Application of Channel Modeling for Indoor Localization Using TOA and RSS

by

Ahmad Hatami

A Dissertation

Submitted to the Faculty

of the

WORCESTER POLYTECHNIC INSTITUTE

in partial fulfillment of the requirements for the

Degree of Doctor of Philosophy

in

Electrical and Computer Engineering

by

May 2006

APPROVED:

_____

Professor Kaveh Pahlavan, Advisor

_____

Dr. Fred J. Looft, Head of Department

Abstract

Recently considerable attention has been paid to indoor geolocation using *wireless local area networks* (WLAN) and *wireless personal area networks* (WPAN) devices. As more applications using these technologies are emerging in the market, the need for accurate and reliable localization increases. In response to this need, a number of technologies and associated algorithms have been introduced in the literature. These algorithms resolve the location either by using estimated distances between a *mobile station* (MS) and at least three reference points (via triangulation) or pattern recognition through *radio frequency* (RF) fingerprinting. Since RF fingerprinting, which requires on site measurements is a time consuming process, it is ideal to replace this procedure with the results obtained from radio channel modeling techniques. Localization algorithms either use the *received signal strength* (RSS) or *time of arrival* (TOA) of the received signal as their localization metric. TOA based systems are sensitive to the available bandwidth, and also to the occurrence of *undetected direct path* (UDP) channel conditions, while RSS based systems are less sensitive to the bandwidth and more resilient to UDP conditions. Therefore, the comparative performance evaluation of different positioning systems is a multifaceted and challenging problem.

This dissertation demonstrates the viability of radio channel modeling techniques to eliminate the costly fingerprinting process in pattern recognition algorithms by introducing novel *ray tracing* (RT) assisted RSS and TOA based algorithms. Two sets of empirical data obtained by radio channel measurements are used to create a baseline for comparative performance evaluation of localization algorithms. The first database is obtained by WiFi RSS measurements in the first floor of the Atwater Kent laboratory; an

academic building on the campus of WPI; and the other by *ultra wideband* (UWB) channel measurements in the third floor of the same building. Using the results of measurement campaign, we specifically analyze the comparative behavior of TOA- and RSS-based indoor localization algorithms employing triangulation or pattern recognition with different bandwidths adopted in WLAN and WPAN systems. Finally, we introduce a new RT assisted hybrid RSS-TOA based algorithm which employs neural networks. The resulting algorithm demonstrates a superior performance compared to the conventional RSS and TOA based algorithms in wideband systems.

Acknowledgments

I would like to express my profound gratitude to my advisor Prof. Kaveh Pahlavan for his continuous guidance, support and wisdom throughout my education.

Special thanks are due to members of my PhD committee, Prof. Fred J. Looft, Prof. Allen Levesque, Prof. Wenjing Lou, and Dr. Farshid Alizadeh for their valuable comments and encouragements.

I am grateful to all my professors in WPI through whom I learned a lot. I would like to thank Prof. Ted Clancy for his thorough editing of my manuscript and his valuable suggestions. I gratefully acknowledge the financial support from WPI, Nokia Corporation, and Draper Laboratory throughout my research.

I wish to thank all my fellow associates who have helped me over the last few years, especially Bardia Alavi, Mohammad Heidari, Ferit Akgul, Nayef Alsindi, Muzaffer Kannan, and all CWINS staff.

I would like to dedicate this work to my wife Shahrzad for her love and support during this journey.

Finally, I am always in debt to the Lord Almighty for giving me the state of well being despite my knowledge and appreciation.

Table of Contents

CHAPTER 1 **INTRODUCTION 1**

1.1. BACKGROUND AND MOTIVATION 1

1.2. LOCALIZATION TERMINOLOGIES 4

1.3. CONTRIBUTIONS OF THIS DISSERTATION 6

1.4. THE OUTLINE OF THIS DISSERTATION 7

CHAPTER 2 **CHANNEL BEHAVIOR AND INDOOR LOCALIZATION 8**

2.1. INTRODUCTION 8

2.2. MULTIPATH AND LOCALIZATION 9

2.2.1. Behavior of TOA Estimation 11

2.2.1.1. Three Classes of Behavior 12

2.2.2. Behavior of RSS Estimation 14

2.3. CHANNEL MODELS FOR LOCALIZATION 17

2.3.1. IEEE 802.11 Recommended Channel Model 18

2.3.2. Channel Modeling Using Ray Tracing 20

2.4. CHANNEL MEASUREMENT SCENARIOS 25

2.4.1. Scenario I : First Floor of AWK 25

2.4.1.1. WiFi RSS Measurement System 27

2.4.1.2. WiFi RSS Measurement vs. RT and IEEE 802.11 Channel Model in Scenario I 30

2.4.2. Scenario II: Third Floor of the AWK 32

2.4.2.1. UWB measurement system for scenario II 33

2.4.2.2. TOA and RSS Measurement vs. RT Simulations in Scenario II 37

CHAPTER 3 **LOCALIZATION SYSTEMS AND ALGORITHMS 45**

3.1. INTRODUCTION 45

3.2. TWO CLASSES OF LOCALIZATION ALGORITHMS 46

3.2.1. Distance Based Localization 47

3.2.2. Pattern Recognition Based Localization *53*

3.3. RSS BASED LOCALIZATION 55

3.3.1. Closest Neighbor (CN) *58*

3.3.2. RT Assisted RSS Based Closest Neighbor (RT-RSS-CN) *58*

3.3.3. Maximum Likelihood RSS Based Location Estimation *59*

3.3.4. RT Assisted RSS Based Maximum Likelihood (RT-MAX-RSS) *62*

3.4. TOA BASED LOCALIZATION 62

3.4.1. Least Square TOA (LS-TOA) *63*

3.4.2. Closest-Neighbor with TOA Grid (CN-TOAG) *65*

3.4.3. RT Assisted TOA Based Closest Neighbor (RT-TOA-CN) *66*

3.5. HYBRID RSS-TOA BASED LOCALIZATION 66

3.5.1. Hybrid RSS-TOA Based Using Neural Networks (RT-HYB-NN) *67*

3.6. SUMMARY 69

CHAPTER 4 **PERFORMANCE COMPARISON OF LOCALIZATION ALGORITHMS 72**

4.1. INTRODUCTION 72

4.2. CHANNEL MODELING AS AN ALTERNATIVE FOR MEASUREMENT IN SCENARIO I 73

4.2.1. Results and Discussions *76*

4.3. TOA VS. RSS BASED LOCALIZATION USING RT IN SCENARIO II 82

4.3.1. Results and Discussions *84*

4.4. TOA VS. RSS BASED LOCALIZATION USING CHANNEL MEASUREMENTS IN SCENARIO II 95

4.4.1. Results and Discussions *97*

4.5. HYBRID RSS-TOA LOCALIZATION USING CHANNEL MEASUREMENTS IN SCENARIO II 100

4.5.1. Results and Discussions *101*

CHAPTER 5 **CONCLUSIONS AND FUTURE RESEARCH 105**

APPENDIX A WIFI RSS MEASUREMENTS IN SCENARIO I 109

APPENDIX B NEURAL NETWORKS 113

APPENDIX C SAMPLE RESULTS OF UWB MEASUREMENTS 118

BIBLIOGRAPHY **120**

Table of Acronyms

AOA	Angle of Arrival
AP	Access Point
BP	Break Point
BS	Base Station
BW	Bandwidth
CCDF	Complementary Cumulative Distribution Function
CDF	Cumulative Distribution Function
CN	Closest Neighbor
CN-TOAG	Closest Neighbor with TOA Grid localization algorithm
DDP	Dominant Direct Path
DME	Distance Measurement Error
DP	Direct Path
FDP	First Detected Path
GPS	Global Positioning system
ISM	Industrial Scientific Medical
LNA	Low Noise Amplifier
LOS	Line of Sight
LS-TOA	Least Square TOA based localization algorithm
MAC	Medium Access Control
MLP	Multi Layer Perceptron
MS	Mobile Station
NDDP	Non-Dominant Direct Path
NN	Nearest Neighbor
POA	Power of Arrival
RMS	Root Mean Square
RSS	Received Signal Strength
RT	Ray Tracing
RT-HYB-NN	RT assisted hybrid RSS-TOA based algorithm using neural networks
RT-MAX-RSS	RT assisted maximum likelihood RSS based algorithm
RT-RSS-CN	RT assisted RSS based with Closest Neighbor algorithm
RT-TOA-CN	RT assisted TOA based with Closest Neighbor algorithm
Rx	Receiver
SNR	Signal to Noise Ratio
TOA	Time of Arrival
Tx	Transmitter
UDP	Undetected Direct Path
WiFi	Wireless Fidelity
WLAN	Wireless Local Area Networks
WPAN	Wireless Personal Area Networks

List of Figures

FIGURE 1-1: FORECAST REVENUE FOR LOCATION BASED SERVICES [1] 2

FIGURE 1-2: A TYPICAL POSITIONING SYSTEM 4

FIGURE 2-1: A SAMPLE CHANNEL IMPULSE RESPONSE FOR A SYSTEM WITH INFINITE BANDWIDTH 9

FIGURE 2-2: A SAMPLE CHANNEL IMPULSE RESPONSE FOR A 200 MHZ SYSTEM 11

FIGURE 2-3: CHANNEL PROFILE CLASSIFICATION 13

FIGURE 2-4: EFFECT OF SYSTEM BANDWIDTH IN TOA ESTIMATION 15

FIGURE 2-5: A SAMPLE IEEE 802.11 PATH LOSS MODEL 20

FIGURE 2-6: A TYPICAL FLOOR PLAN USED BY RT FOR RADIO CHANNEL MODELING 21

FIGURE 2-7: A CHANNEL IMPULSE RESPONSE GENERATED BY RT 22

FIGURE 2-8: TYPICAL CHANNEL IMPULSE RESPONSE 23

FIGURE 2-9: RT PARAMETERS 24

FIGURE 2-10: FIRST FLOOR OF ATWATER KENT LABORATORY (AWK1- SCENARIO I) 26

FIGURE 2-11: RSS CHANNEL MEASUREMENT SYSTEM FOR INDOOR LOCALIZATION 29

FIGURE 2-12: SAMPLE PATH LOSS MEASURED BY IEEE 802.11 PC CARD 29

FIGURE 2-13: RSS DISTRIBUTION AT A FIXED LOCATION OBTAINED BY A WIFI MEASUREMENT SYSTEM 30

FIGURE 2-14: CHANNEL MODELS VS. MEASUREMENTS AT AP1 32

FIGURE 2-15: EXPERIMENTAL SCENARIO FOR A TYPICAL WIDEBAND LOCALIZATION SYSTEM 33

FIGURE 2-16: FREQUENCY DOMAIN MEASUREMENT SYSTEM 34

FIGURE 2-17: A SAMPLE CHANNEL FREQUENCY RESPONSE USING A RECTANGULAR WINDOW 35

FIGURE 2-18: A SAMPLE CHANNEL FREQUENCY RESPONSE AFTER APPLYING A RAISED COSINE WINDOW 35

FIGURE 2-19: SAMPLE CHANNEL IMPULSE RESPONSE 36

FIGURE 2-20: SAMPLE PATH LOSS MEASURED BY WIDEBAND FREQUENCY DOMAIN MEASUREMENT 36

FIGURE 2-21: COMPARISON OF RSS OBTAINED BY MEASUREMENT AND RT USING THE OLD FLOOR PLAN ... 38

FIGURE 2-22: RSS (MEASUREMENT VS. RT) 39

FIGURE 2-23: CDF OF RELATIVE RSS (MEASUREMENT VS. RT) 41

FIGURE 2-24: COMPARISON OF RSS AFTER THE FLOOR PLAN MODIFICATIONS 42

FIGURE 2-25: DME (MEASUREMENT VS. RT) 43
FIGURE 2-26: CDF OF RELATIVE DME (MEAS. VS. RT) 44
FIGURE 3-1: CLASSIFICATION OF LOCALIZATION ALGORITHMS 47
FIGURE 3-2: DISTANCE BASED LOCALIZATION USING RSS 50
FIGURE 3-3: DISTRIBUTION OF RSS FROM EACH AP 50
FIGURE 3-4: DISTRIBUTION OF ESTIMATED DISTANCE FROM EACH AP 51
FIGURE 3-5: CCDF OF LOCALIZATION ERROR 52
FIGURE 3-6: LOCALIZATION USING PATTERN RECOGNITION 53
FIGURE 3-7: APPLICATION OF CHANNEL MODELS IN PATTERN RECOGNITION LOCALIZATION 54
FIGURE 3-8: TYPICAL TOA BASED LOCALIZATION SCENARIO 64
FIGURE 3-9: SUPERVISED LEARNING IN A NEURAL NETWORK 67
FIGURE 3-10: NEURAL NETWORK ARCHITECTURE FOR HYBRID RSS-TOA BASED LOCALIZATION 68
FIGURE 3-11: POSITIONING SYSTEM DESIGN CONSIDERATIONS 70
FIGURE 3-12: LOCALIZATION ALGORITHMS USED IN THIS DISSERTATION 71
FIGURE 4-1: FIRST FLOOR OF ATWATER KENT LAB (AWK1- SCENARIO I) 74
FIGURE 4-2: MAJOR COMPONENTS OF THE TESTBED FOR SCENARIO I 75
FIGURE 4-3: IMPACT OF NUMBER OF REFERENCE POINTS ON LOCALIZATION ERROR USING CN ALGORITHM . 76
FIGURE 4-4: AVERAGE LOCALIZATION ERROR FOR A SYSTEM TRAINED WITH ON SITE MEASUREMENT 77
FIGURE 4-5: AVERAGE LOCALIZATION ERROR FOR A SYSTEM TRAINED WITH RT CHANNEL SIMULATION 78
FIGURE 4-6: AVERAGE LOCALIZATION ERROR FOR A SYSTEM TRAINED WITH IEEE 802.11 MODEL 78
FIGURE 4-7: CCDF OF LOCALIZATION ERROR FOR DIFFERENT TRAINING ALTERNATIVES 79
FIGURE 4-8: THIRD FLOOR OF ATWATER KENT LAB (AWK3 - SCENARIO II) 82
FIGURE 4-9: MAJOR COMPONENTS OF THE SIMULATION FOR SCENARIO II 83
FIGURE 4-10: EFFECT OF UDP CONDITION ON DME (BW: 500 MHZ) 85
FIGURE 4-11: EFFECT OF UDP CONDITION ON RSS (BW: 500 MHZ) 85
FIGURE 4-12: ESTIMATED TRACK 87
FIGURE 4-13: RMS OF LOCALIZATION ERROR AT NUDP POINTS 88
FIGURE 4-14: COMPLEMENTARY CDF OF LOCALIZATION ERROR AT NUDP POINTS 89

FIGURE 4-15: RMS OF LOCALIZATION ERROR AT UDP POINTS 90
FIGURE 4-16: COMPLEMENTARY CDF OF LOCALIZATION ERROR AT UDP POINTS 92
FIGURE 4-17: COMPLEMENTARY CDF OF ERROR FOR ALL THE POINTS 94
FIGURE 4-18: THIRD FLOOR OF ATWATER KENT LAB (SCENARIO II) 95
FIGURE 4-19: MAJOR COMPONENTS OF THE TESTBED FOR SCENARIO II 97
FIGURE 4-20: CCDF OF LOCALIZATION ALGORITHMS 99
FIGURE 4-21: NEURAL NETWORK ARCHITECTURE FOR HYBRID RSS-TOA BASED LOCALIZATION 101
FIGURE 4-22: CCDF OF LOCALIZATION ERROR 102
FIGURE 4-23: CCDF OF LOCALIZATION ERROR FOR NEURAL NETWORK BASED ALGORITHM 104

List of Tables

TABLE 2-1: IEEE 802.11 PATH LOSS MODEL PARAMETERS 19
TABLE 2-2: MEASURABLE RANGE OF WLAN CARDS 28
TABLE 2-3: CORRELATION COEFFICIENTS BETWEEN MEASURED AND SIMULATED RSS 31
TABLE 2-4: MEAN AND STD. DEV. OF RSS FROM AP_1-AP_3 40
TABLE 2-5: MEAN AND STD. DEV. OF DME 42
TABLE 3-1: DME STATISTICS IN DISTANCE ESTIMATION USING RSS 51
TABLE 3-2: COMPARISON OF RSS AND TOA AS LOCALIZATION METRIC 71
TABLE 4-1: CLASSIFICATION OF LOCALIZATION ALGORITHMS 73
TABLE 4-2: COMPARISON OF RADIO MAP GENERATION ALTERNATIVES 81

Chapter 1

Introduction

1.1. Background and Motivation

Localization using radio signals was first introduced in World War II to locate soldiers in emergency situations. During the war in Vietnam the Global Positioning System (GPS) was introduced. This system became available for commercial applications around 1990. In the late 1990s, E-911 technologies and indoor geolocation technologies emerged. The current drive for location based services is mostly limited to emergency and security services required in wireless networks. However, location based applications will play an important role in future wireless markets. A market forecast for the wireless location technology is illustrated in Figure 1-1 [1]. Indoor geolocation is motivated by a number of applications envisioned for indoor location-sensing in commercial, public safety, and military settings [2-5]. Examples of such applications include asset tracking, context aware computing [6], pervasive computing [7], wireless access security [8], mobile advertising [8], locating public safety and military personnel in their indoor missions, and various personal robotics applications [9].

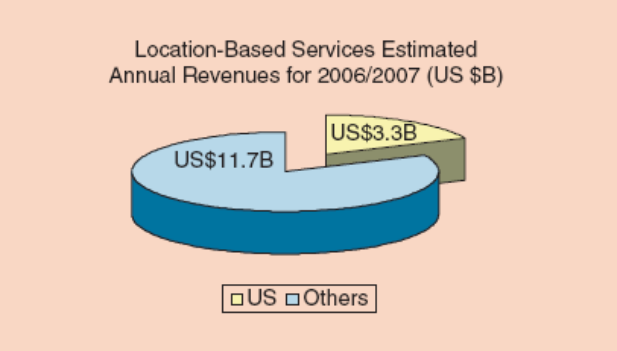

Figure 1-1: Forecast revenue for location based services [1]

More recently, location sensing has found applications in location-based handoffs in wireless networks [10] and location-based ad-hoc network routing [11,12].

The desired accuracy of a localization system is dictated by the application requirements and the environment. For many outdoor applications accuracies of 30-50 m are acceptable [13], while for indoor environment a number of applications demand accuracies of 1-10 m [8]. For example, the required accuracy for E-911 standard (also known as E-112 in Europe) is 100 meters at %67 of the time. However, an application such as child-tracking mandates a locating accuracy within the dimension of a room which is only a few meters. The existence of various applications and their accuracy requirements increases the need for different approaches to the indoor geolocation problem. These needs for more accurate indoor localization have stimulated interest in modeling the propagation environment to assess the accuracy of different sensing techniques [5,14,15], in developing novel technologies to implement the systems [16,17], and in comparative performance evaluation of different technologies.

Most existing localization applications rely on the cellular network infrastructure aimed for outdoor environments. However, increasing deployment of *wireless local area networks* (WLAN) and *wireless personal area networks* (WPAN) creates the opportunity to provide location based services in indoor areas. These new services rely on the existing network infrastructure to determine the position of a mobile user omitting the need for a standalone dedicated network for positioning applications or modifications to existing mobile devices. Nevertheless, many aspects of WLANs and WPANs as location finding applications are not yet fully studied.

References [2,18] identify the complexity of indoor radio propagation and the ad hoc nature of the WLAN and WPAN infrastructure as two main obstacles for accurate indoor localization. Performance, cost, and security are among the main operational challenges in a successful deployment of a localization system [19].

We have already seen implementation of the first generation of indoor positioning products using a variety of technologies [20,21]. The need for a more accurate second generation of products demands extensive research in understanding the channel behavior and development of relevant algorithms. While commercial products and performance studies of indoor geolocation systems are presented in the literature [16,22-25], optimized performance evaluation and deployment techniques that can be used as a framework for efficiently designing indoor geolocation systems are not available. Moreover, there is a literature gap in performance and system bandwidth requirements comparison among RSS and TOA based localization techniques used for indoor geolocation.

This chapter describes some of the localization terminologies and assumptions that have been used throughout this dissertation. Next, the contributions of this research are presented in section 1.3. We conclude this chapter by presenting the outline of this dissertation.

1.2. Localization Terminologies

A network infrastructure deployed to determine the relative coordinates of a *mobile-station* (MS); with respect to some known reference locations (*reference-points*); is called a wireless positioning system. For example a *global-positioning-system* (GPS) receiver determines its relative location with respect to a set of reference satellites and converts that location to a set of latitude, longitude, and altitude values. Figure 1-2 shows the block diagram of a typical positioning system. Positioning systems can be deployed as an overlay service on top of the access network infrastructure. Localization is the process of acquiring the location of MS from a positioning system. This process is also referred to as positioning [26], geolocation [2], and location sensing [27] in the literature. We primarily use the term localization but all of these terms are used interchangeably.

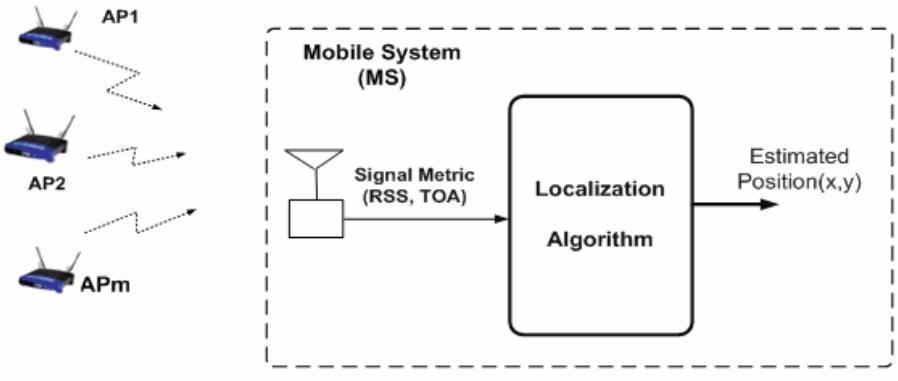

Figure 1-2: A typical positioning system

As shown in Figure 1-2, we use the WLAN terminology, in which an *access-point* (AP) provides the connectivity between a MS and the network infrastructure[1], AP's are the only entities which transmit localization information[2]. A positioning system determines the location of a MS by measuring some signal parameters communicated between the MS and multiple AP's, and using the measured signal parameters in a localization algorithm to provide the final estimate of location. .

In this dissertation we classify the localization algorithms into *distance based* and *pattern recognition* algorithms. A distance based algorithm uses the estimated distances between the MS and at least three reference points in a process called triangulation to find its location. A pattern recognition localization algorithm uses a signal characteristic such as RSS or TOA that form a pattern unique to a reference location and creates a set of reference points with known signal fingerprints called a *radio map* in an offline process called *training* or RF *fingerprinting* [22,23]. During localization, the MS's location is estimated by comparing the observed signals with the existing fingerprints in the radio map. In pattern recognition localization, the radio map is an integrated component of the algorithm. A more accurate radio map can provide a better localization performance. However, RF fingerprinting using on site measurements is a time consuming process and a drawback for an algorithm, it is ideal to replace this procedure with results obtained from suitable radio channel modeling techniques.

[1] In other parts of the literature the connection point of MS to a wireless network is also referred to as *base-station* (BS) [8], or *reference point* [28].
[2] Note that we use the term reference point to identify the points with known locations which are not necessarily colocated with the AP's.

1.3. Contributions of This Dissertation

This dissertation demonstrates the viability of radio channel modeling techniques to eliminate the costly fingerprinting process in pattern recognition algorithms by introducing novel *Ray Tracing* (RT) assisted RSS and TOA based algorithms. Then, we use two sets of empirical data obtained by radio channel measurements to create a baseline for comparative performance evaluation of localization algorithms. The first database is obtained by WiFi RSS measurements in the first floor of the Atwater Kent laboratory; an academic building on the campus of WPI, and the other by UWB channel measurements in the third floor of the same building. We use these measurements to analyze the comparative behavior of TOA- and RSS-based indoor localization algorithms employing triangulation or pattern recognition in different bandwidths adopted in WLAN and WPAN systems. Finally, we introduce a new RT assisted Hybrid RSS-TOA algorithm which employs neural networks.

The results of the research are published in the following manner. Discovering the potentials of using RT algorithms as an alternative to on site measurements to generate the reference radio map for pattern recognition algorithms to reduce the deployment cost of indoor localization is published in [26,29]. In this dissertation we use RT to design new pattern recognition localization algorithms that utilize radio channel behavior to reduce the deployment cost. We compare the performance of the new RT algorithms with traditional algorithms.

Discovering the limits of RSS and TOA approaches for indoor geolocation in practical scenarios involved in *undetected-direct-path* (UDP) conditions and different bandwidths is published in [18,30-32]. In these publications we compare the performance and bandwidth requirement of TOA and RSS based localization algorithms in indoor geolocation systems. Design of an intelligent hybrid TOA-RSS based localization using RT trained neural network algorithm is published in [33].

1.4. The Outline of this Dissertation

This dissertation is organized into five chapters. In Chapter 1 we describe the motivations for this research, present a literature review, and list the contributions of this dissertation. In Chapter 2 we explain the multipath behavior of an indoor radio channel, its impact on TOA and RSS estimation, and applicable models to simulate this behavior. We conclude Chapter 2 by examining the accuracy of channel modeling techniques to fit the empirical RSS and TOA channel measurements in two scenarios which are used throughout this research. Chapter 3 introduces three new RT-assisted algorithms and provides a detailed description of the existing localization algorithms considered for comparative performance evaluations in the dissertation. In Chapter 4 we first investigate the suitability of channel modeling techniques as an alternative to training via on site measurements for RSS based localization. Next, we use RT generated channel profiles as an alternative to on site measurements in both TOA and RSS based localization algorithms to compare the performance of various RSS, TOA, and our novel hybrid RSS-TOA based localization algorithms. Chapter 5 summarizes the results and provides the directions for future research in this area.

Chapter 2

Channel Behavior and Indoor Localization

2.1. Introduction

In this chapter we introduce all channel models and measurement scenarios which are used in the following chapters for design and performance evaluation of both RSS and TOA based indoor localization algorithms. In section 2.2 we describe the multipath behavior of an indoor radio channel and its impact on TOA and RSS estimation. We introduce IEEE 802.11 recommended channel model for simulation of the RSS in addition to the *Ray Tracing* (RT) software for modeling of both RSS and TOA in an indoor environment in section 2.3. In sections 2.4.1 and 2.4.2 we describe two scenarios (scenario I, and scenario II) which are used for channel measurements; (sections 2.4.1.1 and 2.4.2.1 respectively); and performance evaluation of various localization algorithms in Chapter 4. In sections 2.4.1.2 and 2.4.2.2 we examine the accuracy of the channel modeling techniques to fit the empirical RSS and TOA channel measurements in scenario I and scenario II respectively.

2.2. Multipath and Localization

The channel impulse response between a transmitter and a receiver separated by distance d is modeled as [34]:

$$h_d(t) = \sum_{i=1}^{L_p} \beta_i^d \delta[t - \tau_i^d] \qquad (2\text{-}1)$$

where L_p is the number of multipath components, $\beta_i^d = |\beta_i^d| e^{j\phi_i^d}$ and τ_i^d represent location specific random complex amplitude and random propagation delay of the *i*-th path, respectively.

Based on (2-1) a transmitted impulse $\delta(t)$ arrives at the receiver as the sum of multiple delayed impulses with different magnitude and phases due to multipath behavior of an indoor radio channel. A sample channel impulse response is shown in Figure 2-1.

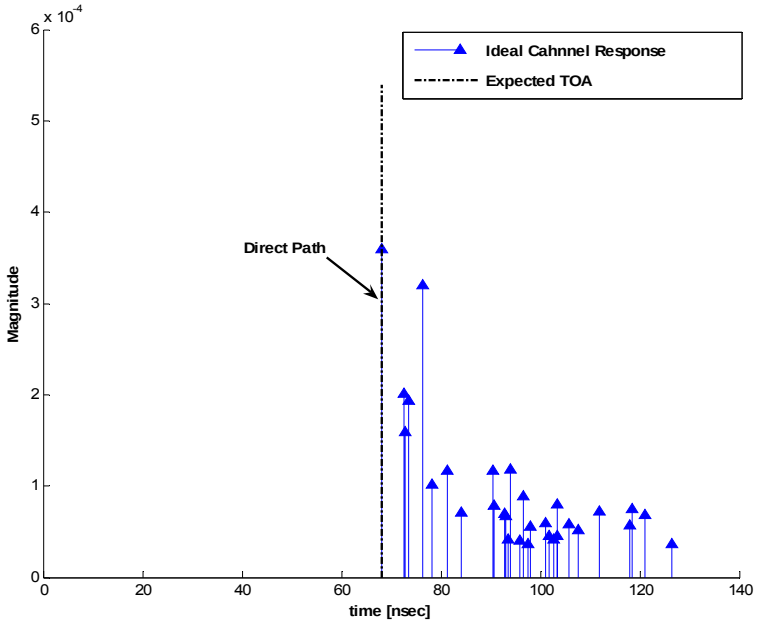

Figure 2-1: A sample channel impulse response for a system with infinite bandwidth

In practice the system has a finite bandwidth; W; due to physical or regulatory constraints and realistic signals are very short duration pulses rather than an ideal impulse. If we represent the transmitted signal by $x_W(t)$, the received signal, $r_d^W(t)$ is given by:

$$r_d^W(t) = \int_{-\infty}^{+\infty} x_W(\tau)\, h_d(t-\tau) d\tau \tag{2-2}$$

In our experiments we use a raised cosine signal defined [35]:

$$x_W(t) = \mathrm{sinc}\left(\frac{2\pi W t}{1+\beta}\right) \times \frac{\cos\left(\frac{2\pi\beta t W}{1+\beta}\right)}{1-16\beta^2 t^2 \frac{W^2}{(1+\beta)^2}} \tag{2-3}$$

or equivalently in the frequency domain [35]:

$$X(f) = \begin{cases} \frac{1+\beta}{2W} & 0 \le |f| \le \frac{1-\beta}{1+\beta} W \\ \frac{1+\beta}{2W}\left[1+\cos\left(\frac{\pi(1+\beta)}{2\beta W}\left(|f| - \frac{1-\beta}{1+\beta} W\right)\right)\right] & \frac{1-\beta}{1+\beta} W \le |f| \le W \\ 0 & W \le |f| \end{cases} \tag{2-4}$$

where β is called the *roll-off* factor and take values in the range $0 \le \beta \le 1$. In our experiments we use $(\beta = 0.5)$

Figure 2-2 shows a sample channel profile generated by transmitting a raised cosine pulse in a system with 200 MHz of bandwidth.

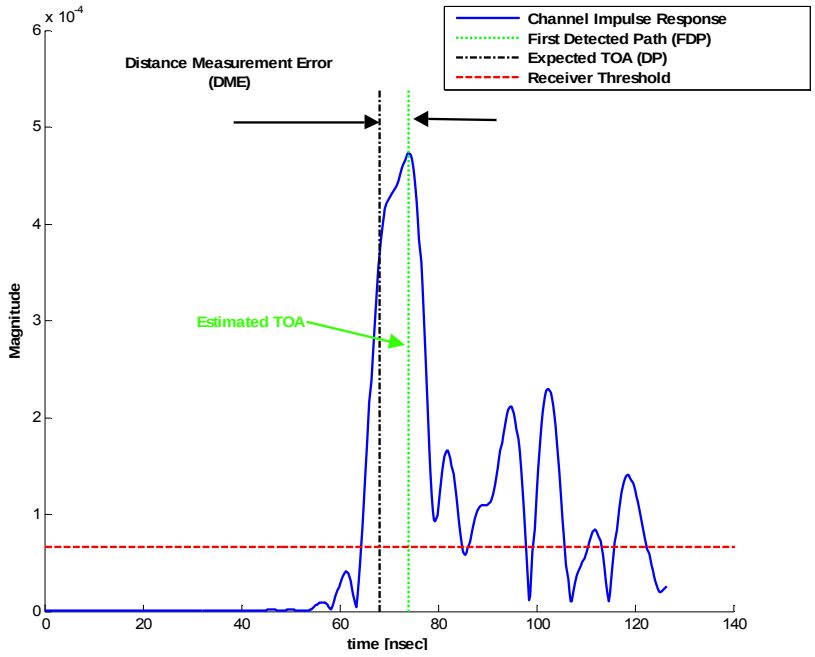

Figure 2-2: A sample channel impulse response for a 200 MHz system

2.2.1. Behavior of TOA Estimation

We define the direct *line-of-sight* (LOS) path between transmitter and receiver antennas as the *direct-path* (DP) and *time-of-arrival* (TOA) of this path indicates the distance between the transmitter and the receiver. In TOA based indoor geolocation systems we use the first detected peak of the channel profile above a detection threshold as the estimated TOA of the DP, we call this peak *first-detected-peak* (FDP). The TOA of FDP, $\hat{\tau}_{1,W}$ is an estimation of the TOA of the DP, τ_{DP}. Therefore the estimated distance between the transmitter and the receiver antennas are obtained from:

$$\hat{d}_W = c \times \hat{\tau}_{1,W} \qquad (2\text{-}5)$$

where c is the speed of light. We use the subscript W to reemphasize that generally $\hat{\tau}_{1,W}$ depends on the receiver's bandwidth W.

In an ideal channel, the actual expected and the estimated DP are the same. However, in multipath conditions, as shown in Figure 2-2, the peak of the channel profile shifts from the expected TOA resulting in a TOA estimation error caused by the multipath condition. We refer to this ranging error as *distance-measurement-error* (DME), which is defined as the error caused by erroneous estimate of the TOA and it is given by:

$$\varepsilon_{d,W} = \left| \hat{d}_W - d \right| \tag{2-6}$$

2.2.1.1. Three Classes of Behavior

Reference [5] classifies wideband channel profiles into *dominant-direct-path* (DDP), *non-dominant-direct-path* (NDDP), and *undetected-direct-path* (UDP) categories. In A DDP channel profile DP which is the strongest path in the profile can be detected by the receiver. In NDDP channel profiles the DP is not the dominant path of the channel impulse response, however, DP can be detected by a more complex receiver. In UDP channels, DP goes below the detection threshold of the receiver while other paths are still detectable, the receiver assumes the FDP as DP which causes large DME values. These classifications are best illustrated in Figure 2-3(a-c), in which the left hand column shows DDP, NDDP, and UDP channel profiles in an infinite bandwidth system and the right hand column shows the same profiles if we use a 200 MHz bandwidth system.

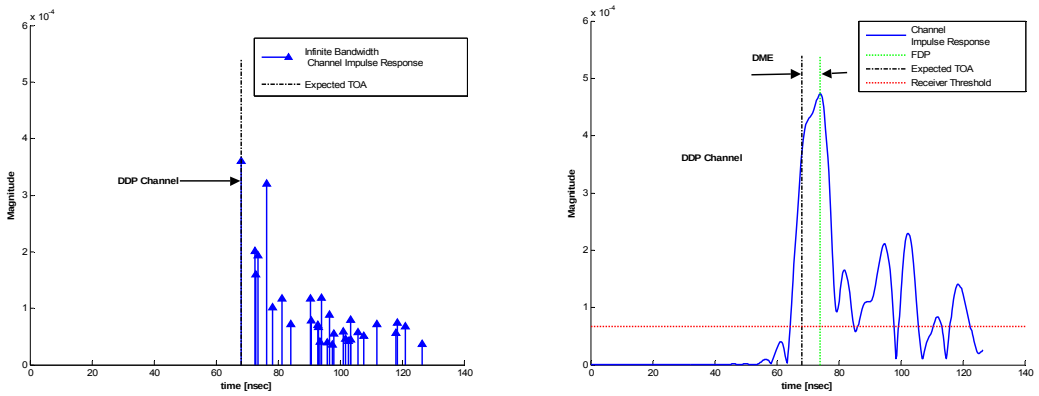

(a) DDP

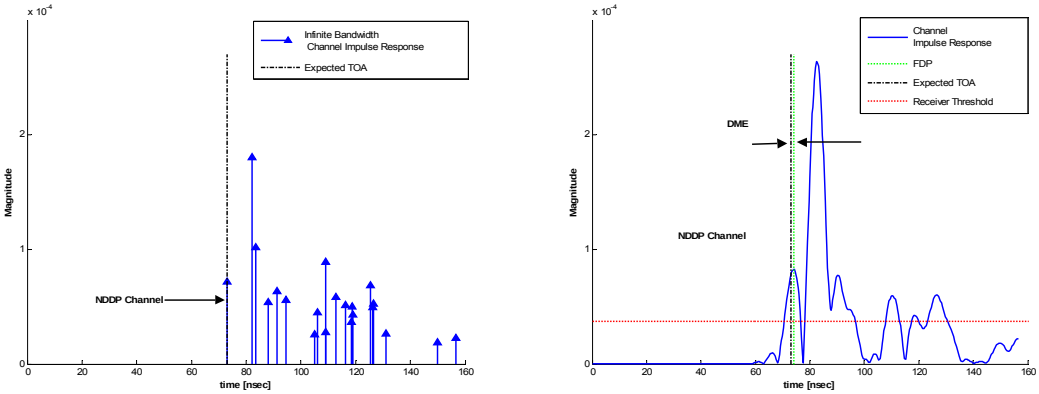

(b) NDDP

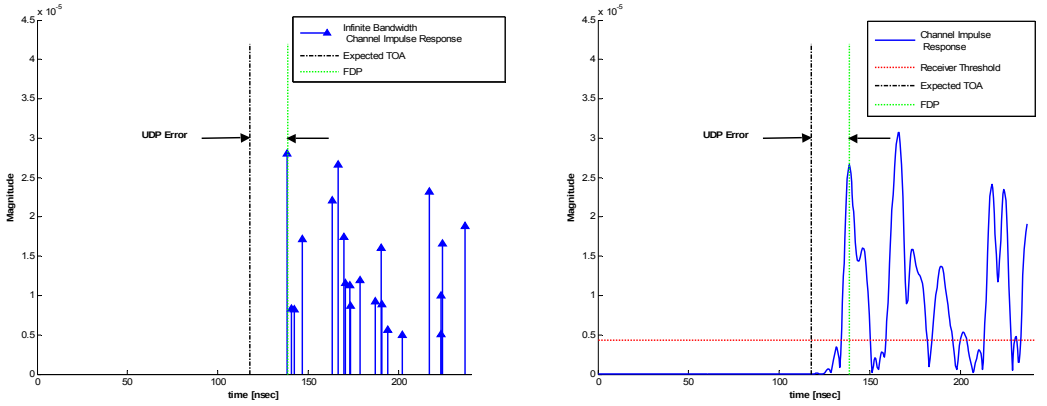

(c) UDP

Figure 2-3: Channel profile classification

The accuracy of TOA estimation depends on the system bandwidth [36]. This relationship is best illustrated by a set of channel profiles. Figure 2-4 (a-b) show the

effect of bandwidth in TOA estimation for the case of a DDP and UDP channel conditions respectively. It can be seen that as the bandwidth increases the channel profiles become more and more similar to the ideal channel profile, i.e. channel impulse response represented on the left hand side of the figure. From a TOA based distance estimation perspective DDP and NDDP channel profiles exhibit similar behaviors. Thus, in this dissertation we classify the channel profiles into *none-UDP* (NUDP) and UDP classes.

The above example demonstrates that increasing system bandwidth reduces DME in NUDP channels. However, increasing bandwidth can not circumvent UDP conditions. In other words increasing system bandwidth does not necessarily reduce DME in UDP conditions [30].

2.2.2. Behavior of RSS Estimation

The total *received-signal-strength* (RSS) at the receiver is defined as:

$$RSS_d = \int_{-\infty}^{\infty} |\, \mathrm{r}_d^W(t)\,|^2 \, dt \tag{2-7}$$

Substituting (2-1) and (2-2) in (2-7) we obtain:

$$RSS_d = \sum_{i=1}^{L_p} \int_{-\infty}^{\infty} |\beta_i^d \, \mathrm{x}_W(t-\tau_i^d)\,|^2 dt \tag{2-8}$$

For the specific case of a system with an infinite bandwidth $\mathrm{x}_W(t) = \delta(t)$:

$$\begin{aligned} RSS_d &= \int_{-\infty}^{\infty} |\, \mathrm{r}_d^W(t)\,|^2 \, dt = \sum_{i=1}^{L_p} \int_{-\infty}^{\infty} |\beta_i^d \delta(t-\tau_i^d)\,|^2 dt \\ &= \sum_{i=1}^{L_p} \left|\beta_i^d\right|^2 \end{aligned} \tag{2-9}$$

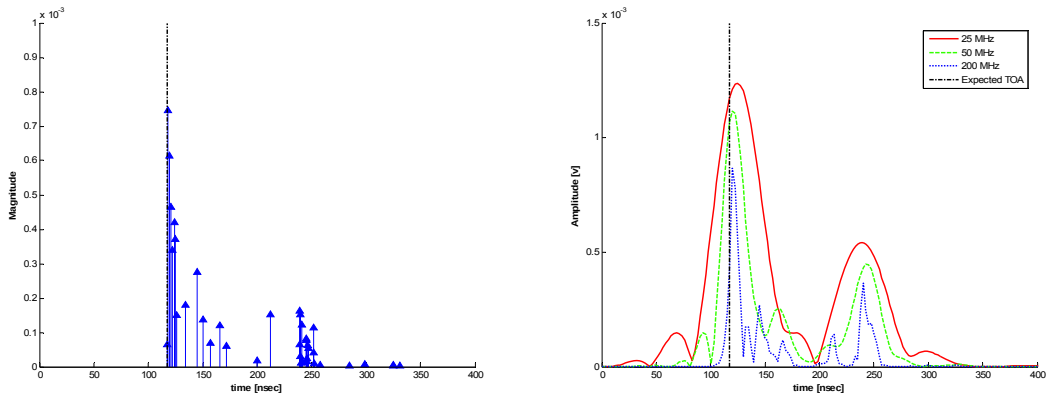

(a) DDP Channel

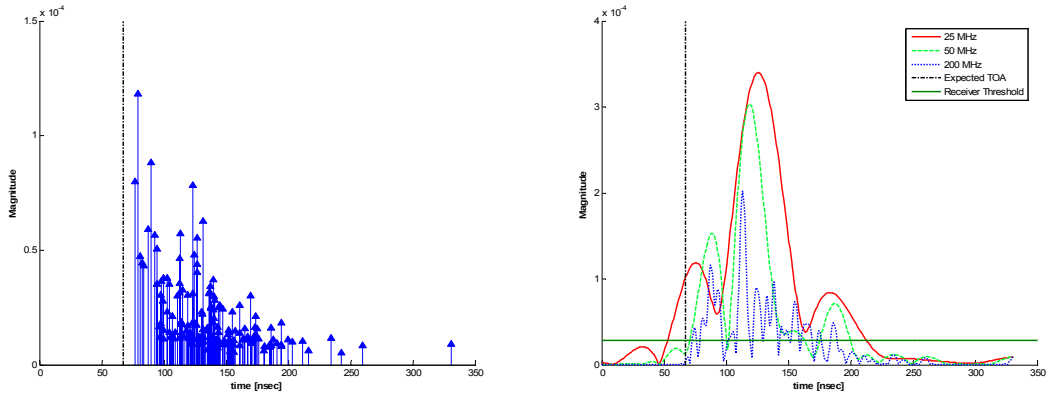

(b) UDP Channel

Figure 2-4: Effect of system bandwidth in TOA estimation

Equation (2-8) is useful for power calculation purpose; however, it does not present an explicit relationship between the average received power and the distance between a transmitter and a receiver.

The relationship between the average received power P_r and the distance d is described by path loss models defined as [22]:

$$p_r = \frac{p_0}{d^{\alpha}} \qquad (2\text{-}10)$$

where p_0 is the received power at one meter from the transmitter and α is referred to as *distance-power-gradient*. This relationship can be described in decibels as:

$$10\log_{10}(p_r) = 10\log_{10}(p_0) - 10\alpha\log_{10}(d) + X \qquad (2\text{-}11)$$

or

$$P_r = P_0 - 10\alpha\log_{10}(d) + X \qquad (2\text{-}12)$$

Where $P_r = 10\log_{10}(p_r)$ and $P_0 = 10\log_{10}(p_0)$ are the received power and the received power at one meter from the transmitter in decibels respectively. The variable X in (2-12) is a zero mean normally distributed random variable with variance σ_x^2:

$$f_X(x) = \frac{1}{\sqrt{2\pi}.\sigma_x} e^{-\frac{x^2}{2\sigma_x^2}} \qquad (2\text{-}13)$$

which represents *shadow fading* in decibels. We define the total path loss L_p in decibels as:

$$L_p = P_t - P_r \qquad (2\text{-}14)$$

where P_t is the transmitted power expressed in decibels. Substituting (2-12) in (2-14) we obtain[1]:

$$L_p = P_t - P_0 + 10\alpha\log_{10}(d) + X \qquad (2\text{-}15)$$

or

$$L_p = L_0 + 10\alpha\log_{10}(d) + X \qquad (2\text{-}16)$$

Where $L_0 = 10\log_{10}\left(\frac{p_t}{p_0}\right)$ represents the path loss in decibels at one meter distance.

[1] Since X is a random variable we use a positive sign.

Equation (2-16) indicates that for a decade increase in distance the path loss increases by 10α in decibels. For a free space path $\alpha = 2$ and for indoor and urban areas the distance power gradient α is highly dependent to the geometry and physical characteristics of the environment [34]. An indoor environment is often non-homogeneous and the overall path loss should be described with multiple distance power gradients, each associated with a segment of the environment. Various channel models with this approach have been addressed in the literature; here we use the IEEE 802.11 recommended channel model in this class because this model has been adopted by IEEE standard committee for WLAN networks.

2.3. Channel Models for Localization

In this research we use channel models in two different contexts. We incorporate channel models in our new localization algorithms to eliminate on site radio measurements; required for the fingerprinting process in existing positioning systems that employ pattern recognition. Moreover, we use channel models to create a repeatable framework for comparative performance evaluation of localization algorithms.

Among the existing channel models we use the IEEE 802.11 recommended channel model for RSS estimation, because it has been adopted as standard for WLAN systems. We also use our two dimensional *ray-tracing* (RT) channel modeling software for UWB channel simulations because it has been shown that RT can generate more realistic channel behavior by using the geometrical and environmental information of the building. The RT generated channel profiles can be used in both RSS and TOA based localization algorithms.

2.3.1. IEEE 802.11 Recommended Channel Model

This model provides an estimation of average path loss [37,38]. Different environments are grouped in five different models (A-E) based on various *rms delay spread* values:

- Model A (optional, should not be used for system performance comparisons), flat fading model with 0 ns rms delay spread (one tap at 0 ns delay model). This model can be used for stressing system performance, occurs small percentage of time (locations).
- Model B with 15 ns rms delay spread.
- Model C with 30 ns rms delay spread.
- Model D with 50 ns rms delay spread.
- Model E with 100 ns rms delay spread.
- Model F with 150 ns rms delay spread.

Among the existing models (B-E) are suitable for indoor channel simulation. The model mapping to a particular environment is presented in Table 2-1.

The path loss model consists of a free space loss, L_{FS} with power distance gradient of α_1 up to a breakpoint distance d_{BP} for distances greater than d_{BP} a different distance power gradient α_2 is used. The free space path loss is defined as:

$$L_{FS}(d) = L_0 + 10.\alpha_1 \log_{10}(d) + X \tag{2-17}$$

The overall path loss for any distance is modeled as:

$$L(d) = \begin{cases} L_{FS}(d) + X & d \le d_{BP} \\ L_{FS}(d_{BP}) + 10\alpha_2 \log_{10}\left(\frac{d}{d_{BP}}\right) + X & d > d_{BP} \end{cases} \tag{2-18}$$

Where L, d, d_{BP}, α_1, α_2 represent path loss in dB, distance in meter, breakpoint distance in meter, power-distance gradient; before and after the breakpoint; respectively. The shadow fading component, X modeled with a zero mean Gaussian probability distribution:

$$f_X(x) = \frac{1}{\sqrt{2\pi}.\sigma_x} e^{-\frac{x^2}{2\sigma_x^2}} \qquad (2\text{-}19)$$

where σ_x is the standard deviation of the shadow fading and defined for different environments (Table 2-1). A sample path loss model based on (2-18) is depicted in Figure 2-5.

In this research we have used the model C in our simulations.

Table 2-1: IEEE 802.11 Path loss model parameters

Model	***Description***	d_{BP} **(m)**	α_1	α_2	**Shadow fading std. dev.** σ_x **(dB)**	
					Before d_{BP} **(LOS)**	**After** d_{BP} ***(NLOS)***
A	(optional)	5	2	3.5	3	4
B	Residential Small Office	5	2	3.5	3	4
C	Typical Office	5	2	3.5	3	5
D	Large Office	10	2	3.5	3	5
E	Large Office	20	2	3.5	3	6
F	Large Space (Indoors and Outdoors)	30	2	3.5	3	6

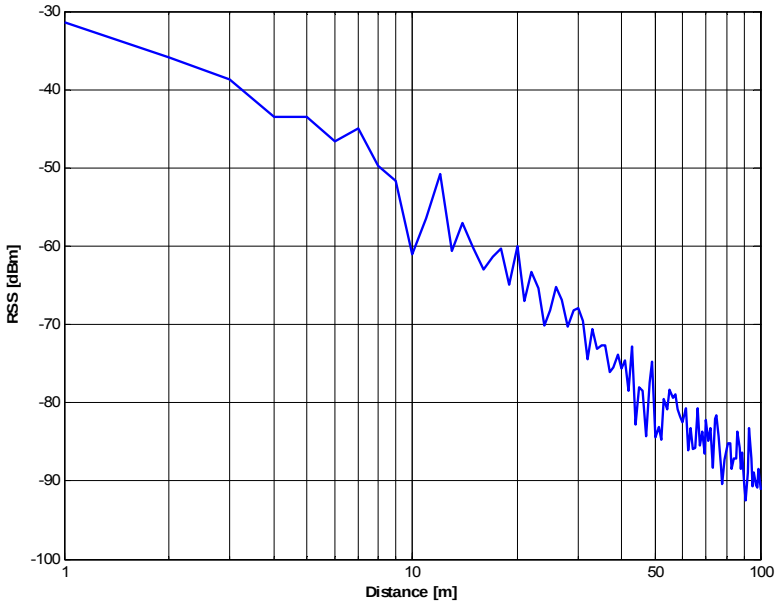

Figure 2-5: A sample IEEE 802.11 path loss model

2.3.2. Channel Modeling Using Ray Tracing

Existing channel models do not use the geometrical characteristics of an environment directly. This is a major shortcoming for these models especially in a multipath rich indoor environment. *Ray-tracing* (RT) is a simulation tool encompassing the geometrical information of a floor plan in addition to the reflection and transmission coefficients of building materials that models the radio channel behavior in different areas [39-42]. For a pair of transmitter-receiver at some known locations, RT determines the necessary information of a channel such as $\beta_i^d = |\beta_i^d| e^{j\phi_i^d}$ and τ_i^d as defined in (2-1), arrival angle, departure angle, phase, number of reflections, and number of transmissions by sending a set of rays from the transmitter and tracing them until they either reach the receiver or largely attenuated that can not be detected by the receiver. The TOA, magnitude, and

phase of each path are recorded for each ray. In small indoor areas with soft surfaced walls reflection and transmission are the dominant mechanisms for radio propagation at frequencies around 1 GHz; whereas for high-rise and urban canyons with roof top antennas diffraction is the main mechanism for signal propagation.

The predictions from ray tracing software are particularly accurate for propagation of radio signals at frequencies greater than 900 MHz where electromagnetic waves can be described as traveling along localized ray paths. This method is shown to be accurate for indoor environments. RT can be used to produce large databases of channel impulse responses for statistical analysis of the channel. Therefore RT is a viable alternative to physical measurement [34]. Figure 2-6 and Figure 2-7 show a set of transmitter-receiver located at the first floor of the Atwater Kent Laboratories and the corresponding RT generated channel impulse response respectively.

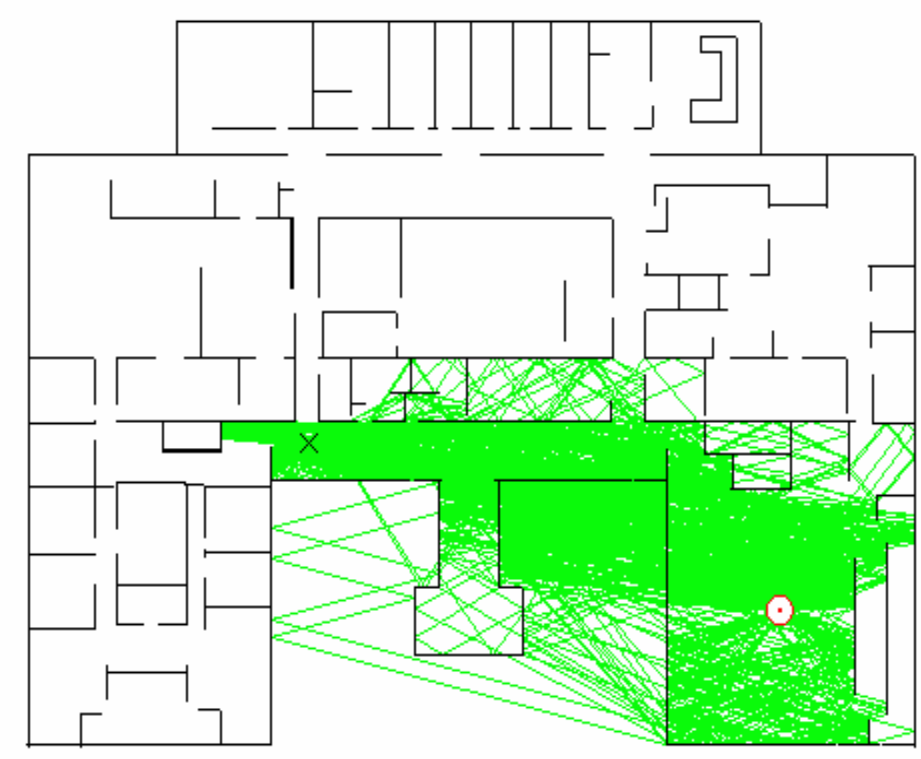

Figure 2-6: A typical floor plan used by RT for radio channel modeling

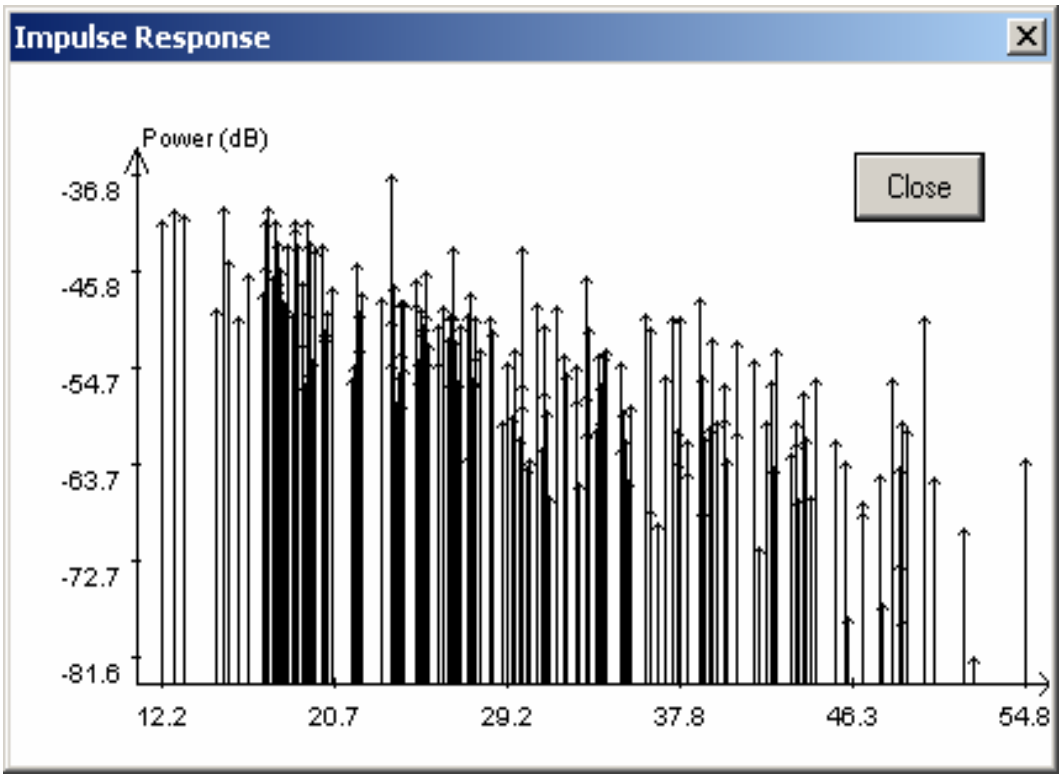

Figure 2-7: A channel impulse response generated by RT

This model contains all the geometrical information of the floor plan such as walls, doors, and windows. To compare the accuracy of RT in channel modeling, two sample channel profiles between known transmitter–receiver locations are shown in Figure 2-8 (a-b) for both an RT simulation and measurement with bandwidths of 500 and 25 MHz respectively. The expected TOA in both cases are shown by the dotted line. This figure illustrates that RT predicts the major paths fairly well. However, it should be noted that the RT must be calibrated for different areas and in general one should compare the statistical characteristics of the channels on a particular area with the results of RT [41]. Although RT is not an appropriate channel estimation technique for real time applications due to its computation complexity, it is a valuable technique for offline coverage study and fingerprinting applications.

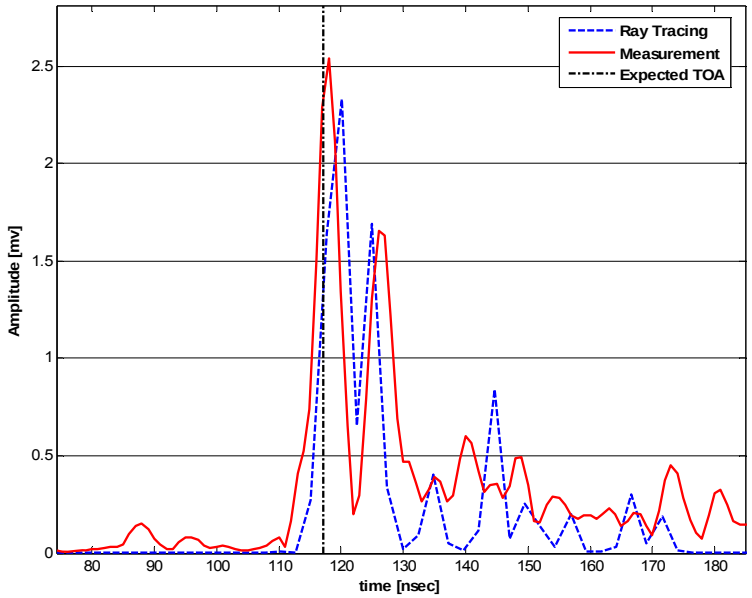

(a)

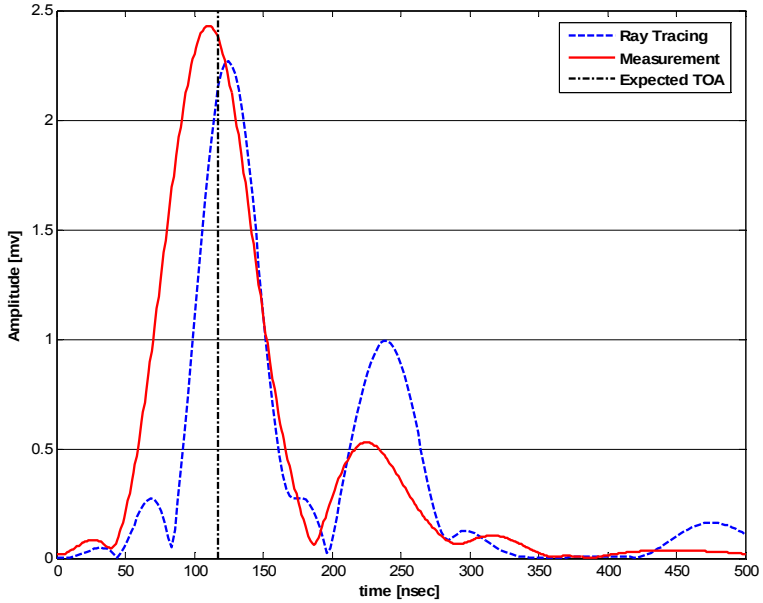

(b)

Bandwidths	:	(a) 500MHz,	(b) 25MHz
DME (RT)	:	(a) 10 [cm],	(b) 2.1 [m]
DME (Meas.)	:	(a) 24 [cm],	(b) 2.2 [m]

Figure 2-8: Typical channel impulse response

Figure 2-9 shows the RT parameters that have been used in this research for channel simulations. The complete descriptions of all RT parameters are available in [43].

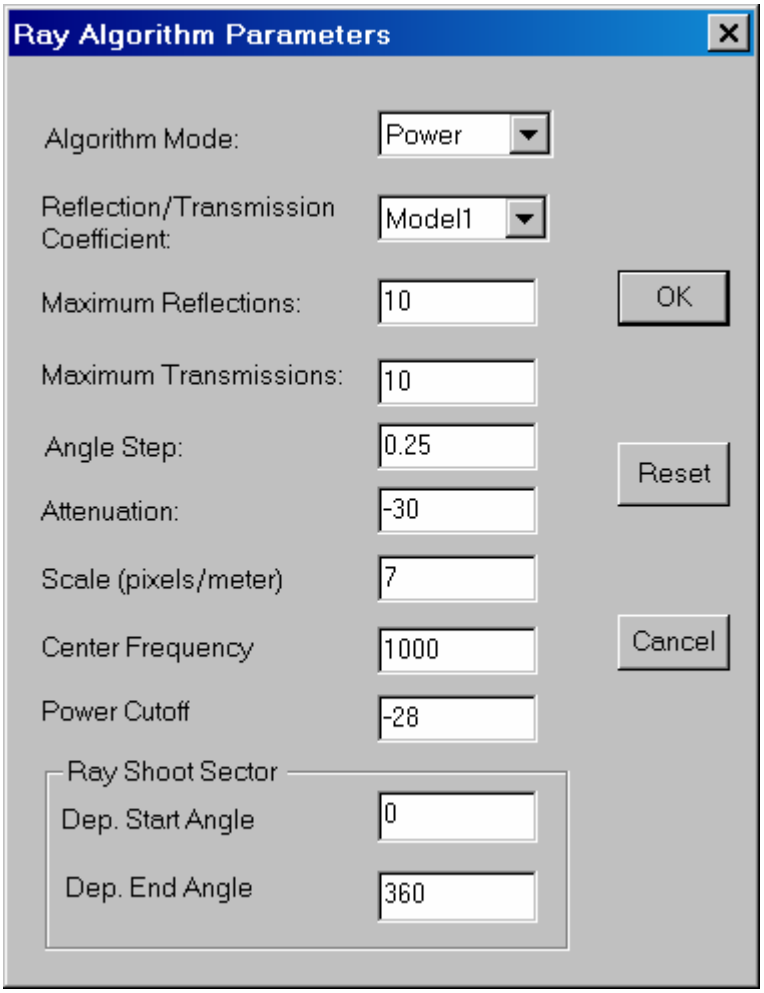

Figure 2-9: RT parameters

2.4. Channel Measurement Scenarios

Indoor radio propagation has been studied extensively for the evaluation of different transmission systems for application in cellular and wireless local area networks. However, most of these studies are aimed towards communication applications. In this section we describe two channel measurement systems that have been used for localization applications.

In this section we introduce two scenarios which are used for comparative performance evaluation of localization algorithms in chapter 4.

Section 2.4.1.1 describes a measurement system which has been used for power measurement required for RSS based localization techniques. The rest of this section describes our RSS measurement campaign scenario, and empirical results compared with the simulated results generated by RT and IEEE 802.11 recommended channel model.

We describe the more complex wideband frequency domain measurement system that have been used for both RSS and TOA based localization applications in section 2.4.2 accompanied with our measurement scenario, and empirical results compared with RT generated channel profiles.

2.4.1. Scenario I : First Floor of AWK

The first scenario for performance evaluation is at the first floor of Atwater Kent laboratory (AWK1) building in Worcester Polytechnic Institute (WPI) campus, which represents a three stories typical office building with more than 1600 square meter area. Figure 2-10 shows the reference points and the location of the AP's in that floor. AP1-AP7 are seven access points which provide wireless network coverage in this floor. The

location of the access points are chosen to provide a comprehensive coverage in populated areas within the building. P1-P257 represent all possible locations where a MS can visit. Rather than creating an exhaustive high resolution grid for reference points, we classified the possible locations in two different categories. The first category includes hallways and places where a user can be walking while using a mobile terminal. The second category is classes and lecture rooms where a mobile host uses the terminal to access a network with limited mobility.

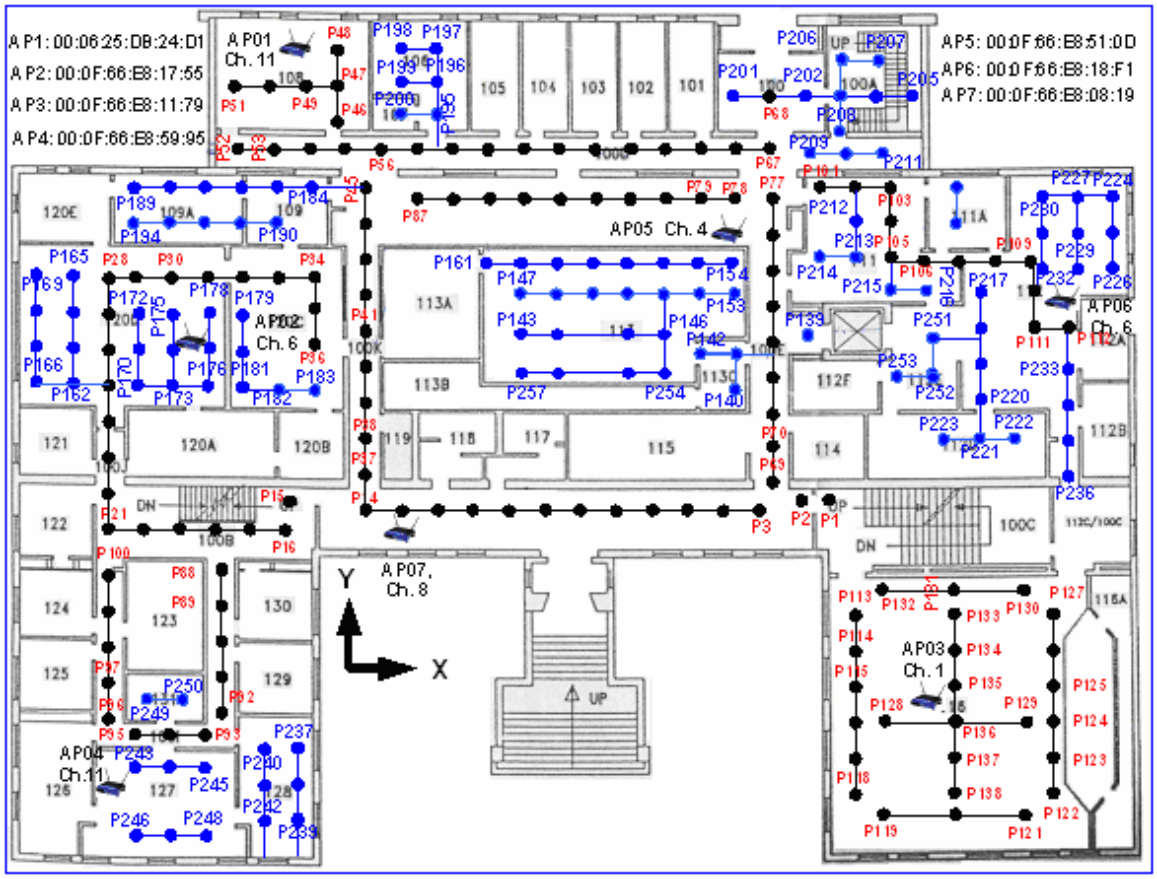

Figure 2-10: First floor of Atwater Kent laboratory (AWK1- Scenario I)

2.4.1.1. WiFi RSS Measurement System

Most off the shelf WiFi devices are able to measure RSS from the available AP's. In this section we explain a WiFi measurement system that we have used to record RSS from a designated AP. Figure 2-11 shows the major components of this measurement system. A Linksys 802.11b/g AP at a known location is used as a transmitter in a designated channel. Since most existing positioning systems use the information provided by the WLAN interface card we used a laptop computer equipped with a dual band Proxim 802.11 PC card as our receiver. We used Airopeek which is a commercial WLAN analyzer software developed by WildPackets™ to log the RSS measurements from AP to the MS over a certain period of time.

There are two alternative options for communicating with an AP. In the first alternative the receiver (an 802.11 card) in a process called active scanning, periodically broadcasts a probe request frame, listens for probe responses from available access points in its neighborhood and records the associated signal strength. The second alternative is passive scanning, in which the receiver sniffs each of the available 802.11 channels periodically to discover the RSS values. Since an AP can be configured to not to respond to broadcast probe requests and we did not want to make any restricting assumption about the WLAN deployment, we relied on the existence of a beacon from each AP and used passive scanning.

An IEEE 802.11b WLAN AP broadcasts a beacon on an assigned channel in the 2.4 GHz band every 10 milliseconds to report network availability as well as link quality information. The 2.4 GHz band is shared by other equipments in the *industrial-scientific-medical* (ISM) band. This band is divided into channels 1-11 each with 26 MHz of

bandwidth with three non-overlapping channels. The link level information available in each beacon frame includes the AP's name, AP's *medium-access-control* (MAC) address, RSS in dBm, noise in dBm, *signal-to-noise-ratio* (SNR) in dB and channel number. There are many factors that can affect the WLAN based RSS measurements such as MS's orientation, time of day, environment, distance from transmitter, interference from other AP's, and make of wireless cards. We used a dedicated channel for our measurements to limit the effect of interference from other AP's in the area. In order to address the MS's orientation factor the measurement was done in multiple directions at the same location. The post processing unit is used to extract the information associated with the desired AP and add a time tag and apply a five seconds averaging window to the collected data.

At the end it should be noted that RSS values reported by most WLAN cards are in integral steps of one dBm. Consequently not all possible RSS values can be represented and the measurement results are dependent on the sensitivity of the WLAN card. The sensitivity of some typical WLAN cards is reported in Table 2-2 [44]. A sample path loss model on a line of site path and a sample RSS distribution at fixed location obtained with this measurement system are depicted in Figure 2-5 and Figure 2-13 respectively.

Table 2-2: Measurable range of WLAN cards

Vendor	**Model**	**Max RSS [dBm]**	**Min RSS [dBm]**	**Range [dB]**
Lucent	Orinoco Gold	-10	-102	92
Lucent	WaveLAN Silver	-10	-94	84
Cisco	Aironet 350 series	-10	-117	107
Proxim	Orinoco gold	-11	-93	82
SMC	EZ Connect SMC2635W	-14	-82	68
D-Link	Airplus DWL-650+	-50	-100	50

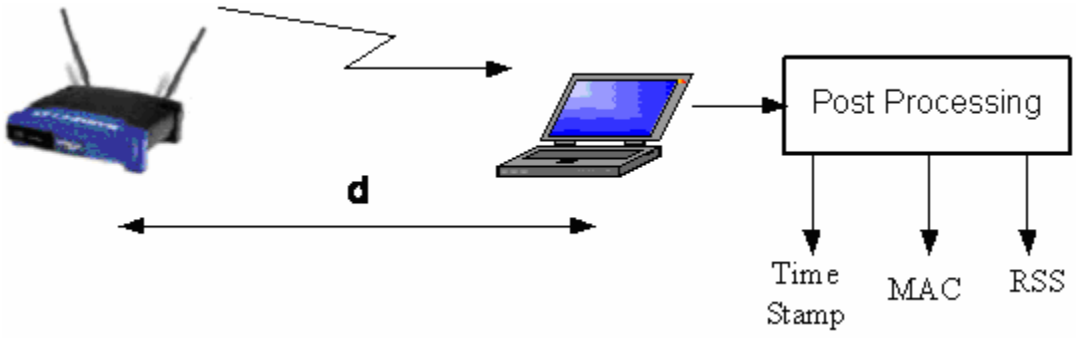

Figure 2-11: RSS channel measurement system for indoor localization

In the path loss depicted in Figure 2-12 the observed distance power gradient is $\alpha = 2.1$ which is similar to a LOS condition. The statistical distribution of the temporal behavior of RSS at a fixed location is depicted in Figure 2-13.

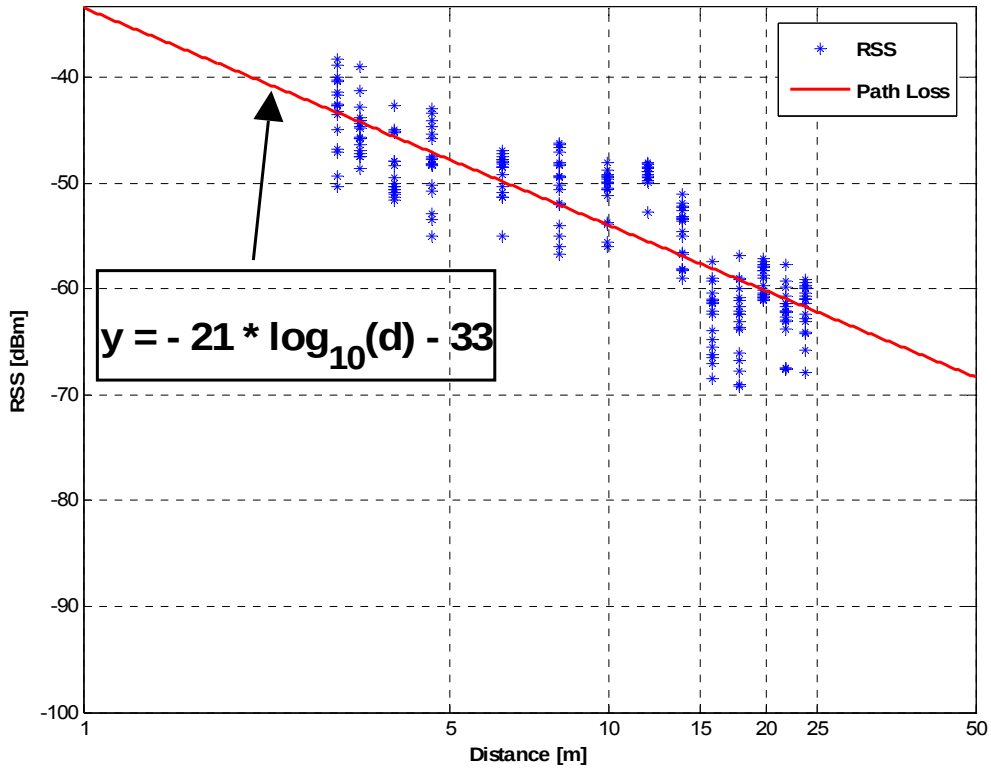

Figure 2-12: Sample path loss measured by IEEE 802.11 pc card

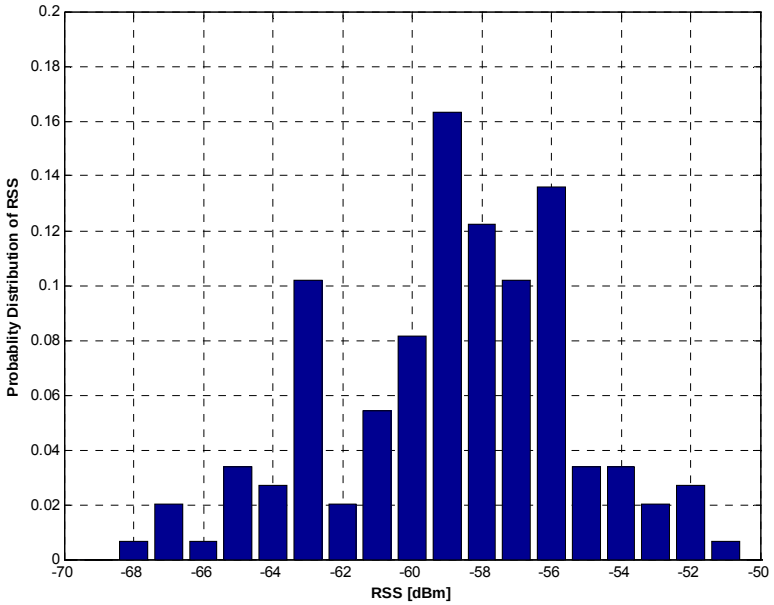

Figure 2-13: RSS distribution at a fixed location obtained by a WiFi measurement system

2.4.1.2. WiFi RSS Measurement vs. RT and IEEE 802.11 Channel Model in Scenario I

We placed seven WiFi AP's at different locations as mentioned in scenario I, and deployed a WiFi RSS measurement campaign using the measurement system we described in 2.4.1.1. We collected 802.11 signal strength values from AP1-AP7 at over two hundred and fifty different locations. Each of the seven 802.11 AP's broadcasts a beacon on an assigned channel (1,4,6,8, and 11) every 10 milliseconds. Channel assignments were conducted in a way to reduce the interference between overlapping channels. The receiver was configured to scan channels 1,4,6,8, 11 periodically for 500 milliseconds. We used the IEEE 802.11 recommended channel model and our two dimensional RT software; as described in sections 2.3.1-2.3.2; to simulate RSS

measurements at the same reference locations in scenario I and compared the simulated values with the measurement results.

Our observation showed that both ray tracing and 802.11 channel model provide an approximation of on site measurement. We have summarized the correlation coefficients between RSS values from each access point (AP1-AP7), obtained by measurements, the results generated by ray tracing and IEEE recommended channel model in Table 2-3. In this table (x,y,z) represent the location of each AP. The smallest correlation coefficient can be justified, by considering the fact that AP3 was located at a lower elevation compared to the other access points in the building. We observed that generally RT provides a better approximation compared to the 802.11 model, mostly because of the indoor multipath fading which is highly dependent to the geometry of the building and is not counted for in IEEE channel model. The RSS from AP1 at all the reference locations are depicted in Figure 2-14. Similar comparative figures for AP2-AP7 are provided in appendix A.

Table 2-3: Correlation coefficients between measured and simulated RSS

Access Point	Location of the AP			Correlation between Measurement &	
	X	Y	Z	Ray-Tracing	IEEE 802.11
AP01	13.4	43.2	2.6	0.94	0.86
AP02	6.3	22.1	3.0	0.91	0.92
AP03	48.4	6.2	0.9	0.74	0.66
AP04	6.0	4.0	2.0	0.91	0.87
AP05	37.4	33.0	3.0	0.84	0.79
AP06	54.4	27.5	2.0	0.89	0.92
AP07	19.0	18.0	3.0	0.82	0.76

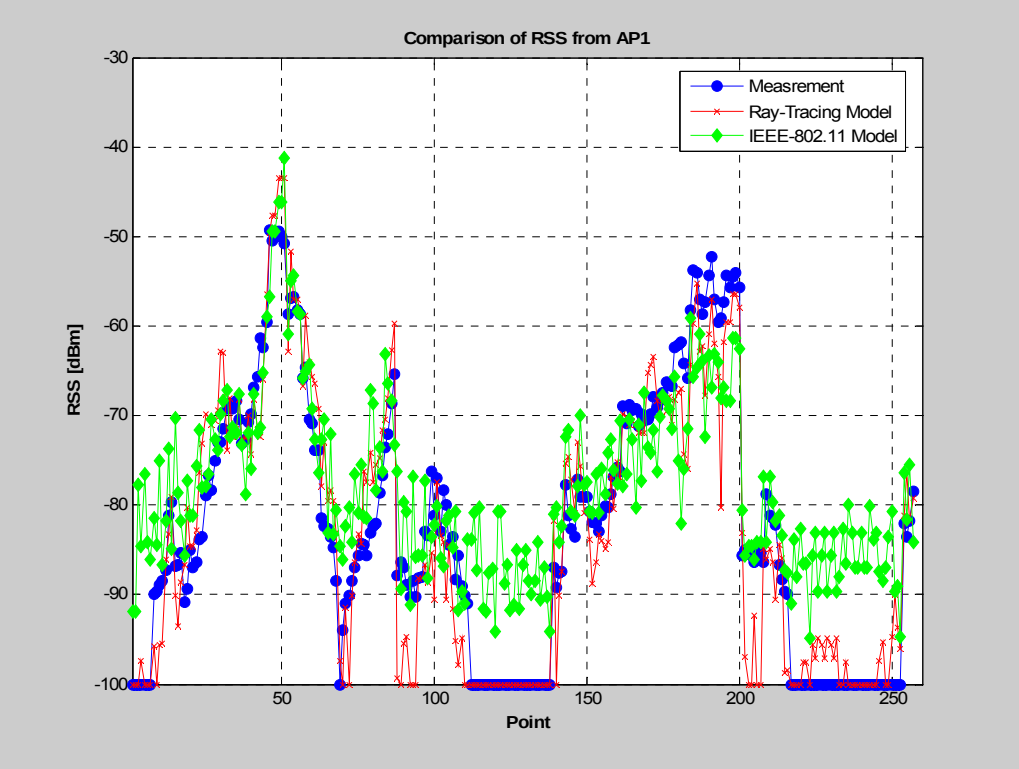

Figure 2-14: Channel models vs. measurements at AP1

2.4.2. Scenario II: Third Floor of the AWK

The second scenario for performance evaluation is at the third floor of Atwater Kent laboratory (AWK3) building in WPI campus. Three *AP's* (AP1-AP3) are located in this floor at known locations (Figure 2-15). The MS moves along existing hallways on this floor. B1 and B2 are a metallic chamber and a service elevator located in this floor, respectively. Both B1 and B2 obstruct the DLOS component of the transmitted signal from AP1 and AP3 in some locations on the path, causing ranging estimation errors by generating UDP channel profiles.

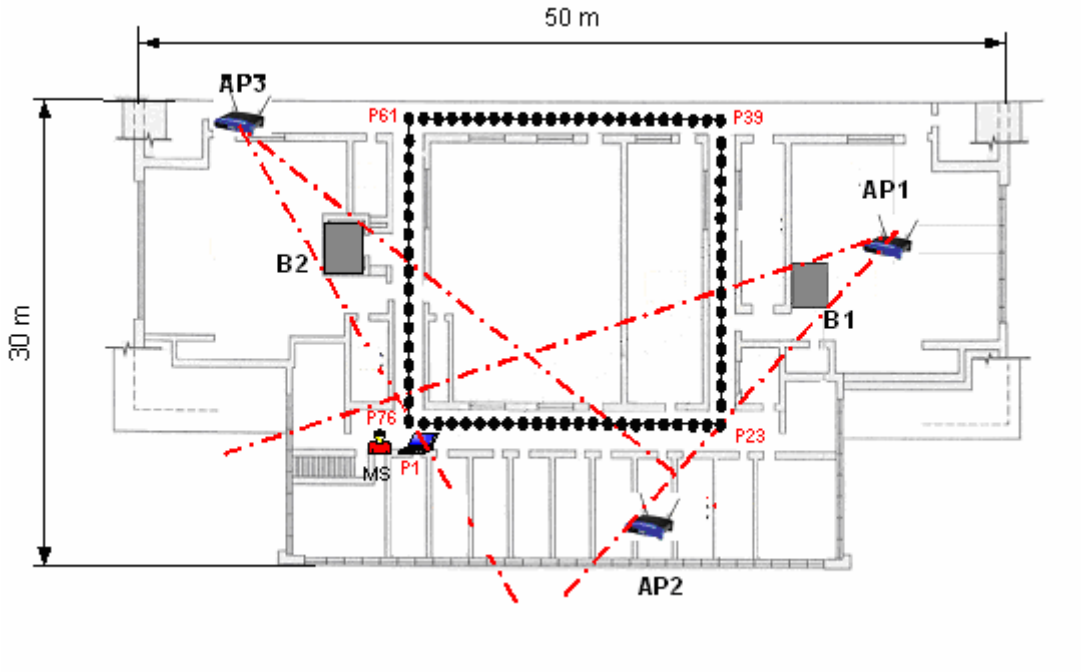

Figure 2-15: Experimental scenario for a typical wideband localization system

2.4.2.1. UWB measurement system for scenario II

Although RSS measurement system provides a convenient and easy to implement measurement system, it does not provide channel impulse response which is required for development of more complex TOA and RSS based localization algorithms. In this section we describe our wideband frequency domain measurement system [5,34,45,46] that determines the channel impulse response by sending a narrow pulse and observing the effect of the channel on the received signal.

The major components of our coherent wideband frequency domain measurement system are shown in Figure 2-16. The wideband network analyzer emulates a coherent transmitter-receiver set. A short duration pulse is generated as a frequency sweep by the network analyzer and transmitted over the air through the transmitter antenna after RF

power amplification. The transmitted signal arrives at the receiver antenna, passes through a low noise amplifier, and appears at the input of the network analyzer. Since transmission of a band-limited signal results in a long duration pulse in the time domain, in order to achieve better spectral characteristic we apply a raised cosine window with 50 percent excess bandwidth ($\beta = \frac{1}{2}$) to the transmitted signal.

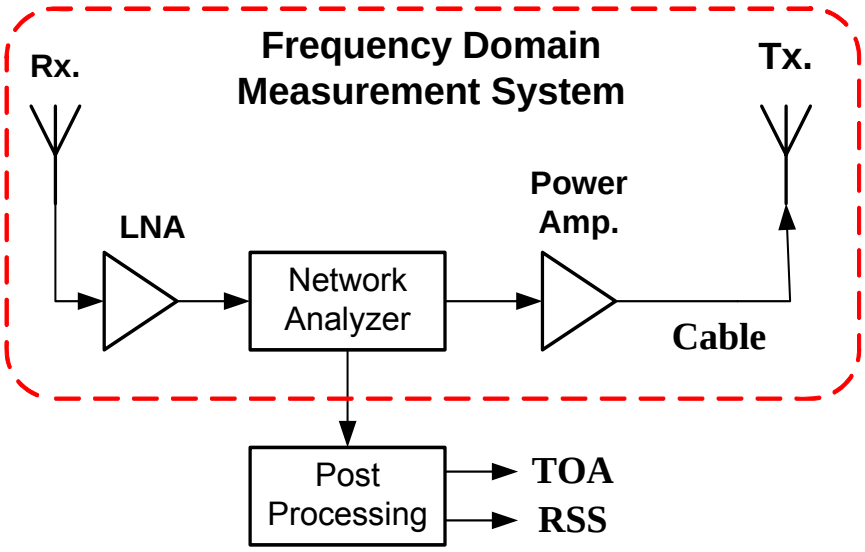

Figure 2-16: Frequency domain measurement system

Figure 2-17 and Figure 2-18 show plot of the magnitude of a typical frequency response with and without applying a pulse shaping window measured at a fixed location respectively. The pulse shaping window reduces both the frequency selective fading effect and out of band interference in the frequency domain. This in turn reduces the number of observed paths in the time domain signal. The corresponding magnitude of the time domain response for the same experiment is shown in Figure 2-19. This system can be used for both TOA and RSS estimation.

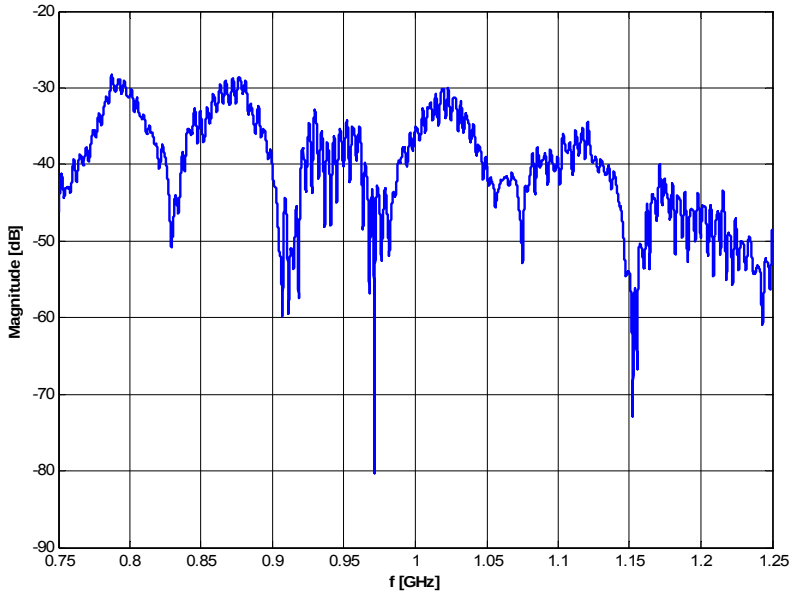

Figure 2-17: A sample channel frequency response using a rectangular window

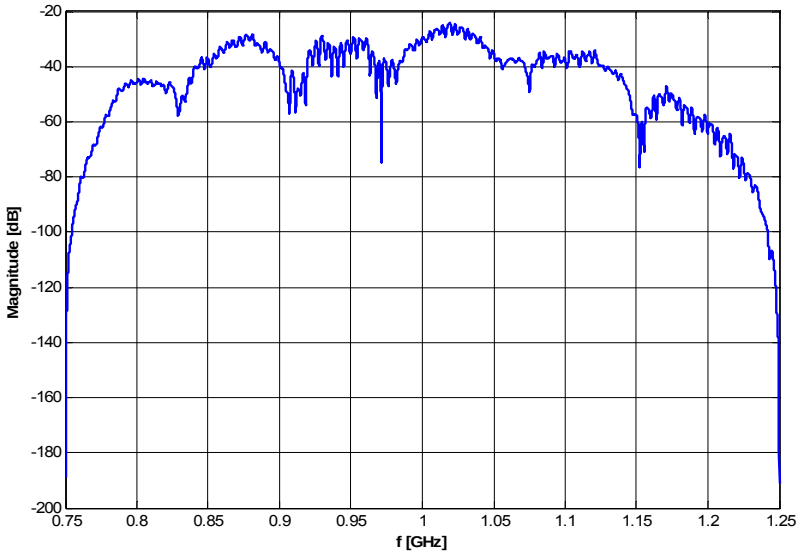

Figure 2-18: A sample channel frequency response after applying a raised cosine window

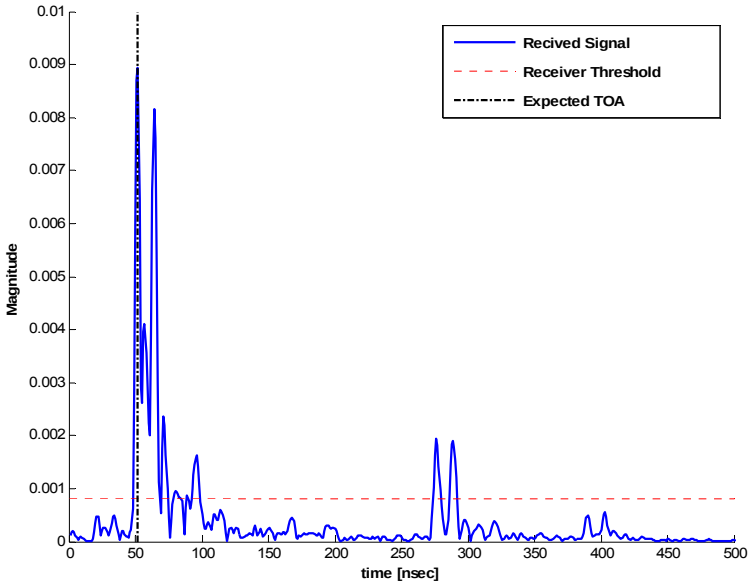

Figure 2-19: Sample channel impulse response

A scatter plot of the power versus the distance on a log scale for a line of site experiment in a 500 MHz system is depicted in Figure 2-20. The path loss model for this experiment is comparable with the model obtained in Figure 2-12. The distance power gradient in both cases is approximately the same ($\alpha \approx 2$).

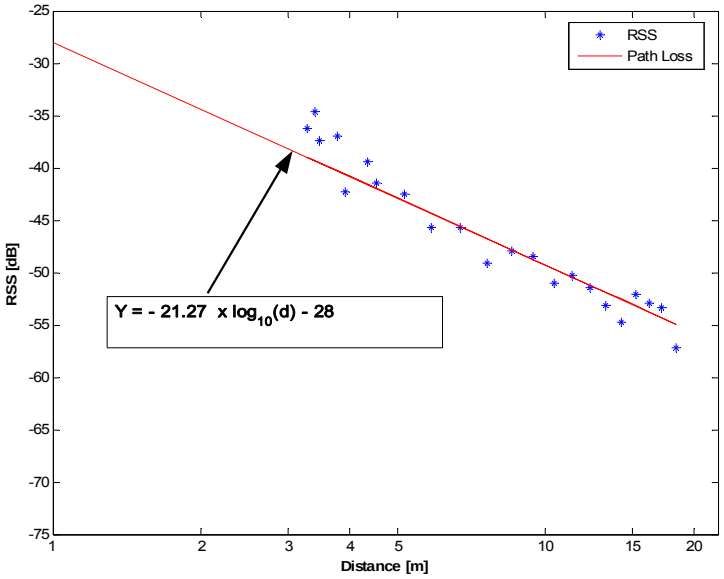

Figure 2-20: Sample path loss measured by wideband frequency domain measurement

2.4.2.2. TOA and RSS Measurement vs. RT Simulations in Scenario II

In section 2.4.1.2 we used RT and IEEE 802.11 recommended channel model to simulate the behavior of a radio channel in indoor environments and examined the accuracy of both techniques in simulating a WiFi measurement system. In this section we generalize the radio channel modeling technique for wideband channel measurement system. In order to study both TOA and RSS based systems we need to model the entire channel profile rather than a single RSS value.

We conducted a frequency domain measurement [5,34] as described in 2.4.2.1 at 76 points along the specified track in scenario II. Our measurement system is centered at 1 GHz with 500 MHz of bandwidth. The transmitting and receiving antennas were both monopole antennas with small metal ground planes whose radiation pattern were assumed to be the same as omnidirectional dipole antennas. Both antennas were mounted at 1.6 m above the floor. We placed the transmitting antenna at AP1-AP3 and the receiving antenna was located at 76 distinct locations along the track representing the MS location. The post processing unit; located at the receiver; applies a raised cosine filter followed by a peak detection; and estimates RSS and TOA of a received signal. The filter can be configured as either a 25 MHz or 500 MHz filter to exemplify WLAN and WPAN systems respectively.

We simulated this scenario with an existing floor plan for AK3 as explained in scenario II. Our objective was to compare signal metrics that are used by localization algorithms, which are RSS, DME and their associated statistics in both 25 MHz and 500 MHz systems. A point by point comparison of RSS values for a 500 MHz system is depicted in Figure 2-21. Although the general pattern of simulated and measured RSS values look the

same but the difference between simulation and measurement at some of the locations was rather large. After some investigation we found that there have been some changes in the floor plan since it was originally created. For example a new wall has been added in the middle of the floor plan, and also the room in which AP2 was located is surrounded by numerous metallic objects which are not counted for in the original floor plan. We decided to add these details to the existing floor plan and simulated the same measurement scenario with RT using a new floor plan. We compared the RT generated channel profiles with channel measurement values using two different bandwidths. We used two systems with 25 MHz and 500 MHz bandwidths to represent WLAN and WPAN devices respectively. A point by point comparison of RSS values from AP1-AP3 along the track for a 500 MHz and a 25 MHz system using the new floor plan is depicted in Figure 2-22 (a-b) respectively.

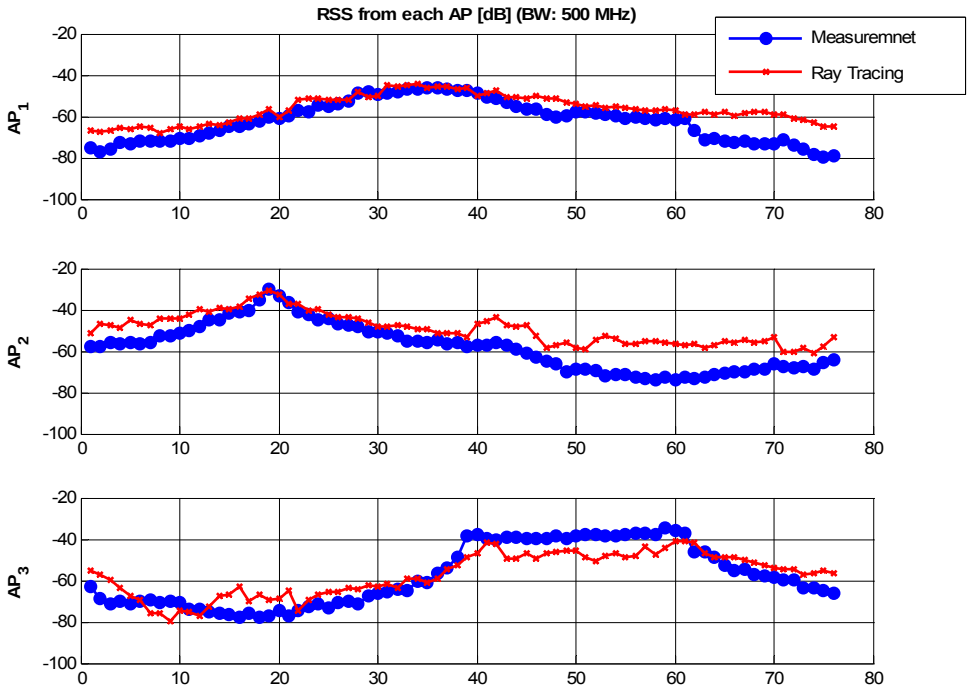

Figure 2-21: Comparison of RSS obtained by Measurement and RT using the old floor plan

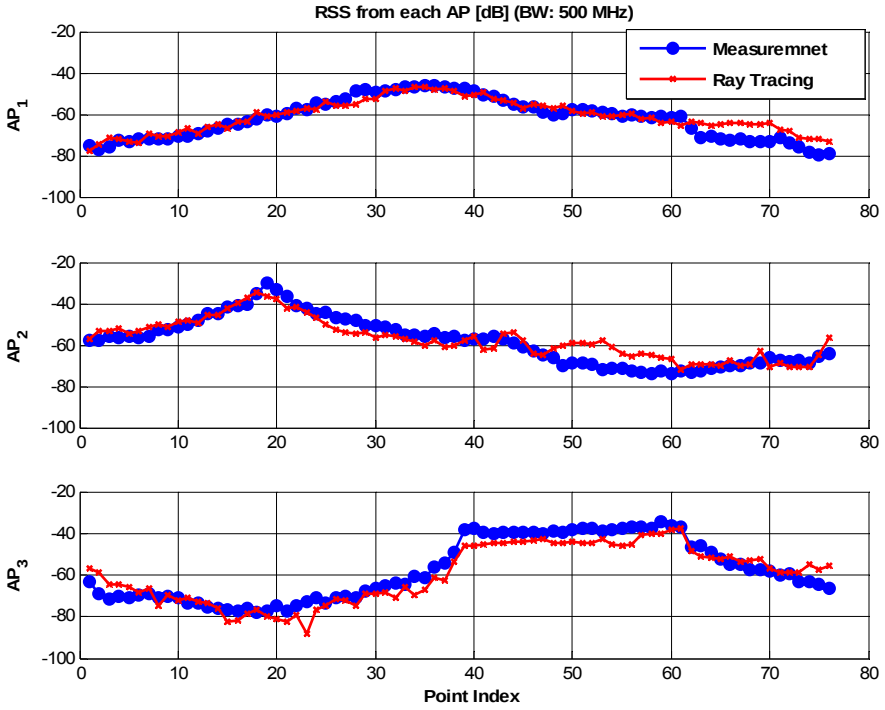

(a) BW: 500 MHz

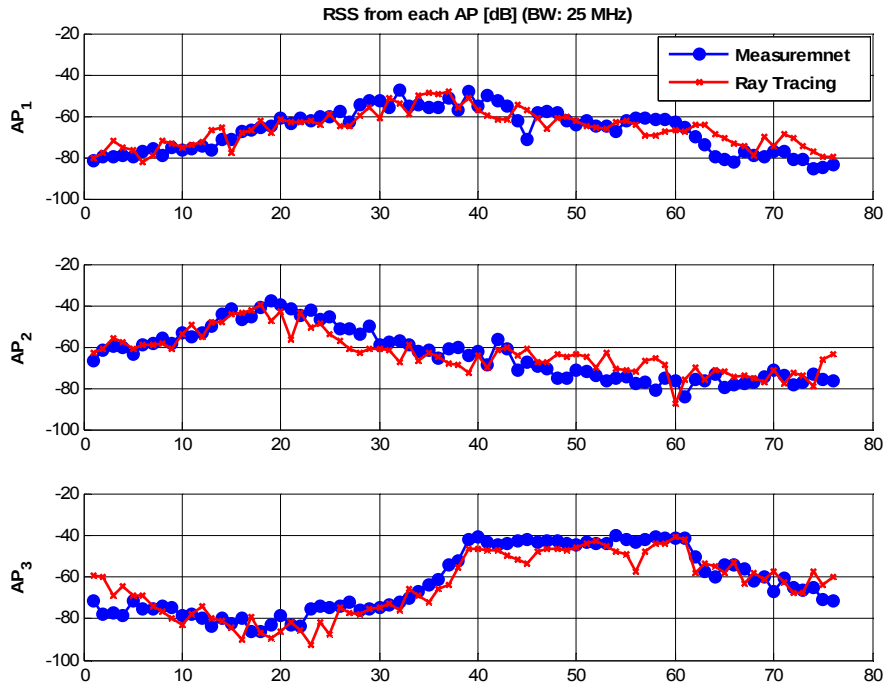

(b) BW: 25 MHz

Figure 2-22: RSS (Measurement vs. RT)

The mean and standard deviation of RSS from AP1-AP3 for both 500 MHz and 25 MHz systems are summarized in Table 2-4. RT simulated RSS values follow the actual measurement values except in certain areas. The average estimated RSS from AP3 is less than the actual measurements while the average RT estimated values from AP1- AP2 are more than the measured values. AP3 is located at the boundary of the building thus some of the rays originated from AP3 pass through the hallway wall and never reflect back into the building. However, in reality a portion of these rays reflect back after hitting adjacent buildings and increase the actual RSS values. The reason for a discrepancy between measurement and RT estimated RSS from AP1 at points 60-70 and form AP2 at points 50-60 is that there are some metallic lab equipment and furniture located at the middle part of the floor plan which are not included in the floor plan used by RT. Thus, a more complete floor plan may be required to improve the RSS estimation at these points. Statistical comparison shows that RT provides an accurate RSS estimation in most points on the track.

Table 2-4: Mean and std. dev. of RSS from AP_1-AP_3

System B.W. [MHz]	RSS Measurement [dB]						RSS RT [dB]					
	AP1		AP2		AP3		AP1		AP2		AP3	
	Mean	Std.	Mean	Std.	Mean	Std.	Mean	Std.	Mean	Std.	Mean	Std.
500	-62.1	9.8	-58	11.4	-57.6	14.8	-61	7.9	-57.1	9.4	-59.6	13.7
25	-66.9	10.4	-63.4	12.4	-62.5	15.4	-66	8.3	-62.9	9.9	-64	14.6

Figure 2-23 shows that at ninety percent of the locations the difference between the estimated and actual RSS value is less than 7.5 dB and 9.5 dB for 500 MHz and 25 MHz systems respectively. In order to compare the results obtained using the original floor plan and the new results using the updated floor plan we compared the associated CDF for both cases in 500 MHz system in Figure 2-24. This figure shows that updating the floor plan has reduced the ninety percentile error of RSS estimation by 6.5 dB.

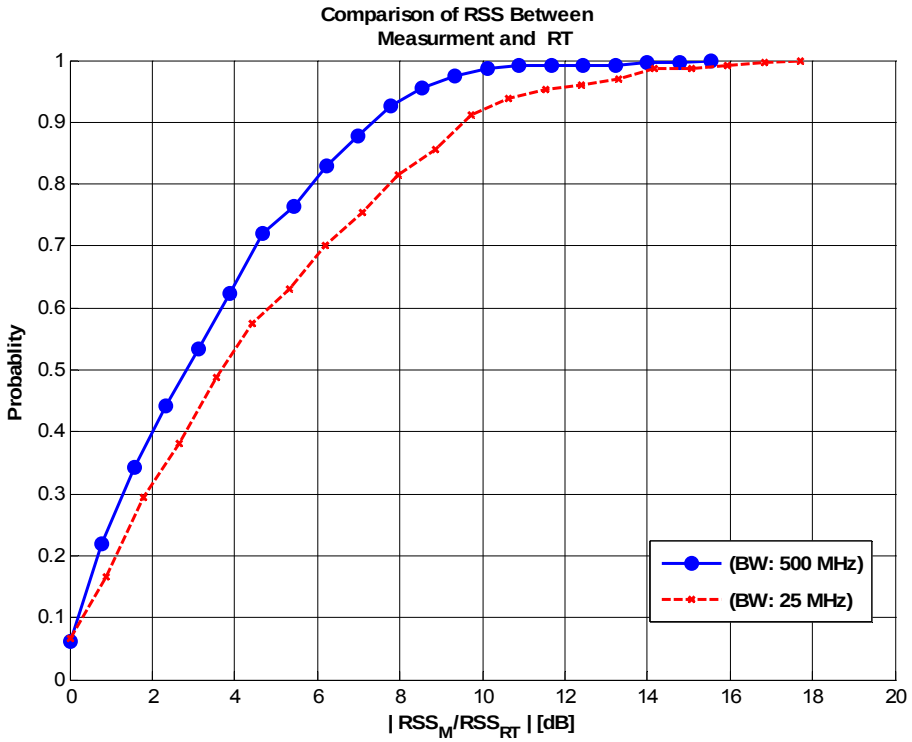

Figure 2-23: CDF of relative RSS (Measurement vs. RT)

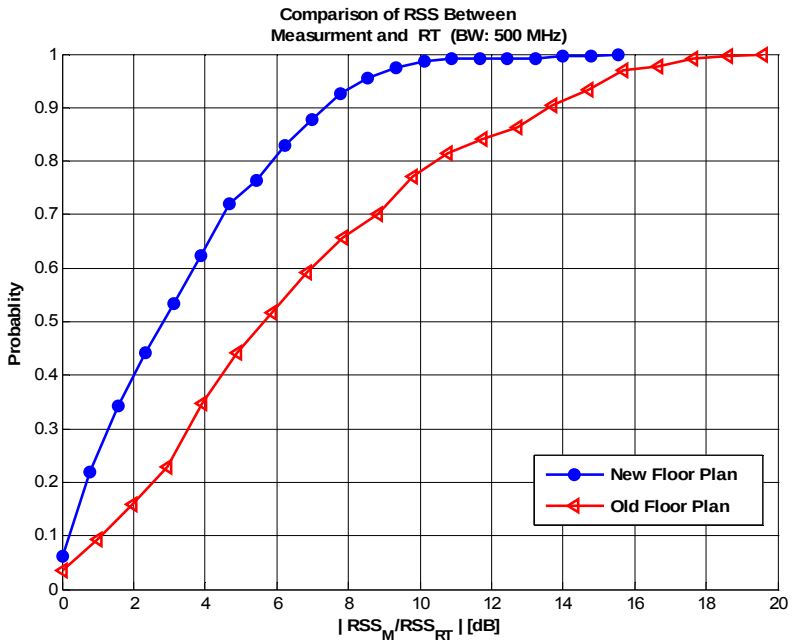

Figure 2-24: Comparison of RSS after the floor plan modifications

The performance of TOA based localization algorithms, are highly dependent on DME. We compared DME values based on RT simulation and measurement in both 500 MHz and 25 MHz systems in Figure 2-25(a-b) respectively. The quantitative values for DME statistics are summarized in Table 2-5. These results show that RT estimated DME values are more optimistic compared to the actual DME.

Table 2-5: Mean and std. dev. of DME

System B.W. [MHz]	DME Measurement [m]						DME RT [m]					
	AP1		AP2		AP3		AP1		AP2		AP3	
	Mean	Std.	Mean	Std.	Mean	Std.	Mean	Std.	Mean	Std.	Mean	Std.
500	2.5	1.2	2.3	1.6	2.6	2.3	1.7	2.2	1.5	1.4	0.9	1.2
25	10.1	7.4	9.2	6.6	10	9.5	4.5	5.2	4.4	3.8	2.8	3.2

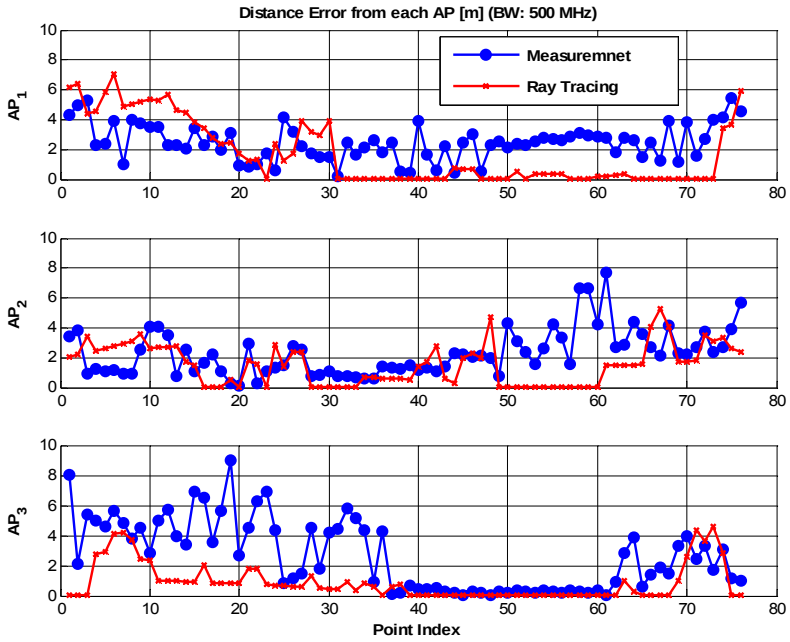

(a) BW: 500 MHz

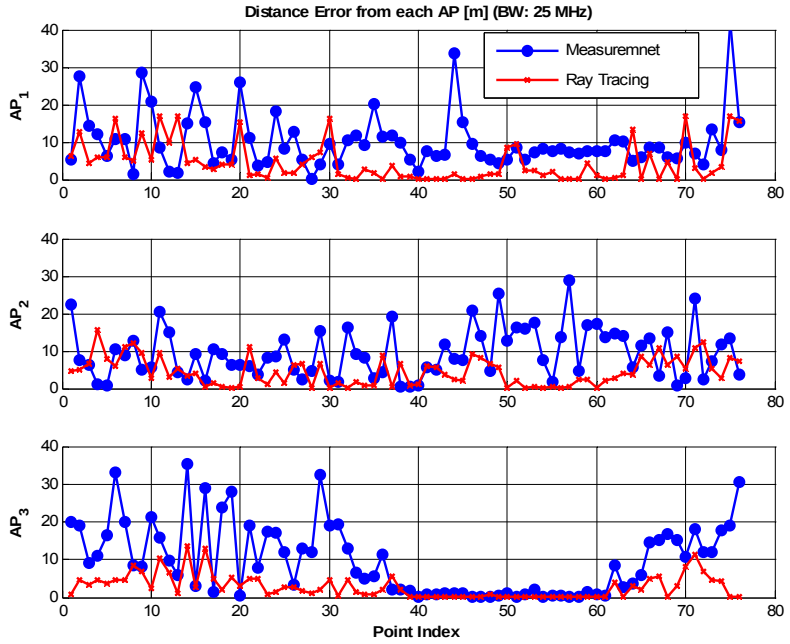

(b) BW: 25 MHz

Figure 2-25: DME (Measurement vs. RT)

The discrepancies between measurement and RT generated DME's are due to lack of detailed floor plan information especially in the middle part of the building. Another observation is that a 25 MHz system experiences much larger DME values compared to a 500 MHz system. Moreover, RT estimated TOA fits the actual TOA better in a wide band system. Figure 2-26 shows the statistical comparison between simulated and actual DME in both 25 MHz and 500 MHz systems. The difference between RT estimated DME and the actual measured DME is less than 4 meters in a 500 MHz system. This difference is increased to 16 meters in a 25 MHz system. TOA based localization systems are very sensitive to distance estimations and large DME values (DME > 2 m) cause large localization errors. In other words, Figure 2-26 shows that a 25 MHz system is not suitable for TOA based localization. RT provides a good approximation for the actual TOA measurements in a 500 MHz system and can be used for TOA based localization.

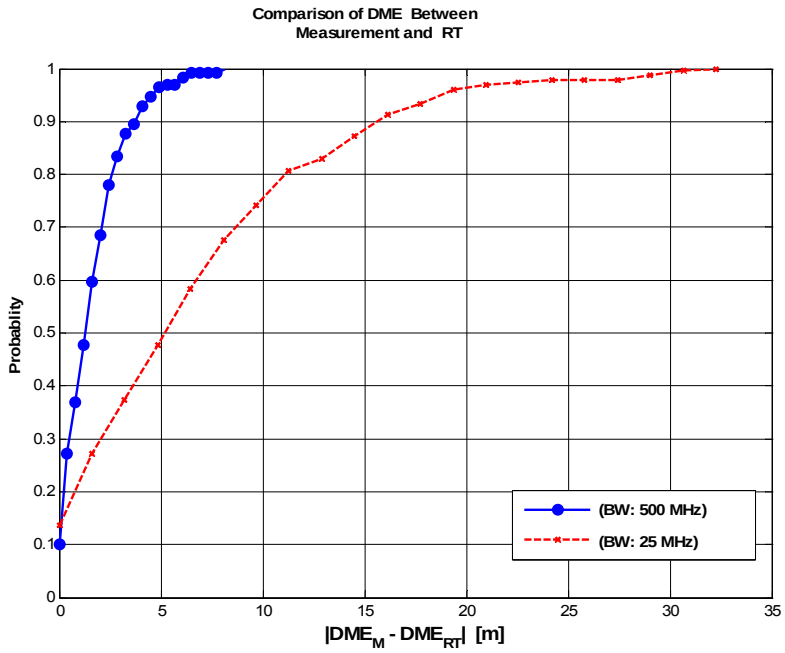

Figure 2-26: CDF of relative DME (Meas. vs. RT)

Chapter 3

Localization Systems and Algorithms

3.1. Introduction

In this chapter we provide an overview of the RSS and TOA based indoor localization techniques considered in this dissertation. These algorithms include a number of traditional algorithms already present in the literature as well as four new channel model assisted algorithms introduced in this dissertation. Indoor positioning systems can be classified by a set of properties such as sensing metric, localization algorithm, scalability, and other system parameters. This taxonomy can be used for characterization and performance evaluation of the positioning system [27,47]. In this dissertation our classification is based on localization algorithm and the sensing metric (RSS or TOA). In section 3.2 we classify the algorithms into distance based and pattern recognition based. Then we provide a detailed description of various RSS and TOA based localization algorithms in sections 3.3 and 3.4, respectively. In section 3.5, we introduce a new hybrid RSS-TOA algorithm which uses neural networks. Finally we conclude this chapter by providing a summary of major design and deployment issues related to localization algorithms in section 3.6.

3.2. Two Classes of Localization Algorithms

An indoor positioning system estimates the location of the MS by using some signal metrics from a number of AP's distributed in the area in a process called localization. We classify indoor localization techniques into *distance based* or *pattern recognition based* methods. A distance based localization algorithm determines the distances between MS and three or more reference points; which may or may not be colocated with the AP's; and locates MS through triangulation. In pattern recognition based algorithms, the localization system gets off line training to create a reference database of possible locations in an environment with an associated fingerprint at those locations. So far as metrics classification is concerned, in this dissertation we restrict our study to those algorithms using RSS, TOA, or a combination of RSS-TOA attribute of a signal. Therefore, as shown in Figure 3-1, we have six classes of algorithms. Distance based localization requires an accurate and reliable distance measurements from three or more reference locations. Since RSS systems can not provide a reliable distance estimate, most practical distance based indoor localization algorithms use TOA rather than RSS. Existing pattern recognition algorithms use on site measurements to create the required reference radio map, in this dissertation we introduce new algorithms by incorporating channel modeling techniques into the localization algorithm to replace the time consuming on site measurements.

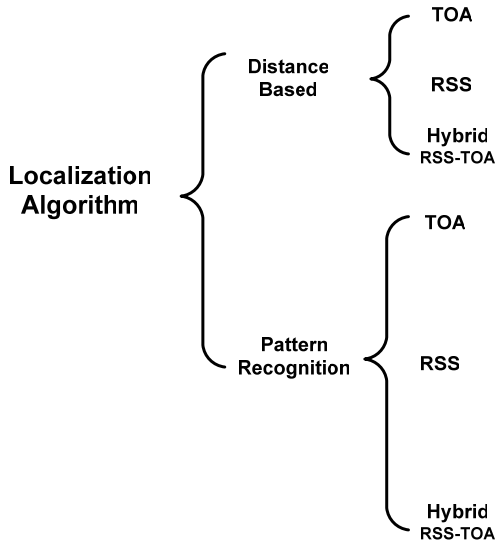

Figure 3-1: Classification of localization algorithms

3.2.1. Distance Based Localization

A distance based localization algorithm determines the distances between MS and each AP[1] and locates MS through triangulation. The distance can be estimated from the attenuation of signal strength based on path loss, *angle of arrival* (AOA), TOA, and *time difference of arrival* (TDOA) of a signal. Distance estimation using TOA, TDOA, and AOA has been studied extensively for outdoor positioning systems [48]. These techniques are suitable for NUDP conditions. However, they suffer from large errors in indoor environments with UDP conditions. Distance estimation via TOA and RSS in indoor environments is described in this section.

As mentioned in section 2.2 a radio channel impulse response between a transmitter and a receiver with infinite bandwidth is modeled as:

[1] In distance based algorithms we consider the location of the AP's as reference points.

$$\mathrm{h_d}(t) = \sum_{i=1}^{L} \beta_i^d \delta[t - \tau_i^d] \tag{3-1}$$

However, in a practical system with limited bandwidth W, the received signal $\mathrm{r}_d^W(t)$ is given by:

$$\mathrm{r}_d^W(t) = \int_{-\infty}^{+\infty} \mathrm{x}_W(\tau)\,\mathrm{h_d}(t-\tau)d\tau \tag{3-2}$$

where $\mathrm{x}_W(t)$ is the transmitted pulse. In a TOA based system the receiver estimates the distance between the transmitter and the receiver ($\hat{d}_W$) by extracting the first detected peak of the channel impulse response and applying (2-5). The error in distance estimation is quantified by DME defined as:

$$\varepsilon_{d,W} = \left|\hat{d}_W - d\right| \tag{3-3}$$

where d represents the actual distance between the transmitter and the receiver. TOA based distance estimation suffers from additive noise, and multipath effects. Extreme cases of multipath effect, causes UDP conditions, which can generate large range errors especially in systems with less bandwidth [49]. For short range measurements where DP exists DME is statistically modeled as Gaussian $\mathrm{N}(c\mu_T, c^2\sigma_T^2)$ where μ_T and σ_T^2 are the mean and variance of the TOA estimation error [50]. However, UDP cases generate large errors that do not follow a zero mean Gaussian distribution [51]. Distance estimation using TOA of a signal has been used in commercial products with good precisions under NUDP conditions in wideband systems. A typical localization algorithm which applies triangulation using distance estimation is least square TOA (LS-TOA) and is described in section 3.4.1.

In general, the relation between the average power in dB, RSS_d, and distance d is given by [34,52]:

$$RSS_d = P_t - 10\alpha \log_{10} d + X \tag{3-4}$$

in which α is the distance-power gradient, X is the shadow fading $\mathrm{N}(0,\sigma_X^2)$, and P_t is the transmitted power in dB. In open outdoor environments α is a constant value, and for a given RSS_d estimated distance follows a log-normal distribution given by [53]:

$$\mathrm{f_d}(d) = \frac{1}{\sqrt{2\pi} d\sigma} \exp\left(-\frac{\left(\ln(d) - \mu\right)^2}{2\sigma^2} \right) \tag{3-5}$$

where:

$$\mu = \frac{P_t - RSS_d}{10\alpha \log_{10}(e)} \; ; \; \sigma = \frac{\ln(10)}{10\alpha} \sigma_X \tag{3-6}$$

Figure 2-24 shows a scenario in which the MS is located in the coverage area of three access points (AP1-AP3) with the following assumptions:

- **Transmit power from each AP :** 0 dBm
- **Constant distance power gradient for AP1-AP3 (** $\alpha = 2$ **)**
- $L_0 = 30[dB]$
- $\sigma_x^2 = 10[dB]$

The actual location of the MS is the cross-section of the three circles.

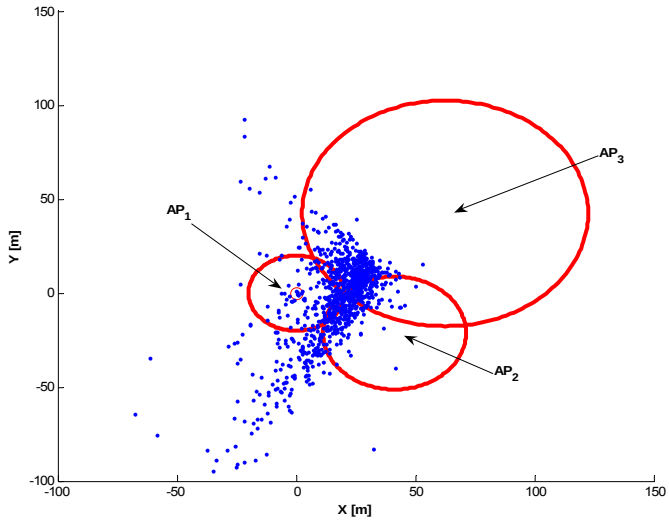

Figure 3-2: Distance based localization using RSS

The estimated location using triangulation by means of RSS based distance estimation is shown as blue dots in Figure 3-2. In spite of high RSS coverage from AP1-AP3 (Figure 3-3) we observe large localization errors due to large DME values.

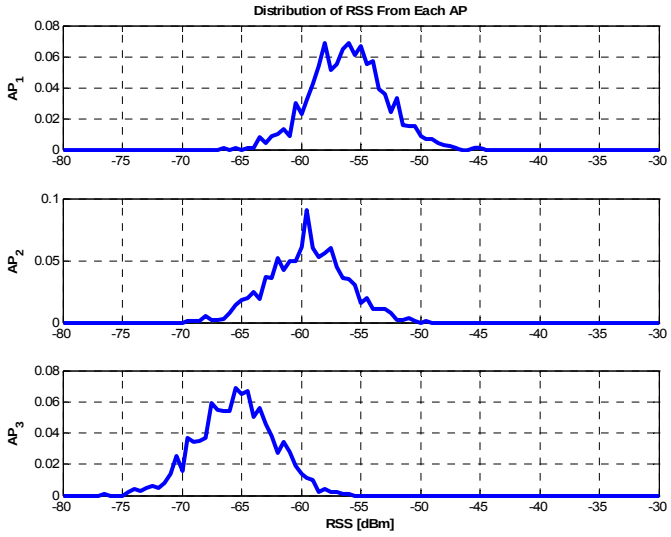

Figure 3-3: Distribution of RSS from each AP

The estimated distances from each AP along with the expected distribution obtained by (3-5) are shown in Figure 3-4. The statistics of DME from each AP is summarized in Table 3-1.

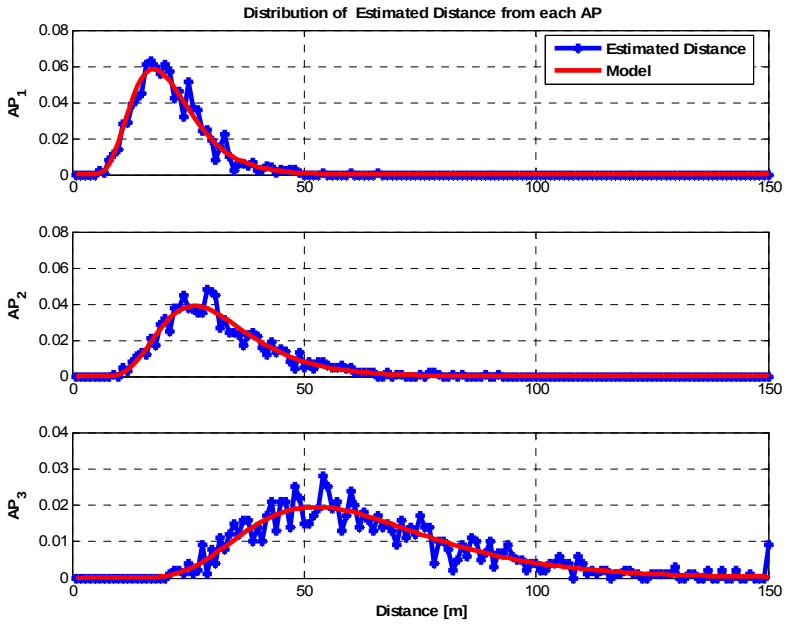

Figure 3-4: Distribution of estimated distance from each AP

Although the average DME is not a large number but the large variation in DME causes large localization errors.

Table 3-1: DME statistics in distance estimation using RSS

AP	Mean(DME) [m]	Std. dev.(DME) [m]
AP1	1.4	7.8
AP2	1.9	12.2
AP3	3.8	24.5

The complementary CDF of the localization error is depicted in Figure 3-5 which presents large errors. In summary (3-4) does not provide good distance estimation in indoor environment because, α changes in different buildings and directions. Moreover, shadow fading is a highly unpredictable component in indoor environment. Therefore, the estimated distance obtained from this equation in indoor environments is very unreliable and most practical distance based indoor localization algorithms use TOA rather than RSS. Example of location-sensing systems that use TOA or TDOA are GPS [27], the Active Bats [54], and the Cricket [55].

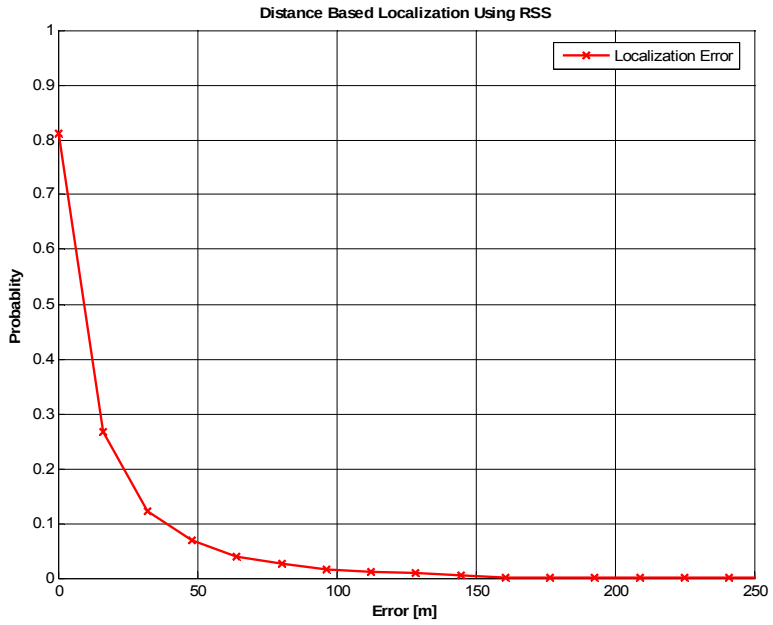

Figure 3-5: CCDF of localization error

3.2.2. Pattern Recognition Based Localization

In recent years, pattern recognition techniques have been used for indoor localization as an alternative to distance based algorithms since distance estimation in a multipath and scatter rich environment is a challenging problem. In pattern recognition based algorithms, the localization system gets off line training to create a reference database of possible locations in an environment with an associated fingerprint at those locations. We refer to this pregenerated database as reference *radio map*. During the localization period, the matching algorithm compares the characteristics of the observed signal with the existing fingerprints in the radio map and chooses the reference point that matches best with the observed data and declares that as the MS's current location. The block diagram of a pattern recognition based localization system is shown in Figure 3-6·

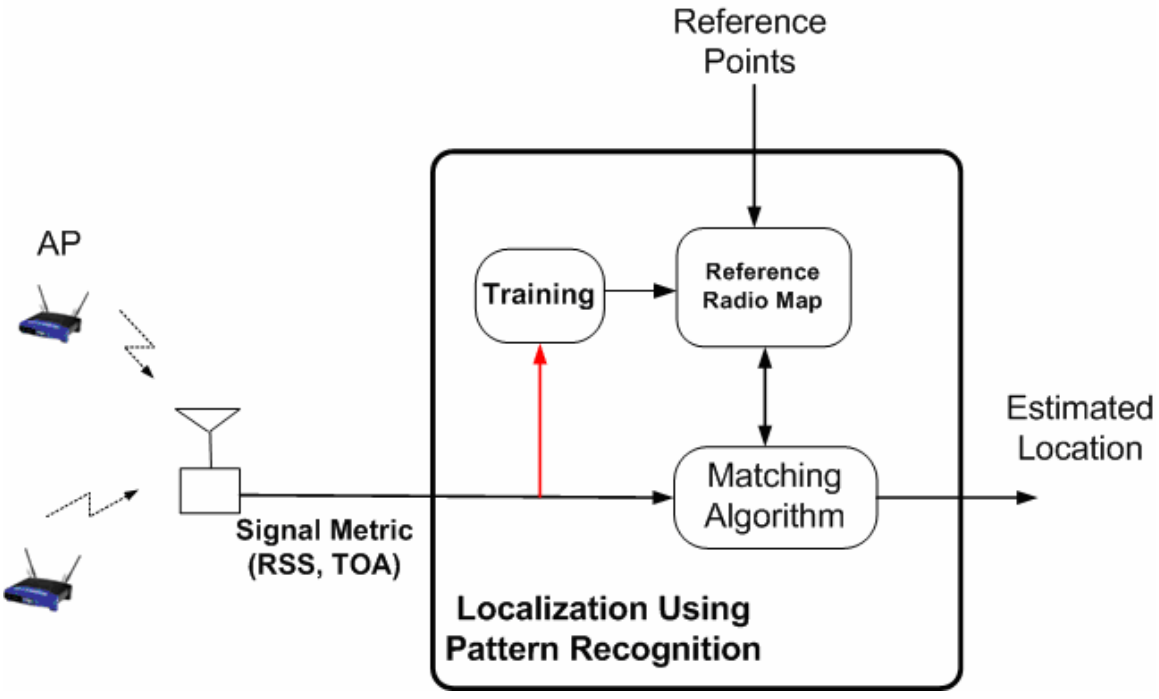

Figure 3-6: Localization using pattern recognition

Pattern recognition techniques generally use a non-geometric attribute feature at a reference location such as RSS or TOA of a signal. Pattern recognition techniques do not require the MS to be in the coverage area of at least three AP's to be able to determine its location. The main disadvantages of pattern recognition based algorithms are the complexity of the localization algorithm, and exhaustive amount of data collection required for the training. Existing pattern recognition algorithms, use extensive on site measurements to create the reference radio map. We introduce new localization algorithms by incorporating channel modeling techniques as part of the algorithm in sections 3.3 - 3.5. A generic block diagram for such an algorithm is shown in Figure 3-7. Using channel assisted localization algorithms, we not only reduce the deployment cost of the system, but also we can improve the performance of the localization algorithm by increasing the number of reference points in the radio map.

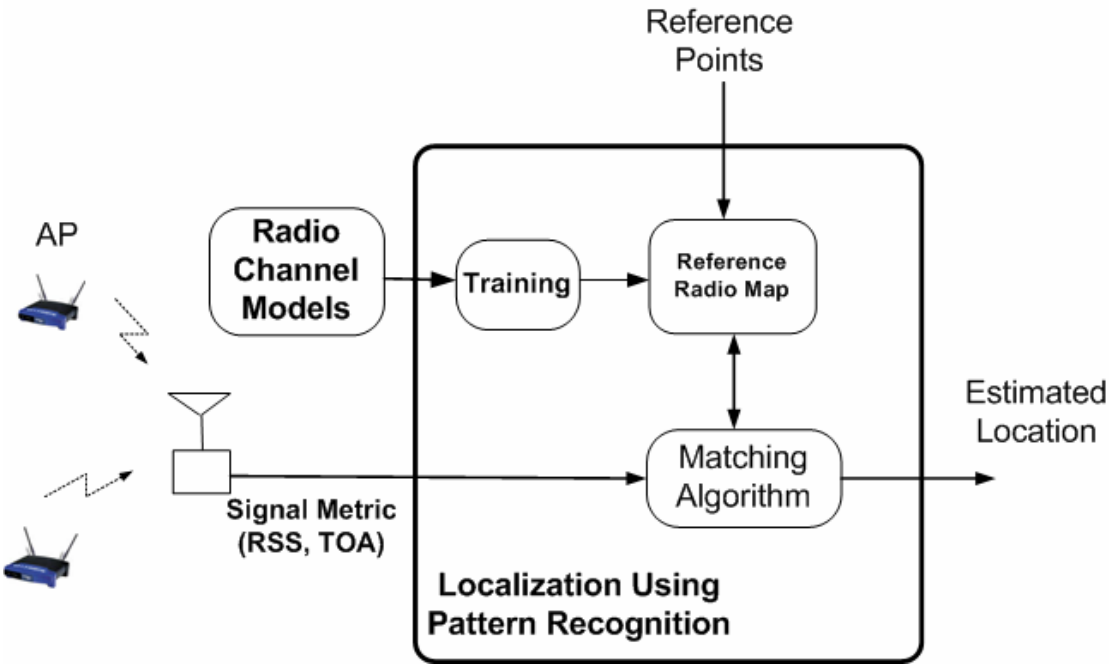

Figure 3-7: Application of channel models in pattern recognition localization

3.3. RSS Based Localization

RSS is a signal metric that most off the shelf wireless devices can measure. As an example the MAC layer of IEEE 802.11 WLAN provides RSS information from all active AP's in a quasi periodic beacon signal that can be used as a metric for positioning [16,22,56]. Since the total RSS value is the sum of signal strengths of each individual path in a multipath environment, RSS based localization algorithms take advantage of the existing multipath diversity in the channel. Furthermore, the timing requirement in RSS based techniques are less rigorous compared to TOA based algorithms, and the system is more tolerant in UDP cases. In open outdoor environments RSS decays linearly with log distance thus a MS can uniquely map an observed RSS value to a distance from a transmitter and consequently identify its location by using distances from three or more AP's. Unfortunately instantaneous RSS inside a building varies over time; even at a fixed location; this is caused largely by channel variations due to shadow fading and multipath fading. Consequently statistical approaches using pattern recognition algorithms to location estimation prevail. In this section we describe pattern recognition algorithms that use RSS metric for indoor localization.

Let (x, y) be the MS location to be determined, $\mathbf{O} = [P_1 \ P_2 \ \ldots \ P_m]$ is an observed RSS vector from $AP_1, AP_2, \ldots, AP_m$ located at $(x_1, y_1), (x_2, y_2), \ldots (x_m, y_m)$ respectively. Let $\mathbf{Z}(x, y) = [Z_1(x, y) \ Z_2(x, y) \ \ldots \ Z_m(x, y)]$ be the vector of expected RSS measurements at (x, y). The MS's location can be estimated as $(\hat{x}, \hat{y})$ where $\mathbf{Z}(\hat{x}, \hat{y})$ provides a good approximation of $\mathbf{O}(x, y) = [P_1 \ P_2 \ \ldots \ P_m]$. We define the error function as:

$$\varepsilon(x,y) = \left\|\mathbf{O}(x,y) - \mathbf{Z}(x,y)\right\|^2 = \sum_{i=1}^{m} (P_i - Z_i(x,y))^2 \tag{3-7}$$

The estimated location for $(\hat{x},\hat{y})$ must minimize (3-7). In other words:

$$\nabla\varepsilon(x,y) = \mathbf{0} \tag{3-8}$$

$$(\hat{x},\hat{y}) = \text{argmin}(\varepsilon(x,y)) \tag{3-9}$$

Applying (3-8) to (3-7) we obtain:

$$\sum_{i=1}^{m} (P_i - Z_i(x,y)) \frac{\partial Z_i(x,y)}{\partial x} = 0 \tag{3-10}$$

$$\sum_{i=1}^{m} (P_i - Z_i(x,y)) \frac{\partial Z_i(x,y)}{\partial y} = 0 \tag{3-11}$$

or in a matrix form:

$$\begin{bmatrix} P_1 - Z_1(x,y) \\ P_2 - Z_2(x,y) \\ . \\ P_m - Z_m(x,y) \end{bmatrix}^T \begin{bmatrix} \frac{\partial Z_1(x,y)}{\partial x} & \frac{\partial Z_1(x,y)}{\partial y} \\ \frac{\partial Z_2(x,y)}{\partial x} & \frac{\partial Z_2(x,y)}{\partial y} \\ . & . \\ \frac{\partial Z_m(x,y)}{\partial x} & \frac{\partial Z_m(x,y)}{\partial y} \end{bmatrix} = \mathbf{0} \tag{3-12}$$

Path loss models are often represented by a constant and a logarithmic component[2] [34 ,52]:

$$Z_i(x,y) = \beta_0 - \beta_1 \ln\left[(x - x_i)^2 + (y - y_i)^2\right] \tag{3-13}$$

where β_0, β_1 are some site specific constant values. Thus:

$$\begin{aligned} \frac{\partial Z_i(x,y)}{\partial x} &= \frac{-2\beta_1 (x - x_i)}{(x - x_i)^2 + (y - y_i)^2} \\ \frac{\partial Z_i(x,y)}{\partial y} &= \frac{-2\beta_1 (y - y_i)}{(x - x_i)^2 + (y - y_i)^2} \end{aligned} \tag{3-14}$$

[2] This is a simplified version of (3-4) if we do not consider the shadow fading effect.

Substituting (3-13) and (3-14) in (3-12) assuming $\beta_1 \neq 0$ we obtain:

$$\begin{bmatrix} P_1 - \beta_0 + \beta_1 \ln\left[(x-x_1)^2 + (y-y_1)^2\right] \\ P_2 - \beta_0 + \beta_1 \ln\left[(x-x_2)^2 + (y-y_2)^2\right] \\ . \\ P_m - \beta_0 + \beta_1 \ln\left[(x-x_m)^2 + (y-y_m)^2\right] \end{bmatrix}^T \cdot \begin{bmatrix} \frac{(x-x_1)}{(x-x_1)^2+(y-y_1)^2} & \frac{(y-y_1)}{(x-x_1)^2+(y-y_1)^2} \\ \frac{(x-x_2)}{(x-x_2)^2+(y-y_2)^2} & \frac{(y-y_2)}{(x-x_2)^2+(y-y_2)^2} \\ . & . \\ \frac{(x-x_m)}{(x-x_m)^2+(y-y_m)^2} & \frac{(y-y_m)}{(x-x_m)^2+(y-y_m)^2} \end{bmatrix} = \mathbf{0} \qquad (3\text{-}15)$$

Equation (3-15) represents a set of nonlinear over-determined equations. To find a numerical solution for the set of nonlinear equations most RSS based use pattern recognition localization by creating a priori conditional probability distribution of RSS vectors in an environment (radio map) during an offline training phase called fingerprinting [22,23,57]. A high resolution grid of reference points at known locations is selected. At each *k*-th reference point on the grid a reference fingerprint vector $Z(x_k, y_k) = [Z_{k1}\ Z_{k2}..Z_{km}]$ is collected. During the localization period MS uses a matching algorithm to map an observed RSS fingerprint vector to a physical location. In this algorithm the MS can determine its location without knowing the exact location of the access points.

3.3.1. Closest Neighbor (CN)

The basic algorithm in pattern recognition class is called the *closest neighbor* (CN) or *nearest-neighbor* (NN) [22]. In this algorithm MS compares an observed RSS vector with all available fingerprints in the reference radio map and finds a reference point with the smallest Euclidean distance in signal space and reports that as the current location of the device. Suppose that MS observes $\mathbf{O} = [P_1 \ P_2 \ \dots \ P_m]$. The Euclidean distance between this vector and the *k*-th reference point entry in the radio map $Z(x_k, y_k) = [Z_{k1} \ Z_{k2} .. Z_{km}]$ is given by:

$$D_k = \left(\sum_{i=1}^{m} (P_i - Z_{ki})^2 \right)^{1/2} \qquad (3\text{-}16)$$

The CN algorithm maps the location of MS to an entry on the radio map. Another variation of this algorithm finds the *M* closest reference points and estimate the location based on the average of the coordinates of these *M* points [57].

3.3.2. RT Assisted RSS Based Closest Neighbor (RT-RSS-CN)

Generally an RSS radio map is generated using on-site measurement in a process called training or fingerprinting. On site measurement is a time and labor consuming process in a large and dynamic indoor environment. In [26] we have introduced two alternative methods to generate a radio map without on site measurements. The RT-RSS-CN algorithm uses RT to generate the reference radio map. During localization MS applies the CN algorithm to the simulated radio map. In this way we can generate a very high

resolution radio map and obtain higher localization accuracy. In order to generate an accurate radio map in this technique the localization system requires knowing the location of the available access points.

3.3.3. Maximum Likelihood RSS Based Location Estimation

The performance of the CN localization algorithm depends on the grid resolution of the reference radio map. Using more reference points on the map provides higher localization accuracy. In order to achieve a fine resolution from a coarse location estimation based on a given radio map, [21,23] apply a machine learning technique to interpolate between several reference points on the map. The advantage of this approach compared to CN is that, in this method the estimated location is not restricted to existing reference points, thus the number of reference points can be reduced. This provides a trade off mechanism between the number of reference points and estimation accuracy.

Our objective is to estimate the location of the MS, given that $\hat{\mathbf{o}} = (\hat{P}_1, \hat{P}_2, .., \hat{P}_m)$ is the RSS vector received from m access points (AP_1-AP_m). The following section describes the training process used to create a likelihood function at each reference point on the radio map through either a measurement campaign or channel simulation.

Given a set of n distinct reference locations $L = \{l_1, l_2, ...l_n\}$; $l_i = (x_i, y_i); i \in \{1, 2, ...n\}$; in area $\mathbf{A}$ and k observations at each location where:

$$\mathbf{O} = \{\mathbf{O}_1, \mathbf{O}_2, ..., \mathbf{O}_n\} \quad (3\text{-}17)$$

$$\mathbf{O}_i = \{\mathbf{o}_{i1}, \mathbf{o}_{i2}, ..., \mathbf{o}_{ik}\};\ i \in \{1, 2, ..., n\} \quad (3\text{-}18)$$

$$\mathbf{o}_{ij} = (P_{ij1}, P_{ij2}, .., P_{ijm}) \tag{3-19}$$

$\mathbf{O}_i$: A set of k observation at reference location $l_i = (x_i, y_i)$
$\mathbf{o}_{ij}$: RSS values from m access points (AP_1-AP_m)
P_{ijt} : j-th RSS observation from AP_t at reference location $l_i = (x_i, y_i)$
m : Number of access points

We denote the probability of observing $\mathbf{o} = (P_1, P_2, .., P_m)$; as $p(\mathbf{o})$ and the prior probability of being at location $l = (x, y)$, $p(l)$ respectively. We obtain the posterior distribution of the location by applying Bayes rule:

$$f_1(l \mid \mathbf{o}) = \frac{f_o(\mathbf{o} \mid l).p(l)}{p(\mathbf{o})} = \frac{f_o(\mathbf{o} \mid l).p(l)}{\sum_{l' \in L} p(\mathbf{o} \mid l')\, p(l')} \tag{3-20}$$

where $f_1(l \mid \mathbf{o})$ and $f_{\mathbf{o}}(\mathbf{o} \mid l)$ are conditional probability distribution functions of being at location $l = (x, y)$ given the observation $\mathbf{o} = (P_1, P_2, .., P_m)$, and the probability distribution function of observing $\mathbf{o}$ given location $l = (x, y)$, respectively. Generally, the prior probability density function of $p(l)$ is a mechanism to incorporate previous tracking information to this system. Here for simplicity we assume that $l = (x, y)$ follows a uniform distribution, and $p(\mathbf{o})$ does not depend on location l so it can be considered as a normalization factor. Application of these assumptions reduces (3-20) to (3-21), where η is a constant normalization factor.

$$f_1(l \mid \mathbf{o}) = \frac{f_o(\mathbf{o} \mid l).p(l)}{p(\mathbf{o})} = \eta.f_o(\mathbf{o} \mid l) \tag{3-21}$$

The term $f_{\mathbf{o}}(\mathbf{o} \mid l)$ is called the likelihood function, which in discrete domain gives the probability of observing a profile $\mathbf{o} = (P_1, P_2, .., P_m)$ at a given location $l = (x, y)$.

Equation (3-21) shows that estimation of the likelihood function $\mathrm{f}_{\mathbf{o}}(\mathbf{o}\,|\,l)$ leads to finding $\mathrm{f}_{\mathrm{l}}(l\,|\,\mathbf{o})$. The posterior distribution function $\mathrm{f}_{\mathrm{l}}(l\,|\,\mathbf{o})$ can be used to find the optimum location estimator based on any desired loss function. In particular, using expected value of the location minimizes the mean squared error and (3-22) shows this estimation:

$$\mathrm{E}\left[l\,|\,\mathbf{o}\right]=\eta.\sum_{l'\in L} l'\ .\mathrm{f}_{\mathrm{o}}(\mathbf{o}\,|\,l') \tag{3-22}$$

Here we use a Gaussian kernel function to model the likelihood function $\mathrm{f}_{\mathbf{o}}(\mathbf{o}\,|\,l)$. Suppose we have k observations at point $l=(x,y)$. Equation (3-23) defines one prospective likelihood function:

$$\mathrm{f}_{\mathbf{o}}(\mathbf{o}\,|\,l)=\frac{1}{k}\sum_{i=1}^{k}\mathrm{K}(\mathbf{o},\mathbf{o}_i) \tag{3-23}$$

$\mathbf{o}=(P_1,P_2,..,P_m)$ and $\mathbf{o}_i=(P_{i1},P_{i2},...,P_{im})$

where $\mathrm{K}(\mathbf{o},\mathbf{o}_i)$ denotes the kernel function. We assume that RSS P_t from access point t is a Gaussian random variable $\mathrm{N}(\mu=P_t,\sigma^2)$; where σ^2 is an adjustable parameter. If we assume that the consecutive values of P_t are independent, we can use a Gaussian kernel function and obtain:

$$\mathrm{K}_{\mathrm{Gauss}}(P_1,...P_m\,,P_{i1},...,P_{im})=\frac{e^{-\frac{1}{2\sigma^2}\sum_{r=1}^{m}(P_r-P_{ri})^2}}{\left(\sqrt{2\pi}\sigma\right)^m} \tag{3-24}$$

Combining (3-23), and (3-24) we conclude:

$$\mathrm{f}_{\mathrm{p_1..p_m}}(P_1,..,P_m\,|\,l)=\frac{1}{k(\sqrt{2\pi}\sigma)^m}\sum_{i=1}^{k}e^{-\frac{1}{2\sigma^2}\sum_{r=1}^{m}(P_r-\mathrm{P}_{ri})^2} \tag{3-25}$$

This is the likelihood function of observing $\mathbf{o} = (P_1, P_2, .., P_m)$ at location $l = (x, y)$. We generate these likelihood functions at each reference point on the radio map during the offline training phase. In order to find the location of the MS when it observes the RSS vector $\hat{\mathbf{o}} = (\hat{P}_1, \hat{P}_2, .., \hat{P}_m)$, we apply this observation to (3-21) and (3-22) at each reference point on the map to find the expected value of the location.

3.3.4. RT Assisted RSS Based Maximum Likelihood (RT-MAX-RSS)

In this algorithm we use RT channel simulations to create the required likelihood functions $\mathrm{f}_o(\mathbf{o} \mid l)$ in (3-22) at each reference point. RT simulated RSS values are applied in (3-23) to obtain the likelihood function $\mathrm{f}_o(\mathbf{o} \mid l)$. The variance σ^2 in the Kernel function is an adjustable parameter which can be tuned based on the environment. In the rest of this dissertation we refer to this algorithm as RT-MAX-RSS algorithm.

3.4. TOA Based Localization

There are two shortcomings with current RSS based localization techniques. The first limitation is caused by the fact that RSS based systems do not use the physical characteristics of the signal directly and rely on an environment dependent radio map which needs to be generated and calibrated for each and every building, thus RSS based algorithms are restricted to a campus or inside a building area, and do not scale well for large service areas. The second shortcoming of RSS based algorithms is low accuracy. In mission critical applications such as public safety, patient tracking, *etc*. the positioning system must be able to find the location with an estimation error of less than 1-5 meters

in indoor areas. In order to achieve such a high accuracy the localization algorithm must rely on other signal metrics such as TOA of a signal. In this section we describe TOA based localization techniques that can be used for indoor geolocation applications.

3.4.1. Least Square TOA (LS-TOA)

Let (X_M, Y_M) be the location of MS to be determined, r_1, r_2, and r_3 are estimated distances between MS and AP_1, AP_2, AP_3 which are located at $(x_1, y_1), (x_2, y_2)$, and (x_3, y_3) respectively. We can find by solving the following set of equations:

$$(X_M - x_1)^2 + (Y_M - y_1)^2 = r_1^2 \quad (3\text{-}26)$$

$$(X_M - x_2)^2 + (Y_M - y_2)^2 = r_2^2 \quad (3\text{-}27)$$

$$(X_M - x_3)^2 + (Y_M - y_3)^2 = r_3^2 \quad (3\text{-}28)$$

In an ideal system if these circles overlap, all three equations will be satisfied. In other words we can select any two of theses equations, find two candidate solutions for (X_M, Y_M). One of the candidate solutions will satisfy the third equation and that corresponds to the location of MS. However, in a more realistic scenario these circles may not overlap or they may not overlap at the same location. Thus, none of the candidate solutions will satisfy the third equation. Furthermore, the number of AP's might be more than three (Figure 3-8). Thus we need to combine all these equations in order to find an optimal solution. For a set of *n* AP's this problem can be described by:

$$X = \begin{bmatrix} X_M \\ Y_M \end{bmatrix} \quad ; \quad HX = b \quad (3\text{-}29)$$

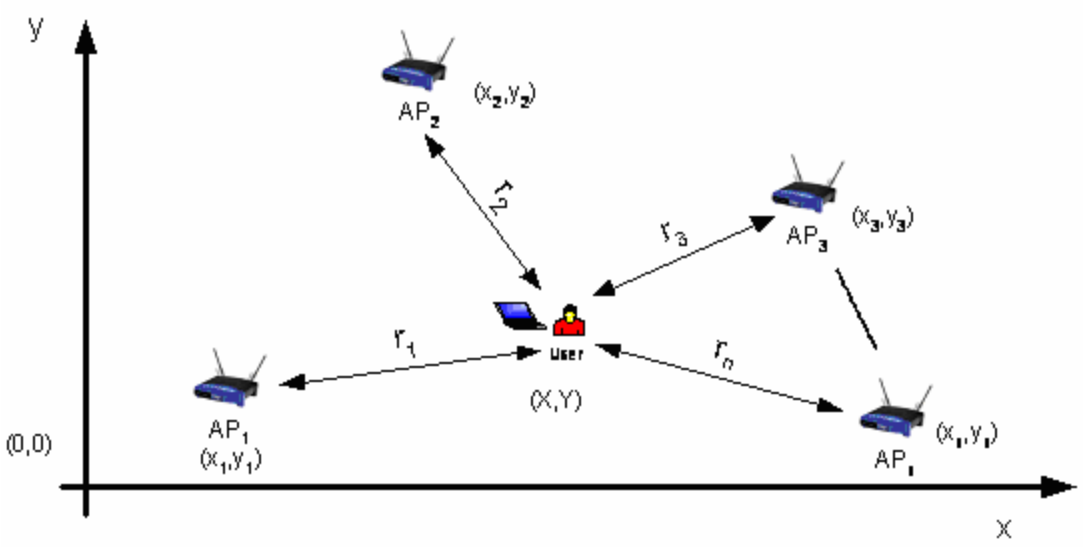

Figure 3-8: Typical TOA based localization scenario

where:

$$H = \begin{bmatrix} x_2 - x_1 & y_2 - y_1 \\ x_3 - x_1 & y_3 - y_1 \\ . & . \\ x_n - x_1 & y_n - y_1 \end{bmatrix} \; ; \; K_i^2 = x_i^{\,2} + y_i^{\,2} \tag{3-30}$$

$$b = \frac{1}{2}\left(\begin{bmatrix} K_2^2 - r_2^2 + r_1^2 \\ K_3^2 - r_3^2 + r_1^2 \\ . \\ K_n^2 - r_n^2 + r_1^2 \end{bmatrix} - \begin{bmatrix} x_1^2 + y_1^2 \\ . \\ . \\ x_1^2 + y_1^2 \end{bmatrix} \right) \tag{3-31}$$

The least square solution for this over-determined set of equations can be derived as [58]:

$$\hat{X} = \begin{bmatrix} \hat{X}_m \\ \hat{Y}_m \end{bmatrix} = \left(H^T H \right)^{-1} H^T b \tag{3-32}$$

where H and b are $(m\text{-}1) \times (m\text{-}1)$ and $(m\text{-}1) \times 1$ constant matrices. Various techniques for finding numerical solutions for (3-29) have been used in the literature [59,60]. All the

algorithms in this class are challenged by UDP channel conditions in a multipath and scatter rich indoor environment [61].

3.4.2. Closest-Neighbor with TOA Grid (CN-TOAG)

The performance of LS-TOA algorithm is very sensitive to UDP conditions [30]. Reference [28] introduces a TOA based pattern recognition localization technique; Closest-Neighbor with TOA Grid (CN-TOAG) Algorithm; where the observed distance measurement vector is compared to vectors of expected distances in the radio map that characterize a given indoor area. Associated with each point in radio map is a vector of distances from each AP. This vector is known as the *range signature*. The CN-TOAG algorithm compares the vector of observed distance measurements to the range signature at each point, and selects the point with the minimum Euclidean distance as the location estimate. The range signature associated with each point is exact, since it is based on straightforward geometrical calculations. In this way the localization system does a database search rather than a complex operation to solve (3-29). The second advantage of this technique is that it makes the estimation error a bounded value. Application of equation (3-32) for an indoor environment, with UDP conditions can generate very large errors but CN-TOAG estimated location must be a reference point within the radio map. It must be noted that the estimation accuracy of the CN-TOAG algorithm; like most pattern recognition based localization algorithms; depends on the granularity of the radio map, which is determined by the spacing between the reference points.

3.4.3. RT Assisted TOA Based Closest Neighbor (RT-TOA-CN)

CN-TOAG [28] algorithm uses a deterministic TOA radio map which consists of vectors of expected distances from multiple access points, and characterizes a given indoor area. During localization an observed distance measurement vector is compared to vectors of expected distances in the radio map and the reference point with the minimum Euclidean distance is reported as the location estimate. This technique like other TOA based algorithms is sensitive to the occurrence of UDP conditions as well as system bandwidth. The performance of CN-TOAG can be improved by incorporating site specific TOA estimation at each reference point on the radio map rather than an expected deterministic value. This can be accomplished by a fingerprinting process either through an on site measurement or a wideband channel modeling tool such as RT. In RT-TOA-CN algorithm we use RT to generate the reference radio map. During localization MS applies the CN algorithm to the simulated radio map to estimate the location. By using a high resolution radio map, we obtain higher localization accuracy.

3.5. Hybrid RSS-TOA Based Localization

As we discussed in previous sections, RSS based localization techniques are less sensitive to multipath, UDP conditions, and system bandwidth [30]. TOA based localization algorithms on the other hand are more accurate at NUDP points provided that we use a wideband receiver (BW > 200 MHz). The complementary behavior of TOA and RSS based localization techniques creates a motivation to develop a hybrid RSS-TOA algorithm. We use neural networks for this hybrid algorithm because it provides a

flexible learning and modeling capability which are the essential requirements for solving a nonlinear and complex pattern recognition indoor localization problem.

In this section we explain the general architecture of the neural network that can be used as a hybrid RSS-TOA pattern recognition algorithm.

3.5.1. Hybrid RSS-TOA Based Using Neural Networks (RT-HYB-NN)

Neural networks are composed of simple interconnected elements (*Neurons*) operating in parallel. The overall function of the network is largely determined by the connection of neurons. A neural network can be trained to perform a complex pattern recognition function by adjusting the connection between neurons [62]. In most application a neural network is trained so that a particular input generates a predefined target output. For example the neural network in Figure 3-9 is adjusted based on a comparison of the output and the target signal. In a practical system many pairs of input target values are used in this *supervised learning* process to train this network. A brief introduction to neural networks is presented in appendix B.

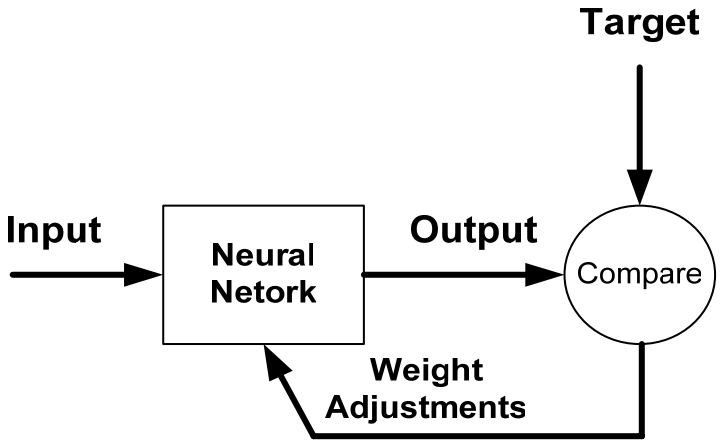

Figure 3-9: Supervised learning in a neural network

A trained neural network can be viewed as a black box processing unit which estimate the location of MS based on the current RSS and TOA observations. A neural network does not require any environmental information such as location of the transmitters or the geometry of the environment. RSS based pattern recognition localization algorithms using neural networks have been used in WLAN systems [63-65]. The accuracy and the precision performance of neural networks was reported to be slightly better than nearest neighbor algorithm [66].

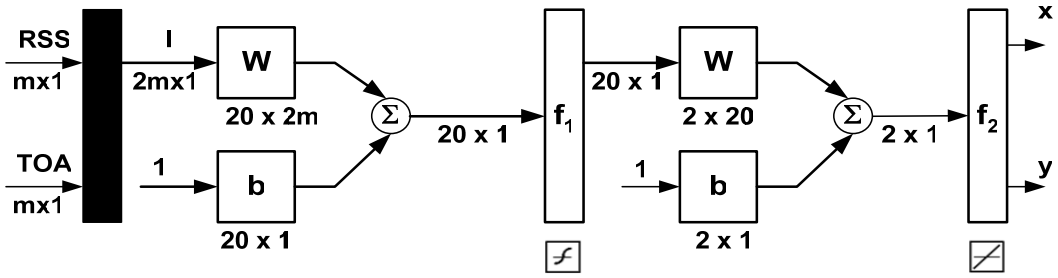

Figure 3-10: Neural network architecture for hybrid RSS-TOA based localization

We use a multilayer-perceptron (MLP) neural network (Figure 3-10) developed through supervised learning, as an underlying engine for a hybrid RSS-TOA based localization algorithm. Two sets of input lines are assigned to RSS and TOA measurements from AP_1-AP_m in this neural network. The output (x, y) is the current location of MS. It has been shown that a MLP with a single hidden layer is sufficient to approximate any continuous function to some desired accuracy provided that we use sufficient number of neurons [67]. The performance function of such a network has the form of a sum of squares:

$$\mathrm{E}(w) = \frac{1}{2}\sum_{i=1}^{N}(T_i - \mathrm{O}_i(w))^2 \qquad (3\text{-}33)$$

Where T_i and $O_i(w)$ are the target and current output values for pattern i as a function of the network weights w and N is the number of training points. We use *tan-sigmoid* defined by (3-34) and the identity function as transfer functions for the hidden layer and the output layer respectively.

$$\text{tansig}(x) = \frac{2}{1+e^{-2x}} - 1 \qquad (3\text{-}34)$$

This neural network is trained with RT generated radio map using *Levenberg-Marquardt* algorithm [68].

3.6. Summary

For a successful deployment of a positioning system, a designer needs to determine the suitable localization algorithm based on the following interrelated system parameters: (Figure 3-11)

- **Application and environment:** The application and environment where the system needs to be deployed in, determines the required accuracy and coverage area.
- **System bandwidth**: This is usually dictated by the available access network infrastructure and has a large impact on TOA based localization algorithms and system performance.

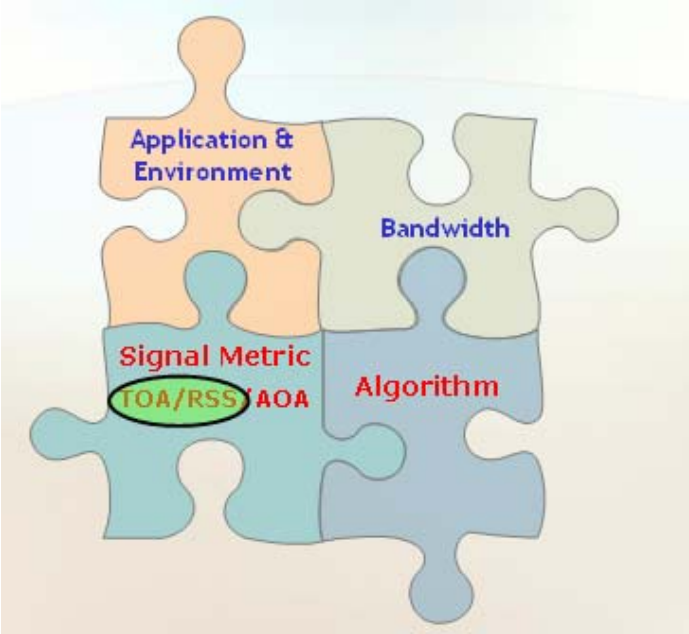

Figure 3-11: Positioning system design considerations

- **Signal Metric**: The attribute of the signal which is used for localization. RSS and TOA are the two signal metrics that have been used in this dissertation. The advantages and disadvantages of each metric are listed in Table 3-2.
- **Localization algorithm**: Using more complex algorithms results in a more accurate system. In other words localization algorithm can be used as a trade off mechanism between system complexity and localization accuracy.

Figure 3-12 summarizes all localization algorithms used in this dissertation with the newly introduced algorithms in red boxes. We compare the performance and bandwidth requirement of each algorithm in scenario I and scenario II in Chapter 4.

Table 3-2: Comparison of RSS and TOA as localization metric

Signal Metric	Advantages	Disadvantages
TOA	• Accurate at NUDP conditions • No need for exhaustive training • Good scalability	• More bandwidth requirement • Complex hardware • Very sensitive to bandwidth and UDP conditions • Complex timing requirements
RSS	• Simple hardware • No need for complex timing • More resilient to UDP conditions • Less sensitive to system bandwidth	• Not as accurate as TOA based localization at NUDP conditions • Long training procedure • Complex algorithms • Does not scale easily to large areas

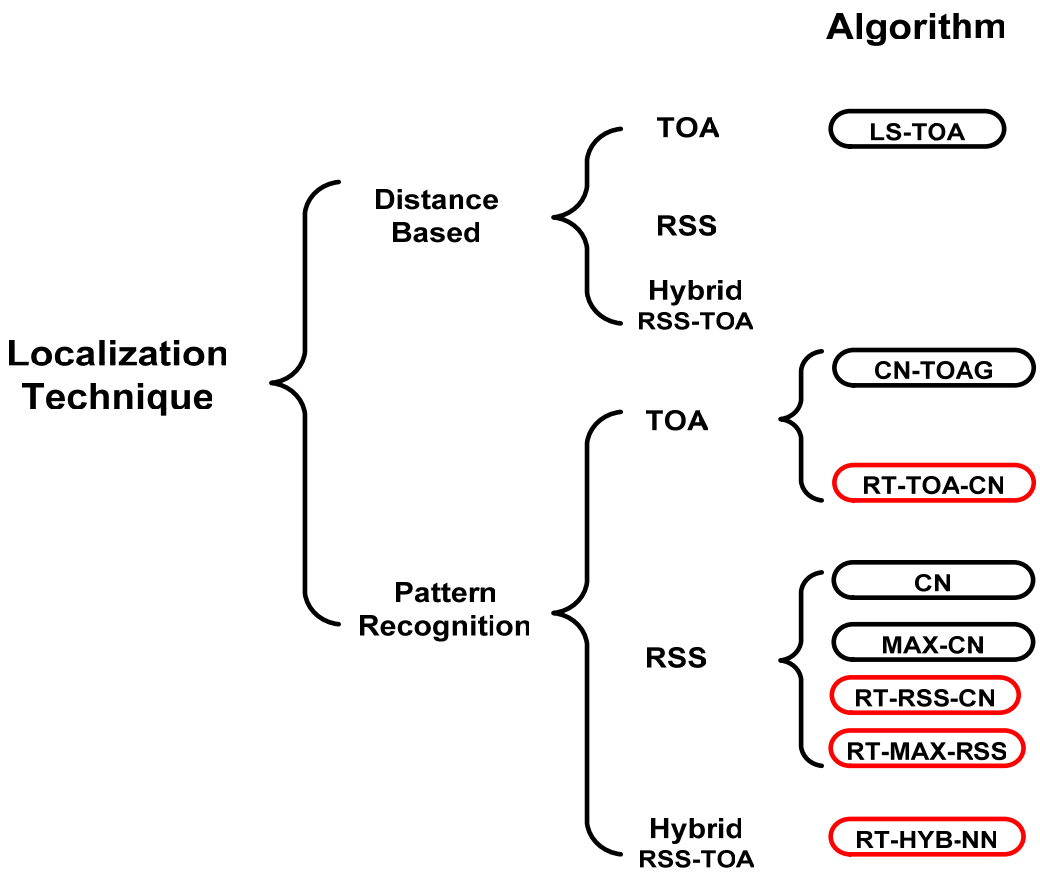

Figure 3-12: Localization algorithms used in this dissertation

Chapter 4

Performance Comparison of Localization Algorithms

4.1. Introduction

In this chapter we compare the performance of various TOA and RSS based algorithms introduced in Chapter 3 using scenario I and scenario II described in chapter 2. Section 4.2 investigates the potential use of RT and IEEE 802.11 recommended channel model as alternatives for on site measurements in traditional RSS-based WiFi indoor positioning systems. In particular we compare the performance of our channel model assisted algorithms with the performance of the Ekahua™ commercial indoor positioning product [69] in scenario I in the first floor of Atwater Kent Laboratory. Section 4.3 compares the performance of LS-TOA, CN-TOAG, RT-RSS-CN, and RT-MAX-RSS., localization algorithms using systems with bandwidths of 25 MHz and 500 MHz in scenario II at the third floor of the Atwater Kent Laboratory. In this section we use RT for both training of the algorithms and generation of channel profiles used for performance evaluation. Section 4.4 uses UWB measurements for performance evaluation of LS-TOA, CN-TOAG, RT-TOA-CN, and RT-RSS-CN in scenario II. We conclude this chapter in

section 4.5 by describing an RT trained neural network architecture adopted for hybrid RSS-TOA based localization. In this section we also compare the performance of this algorithm with LS-TOA, CN-TOAG, RT-TOA-CN, RT-RSS, and CN in both 25 MHz and 500 MHz systems in scenario II. Table 4-1 summarizes all the algorithms that we use in this chapter and highlights the newly introduced algorithms in bold and red.

Table 4-1: Classification of localization algorithms

Scenario	Localization Algorithm			
	Distance Based	Pattern Matching		
	TOA	TOA	RSS	Hybrid
I : (WLAN) (BW: 26 MHz)			CN Max-RSS **RT-RSS-CN** **RT-Max-RSS** **IEEE-RSS-CN**	
II: (WPAN, UWB) (BW: 25 + 500 MHZ)	LS-TOA	CN-TOAG **RT-TOA-CN**	**RT-RSS-CN** **RT-Max-RSS**	**RT-Hybrid-NN**

4.2. Channel Modeling as an Alternative for Measurement in Scenario I

In section 2.4.1.2 we compared the accuracy of RT and IEEE 802.11 recommended channel models in RSS estimation. Here we use the same testbed (Figure 4-1) with the following objectives:

1. Study the possibility of using channel simulated results as alternative to on site measurements for RSS based indoor localization using two typical RSS based

algorithms and compare the results with a commercial RSS based localization system trained by on site measurements.

2. Find the average localization error as a function of radio map resolution in a typical RSS based localization system.

Major components of this testbed are shown in Figure 4-2. Three reference radio maps are generated by on site measurement, RT, and IEEE 802.11 recommended channel model. We have considered nearest neighbor[1] and maximum likelihood RSS based localization as typical localization algorithms. Ekahau™ [69] is a commercial RSS based indoor positioning system which uses WiFi technologies. We used Ekahau positioning engine trained with on site measurements to create a baseline for performance comparison. RSS observation from AP1-AP7 at different locations are simultaneously fed to the localization algorithms and two instances of Ekahau positioning engine; trained at 4 and 13 reference points respectively. The estimated location reported by the system and Ekahau positioning engines are compared with the actual location of the MS.

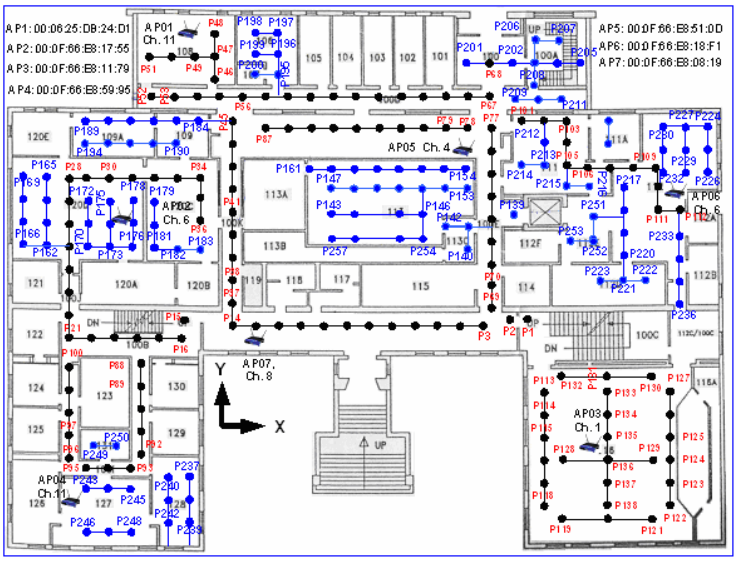

Figure 4-1: First floor of Atwater Kent lab (AWK1- Scenario I)

[1] We use the term nearest neighbor and closest neighbor interchangeably.

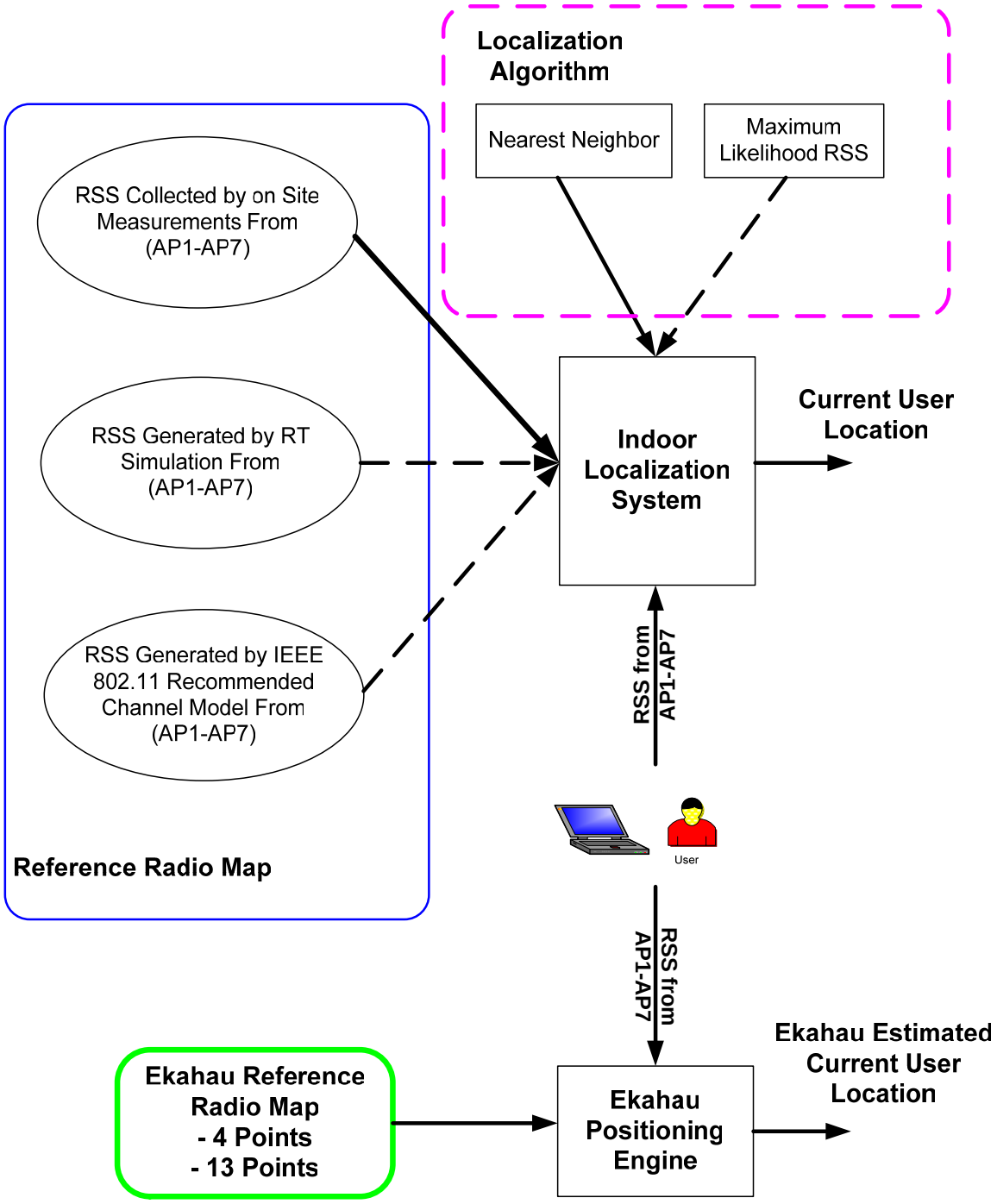

Figure 4-2: Major components of the testbed for scenario I

4.2.1. Results and Discussions

The most important performance metric in a positioning system is the localization error which depends on the resolution of the reference radio map. The performance of a typical localization algorithm can be improved by using a finer grid of reference points. Figure 4-3 shows the impact of the number of reference points on the distribution of the localization accuracy in a system using nearest neighbor localization algorithm. Increasing the number of reference points from 4 to 250 reduces the ninety percentile of the localization error from 20 meters to 5 meters.

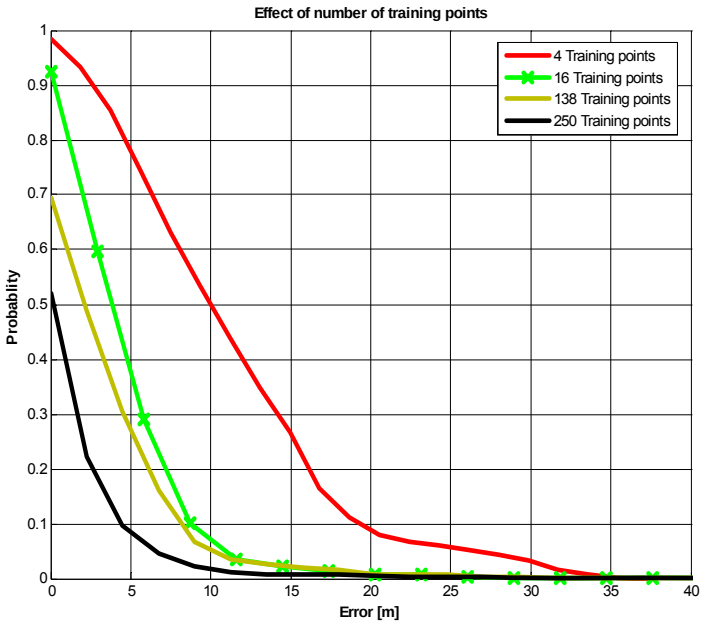

Figure 4-3: Impact of number of reference points on localization error using CN algorithm

Although we can increase the number of reference points to achieve any desired accuracy for scientific empirical performance comparisons, in real-world situations this approach is impractical. Creating and maintaining a high resolution reference radio map using on

site measurements is a challenging process in a dynamic WLAN environment. In other words, for practical applications the optimal obtainable accuracy is often not the most important goal, but the issue is how easy it is to obtain a practically applicable accuracy. Here we explore the feasibility of radio channel modeling techniques to answer this question by demonstrating the average error as a function of the reference grid resolution. We used nearest neighbor and maximum likelihood localization algorithm as two typical RSS based localization algorithms. We applied both algorithms to three different radio maps generated by means of on site measurement, ray tracing, and IEEE 802.11 recommended channel model with different number of reference points.

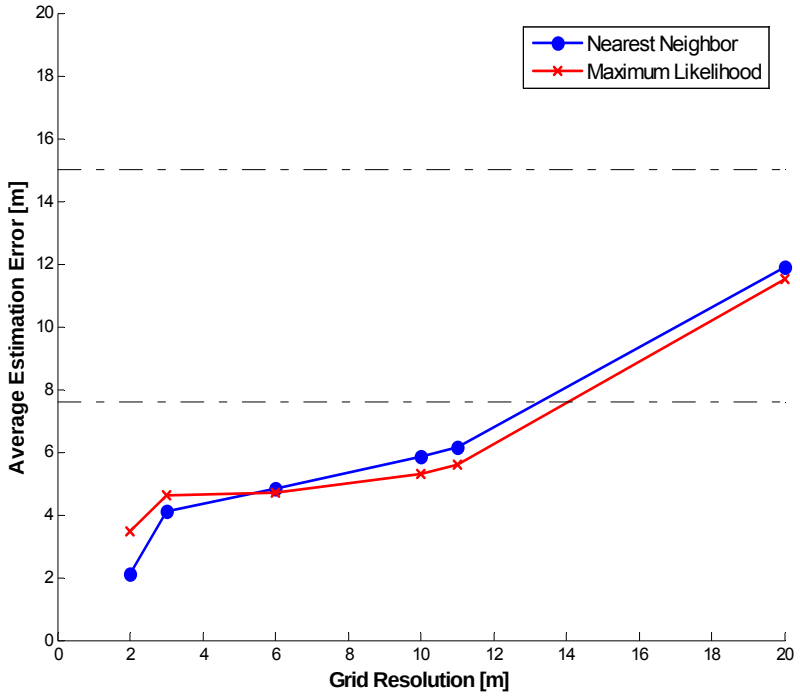

Figure 4-4: Average localization error for a system trained with on site measurement

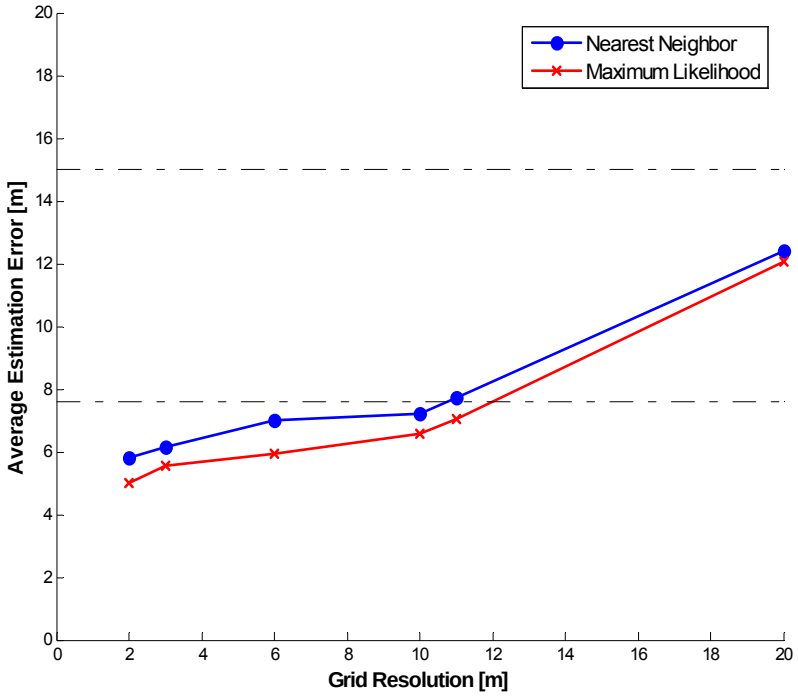

Figure 4-5: Average localization error for a system trained with RT channel simulation

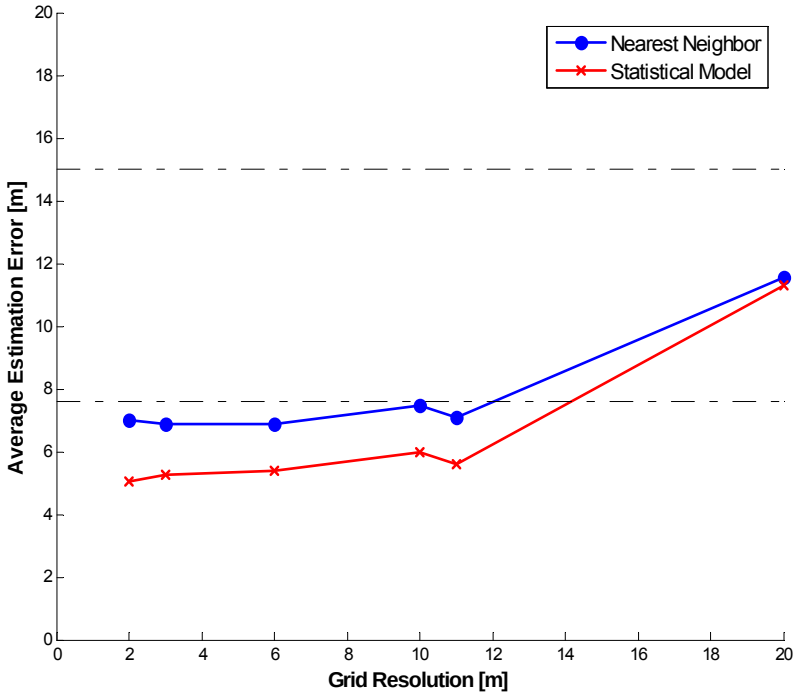

Figure 4-6: Average localization error for a system trained with IEEE 802.11 model

Figure 4-4 - Figure 4-6 show the average distance error estimation of both algorithms as a function of grid resolution for these radio maps. The two horizontal lines in those graphs are the average estimation error reported by Ekahau positioning engine with four and thirteen training points. Using these curves, a system designer can determine the optimum number of reference points to achieve a desired localization accuracy which is dictated by the application requirements. From these plots we can see that the performance of an RT trained RSS based localization system is comparable to a system which is trained by on site measurements. For example Figure 4-5 shows that the average localization error for nearest neighbor algorithm in a system which uses an RT generated reference radio map with 10 m grid resolution is 7.2 meters which is a good approximation for the corresponding average error in Figure 4-4 for any practical deployments. This is further illustrated in Figure 4-7 which shows the performance of the nearest neighbor algorithm

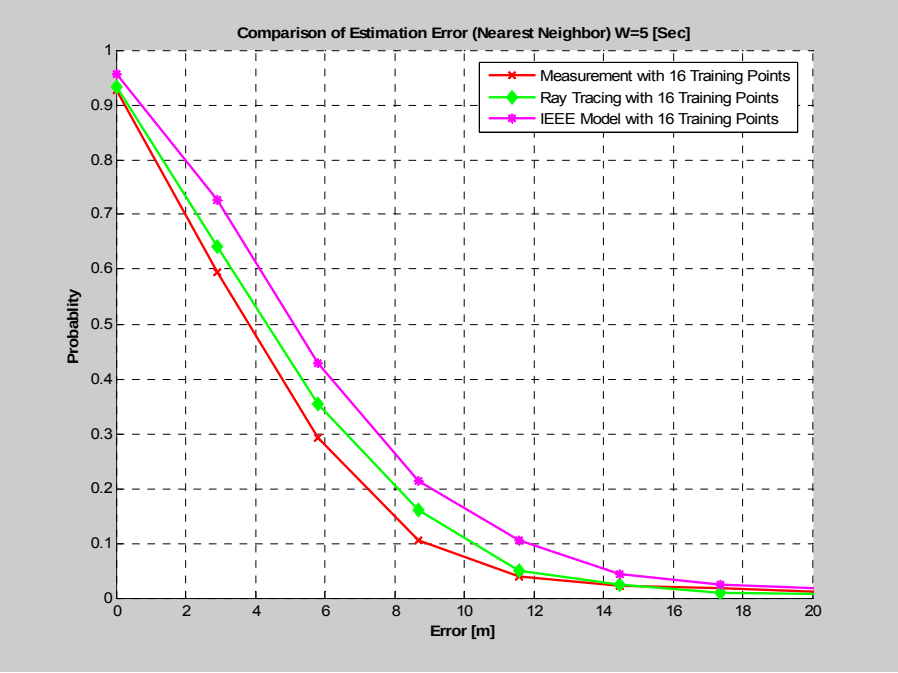

Figure 4-7: CCDF of localization error for different training alternatives

using the three reference radio maps, provided that the system is trained at sixteen training points. Between the two channel modeling methods, RT proved to be a more robust technique because it uses the physical and geometrical information of a building, in addition to the distance between the MS an AP to simulate the radio channel behavior. Usage of a generic model such as the IEEE 802.11 recommended channel model is not validated for all types of indoor environments. On the other hand, the IEEE 802.11 recommended channel model can be employed more easily because it does not require a detailed floor plan and the RT software to create a reference radio map. Using channel modeling techniques, we can easily increase the grid resolution to achieve higher localization accuracy while increasing the number of reference points using on site measurements is a real challenge. In both channel modeling techniques the system needs to know the exact locations of the AP's in order to create the reference radio map. However, a positioning system trained with on site measurements does not require knowing the location of the AP's.

In summary we demonstrated that RT and IEEE 802.11 channel models can be used to generate a reference radio map for RSS based localization in scenario I. We have summarized the advantages and disadvantages of each training alternatives in Table 4-2.

Table 4-2: Comparison of radio map generation alternatives

Method	Advantages	Disadvantages
On site Measurements	• High reliability. • Generally algorithm does not need to know about the location of access points. • No need for accurate floor plan	• Expensive • Positioning fails if there is no training • The number of required measurements grow exponentially with grid resolution • Any minor changes in the geometry of the network needs a new set of measurements
Ray Tracing	• No need for measurement • Higher resolution is achievable by using a finer grid with no substantial cost increase • Changes in network geometry can be reflected in a new set of simulations • Grid resolutions can be adjusted based on the application	• Need for a third party software (RT) • An accurate floor plan of the building is needed • The location of all AP's must be known in advance • Generally less accurate results compared to on site measurements.
IEEE 802.11 Model	• No need for measurement • Higher resolution is achievable by using a finer grid with no substantial cost increase • Changes in network geometry can be reflected in a new set of simulations • Grid resolutions can be adjusted based on the application	• The location of all AP's must be known in advance • The results are less accurate compared to ray tracing or on site measurements.

4.3. TOA vs. RSS Based Localization Using RT in Scenario II

This section presents experimental results that demonstrate a systematic comparison between RSS and TOA based localization techniques. We use RT to create a common framework for performance evaluation of localization algorithms. We present a comparison among LS-TOA and CN-TOAG algorithms from the TOA based algorithms, with RT-RSS-CN and RT-Max-RSS from the RSS based algorithms for applications with bandwidths of 25 MHz and 500 MHz, representing typical WLAN and WPAN positioning applications. We use RT to simulate UWB radio channel behavior in scenario II (Figure 4-8) which was introduced in section 2.4.2. We select 578 points on the middle path as all the possible locations where the MS can be present.

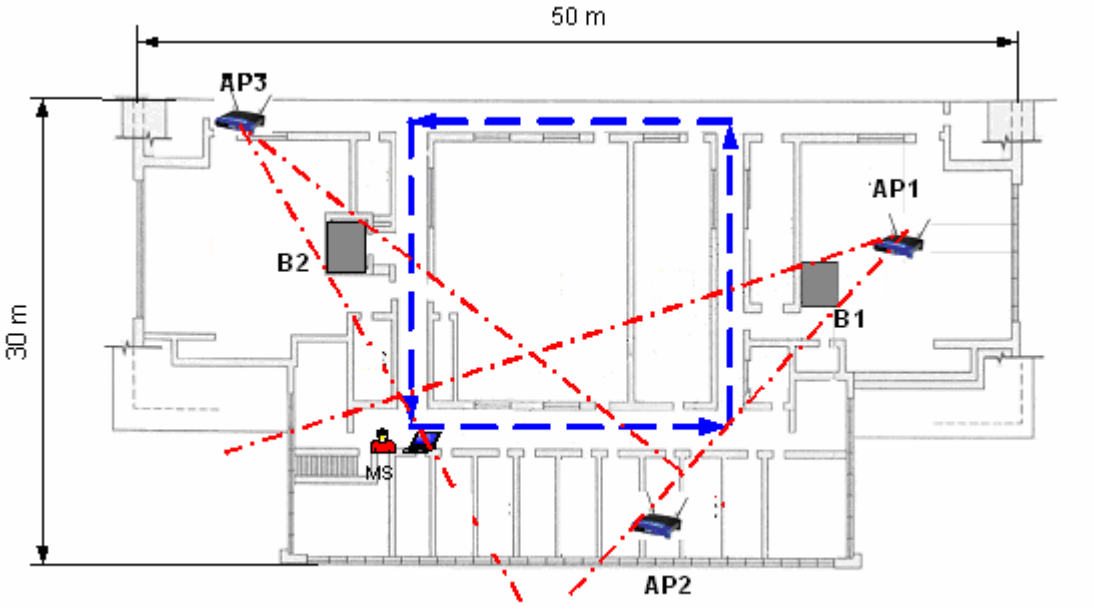

Figure 4-8: Third floor of Atwater Kent lab (AWK3 - Scenario II)

B1 and B2 obstruct the direct line of site (DLOS) component of the transmitted signal from AP1 and AP3 in some locations on the path, causing ranging estimation errors by generating UDP channel profiles.

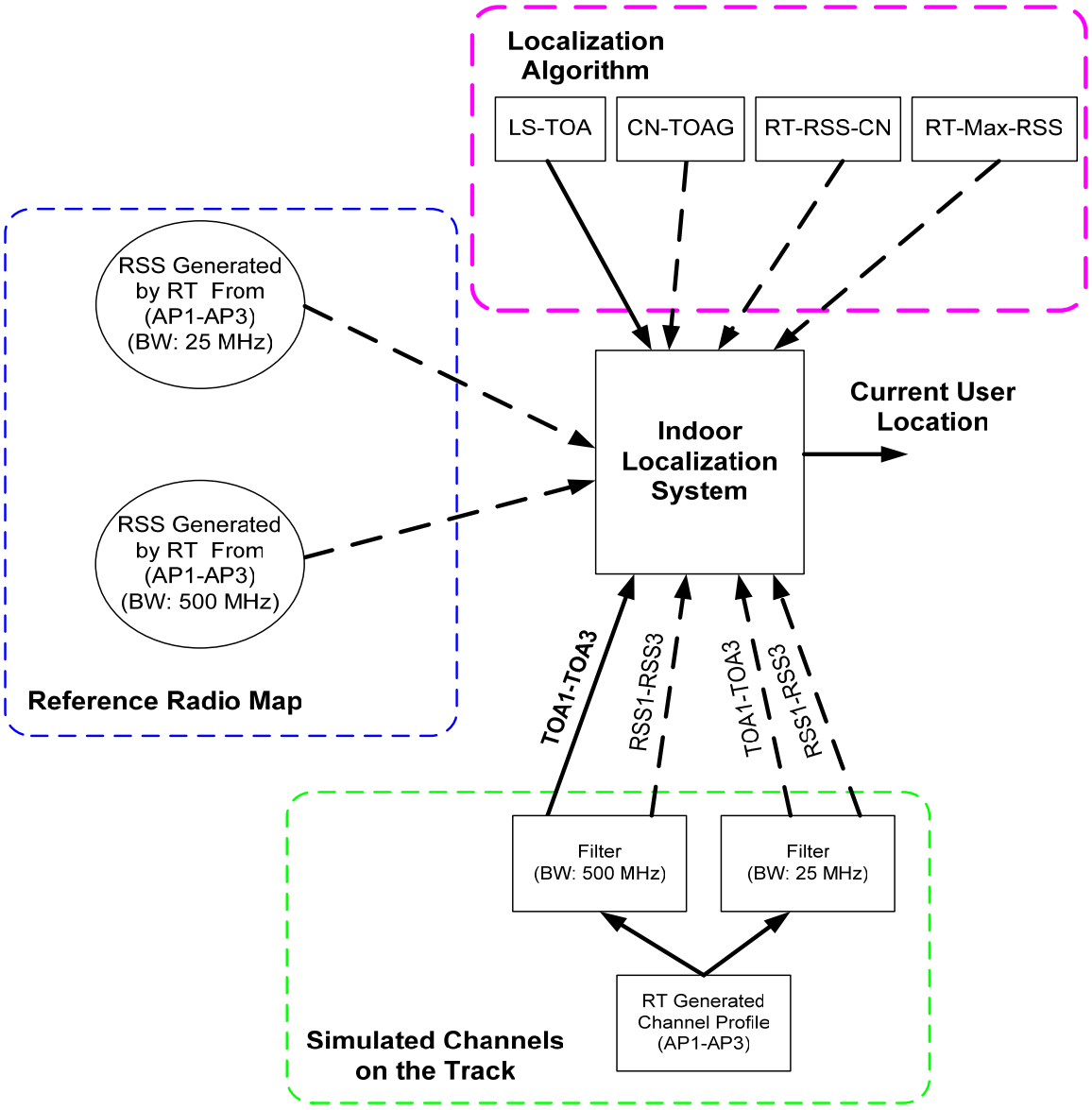

Figure 4-9: Major components of the simulation for scenario II

Major components of this simulation scenario are depicted in Figure 4-9. The required radio map for RT-RSS-CN and RT-Max-RSS are generated by RT using 1040 reference points covering the entire floor plan in scenario II. The reference radio maps can be configured as a map generated by a system with 25 MHz or 500 MHz of bandwidths. Note that both the reference radio map and the MS's observations along the path are simulated by RT. We apply a filter to simulate the behavior of either a 25 MHz or 500 MHz system representing WLAN and WPAN systems respectively. We assume that AP1-AP3 are time synchronized so we can apply any TOA based localization algorithms. The objective of this experiment is to determine the X-Y location of the MS by applying various TOA and RSS based localization techniques, and compare the performance and bandwidth requirements for each algorithm. The required signal metrics for each algorithm are fed to the localization algorithm and the estimated location is compared with the actual MS location.

4.3.1. Results and Discussions

The effect of UDP conditions in DME in a 500 MHz TOA based distance estimation from AP1 and AP3 are shown in Figure 4-10 (a-b) respectively. The existence of the metallic objects B1 and B2 cause large DME values at some locations on the path. The light shaded areas represent the locations with UDP conditions. The DME values in these areas are more than 5 m. This situation can be caused by two reasons. First the MS might be out of the coverage area of an AP and the received signal is largely attenuated. In this case the MS experiences large DME and low RSS values. The second reason for UDP condition, is the obstruction of the DP while the other paths are not largely attenuated.

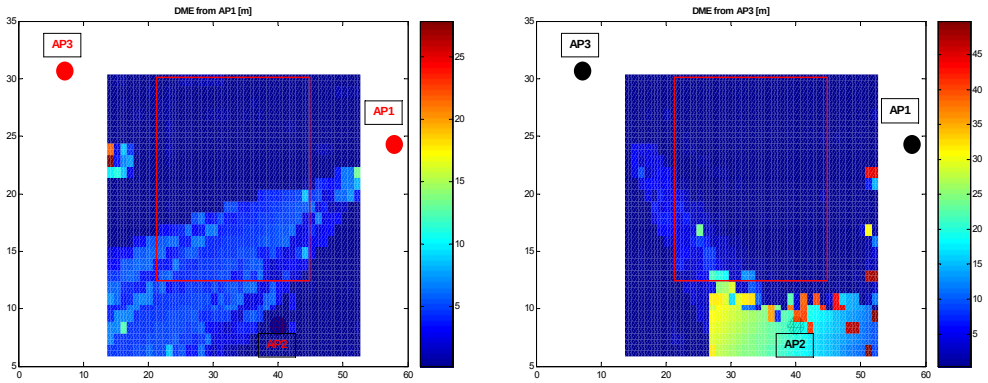

a) DME from AP1 b) DME from AP3

Figure 4-10: Effect of UDP condition on DME (BW: 500 MHz)

For example the required receiver sensitivity for WLAN communications is around -85 dBm which indicates that if MS observes RSS levels in the range of -60 to -75 dBm from an AP, it is located well within the coverage area of the AP. However, being in the coverage area of an AP does not guarantee the existence of the DP. To further illustrate this situation the RSS values from AP1 and AP3 at all locations in the floor plan are depicted in Figure 4-11.

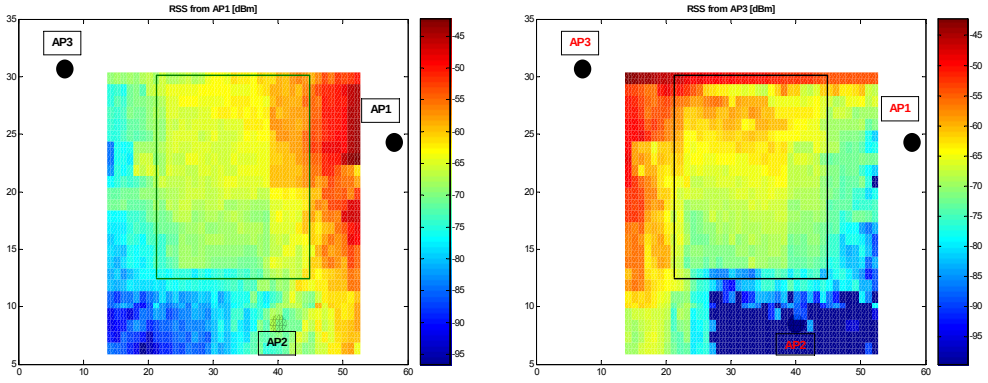

a) RSS from AP1 b) RSS from AP3

Figure 4-11: Effect of UDP condition on RSS (BW: 500 MHz)

Comparison of Figure 4-10 and Figure 4-11 reveals that, in spite of good RSS coverage at certain points on the map we observe large DME values due to the UDP conditions. Large DME values between MS and both AP1 and AP3 at the lower segment of the path, cause significant localization errors in TOA based algorithms. The overall track of movement of MS along with the estimated track by LS-TOA algorithm in a 500 MHz system and the estimated track by RT-Max-RSS algorithm with only 25MHz of bandwidth are depicted in Figure 4-12(a-b) respectively. The starting point index on the track is the lower left corner of the path. We observe that LS-TOA algorithm experiences large localization errors ($10 < \text{error} < 40$ m) on the lower horizontal part of this track, while it provides very accurate estimation ($0 < \text{error} < 1$ m) on the other parts of the path.

This observation motivates us to classify the points on the path into two distinct classes. A point is defined as an *NUDP point* if it observes NUDP channel profiles from all three access points. On the contrary we define a *UDP point* as a point that observes at least one UDP channel from an access point. Based on our simulations all UDP points are located at the lower part of the path as shown in Figure 4-10 (a-b). This observation explains the poor performance of the LS-TOA algorithm along the lower part of the path in Figure 4-12a. However, RT-Max-RSS algorithm with 25 MHz of bandwidth provides better location estimation along the same region compared to the LS-TOA with 500 MHz of bandwidth. If we limit our experiment to all NUDP points on the path and use a 500 MHz receiver, we see that TOA based systems perform better than RSS based systems.

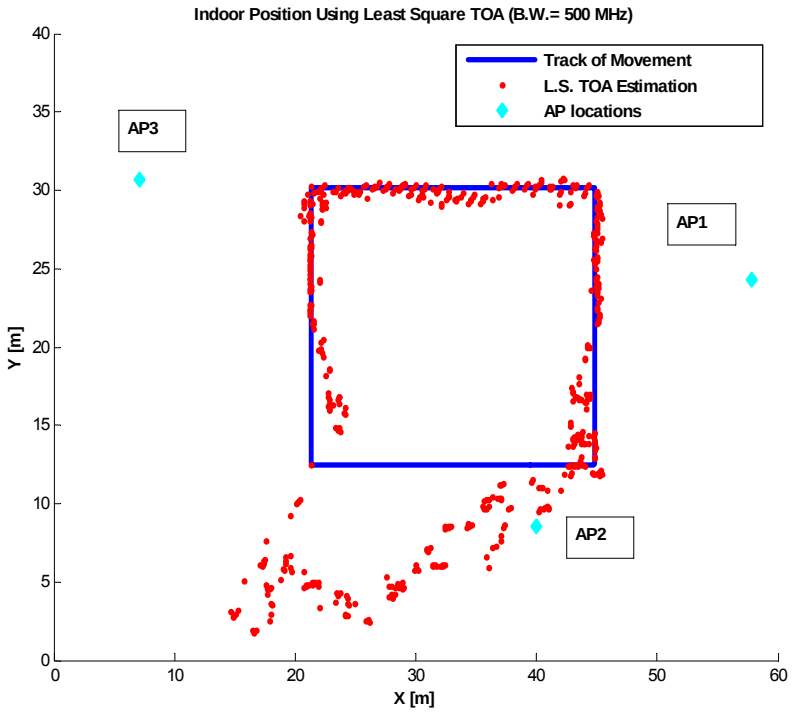

(a) LS-TOA (BW: 500 MHz)

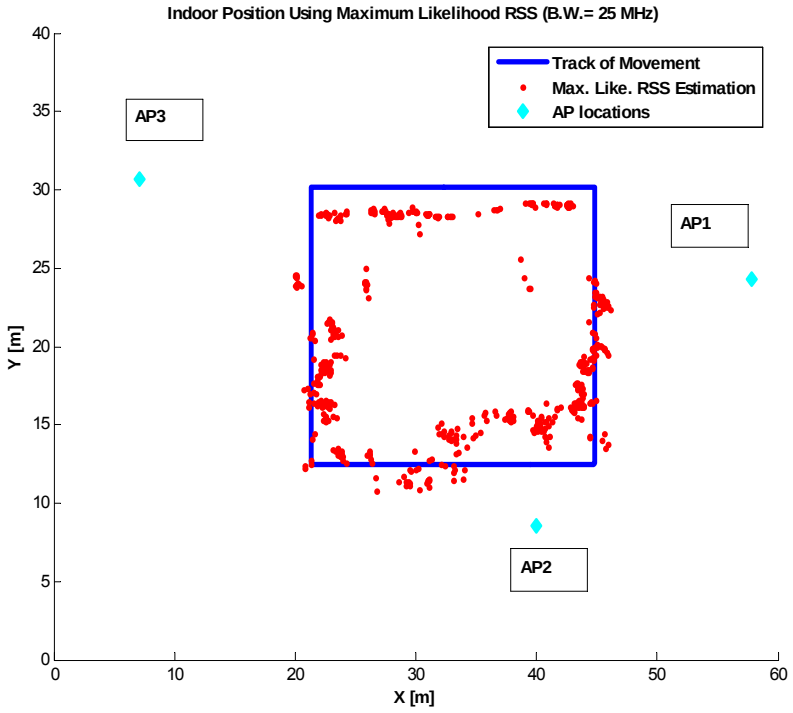

(b) Max. Like. RSS (BW:25 MHz)

Figure 4-12: Estimated track

In order to further clarify the effect of bandwidth on localization error at NUDP points, we have provided the RMS of the localization error for all the algorithms at NUDP points in Figure 4-13 which shows that increasing system bandwidth improves the performance of TOA based localization techniques while having no major effects on performance of RSS based localization.

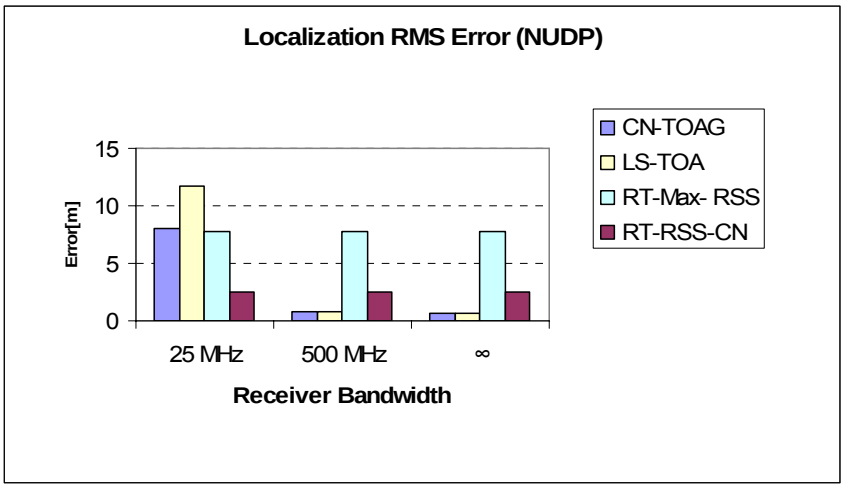

Figure 4-13: RMS of localization error at NUDP points

Statistical comparison of the localization error among each individual algorithm at NUDP points for both 25 MHz and 500 MHz systems are illustrated in Figure 4-14 (a-b). Note the superior performance of the RSS based localization algorithms in a 25 MHz system. On the other hand, TOA based algorithms achieve much better localization performance compared to RSS based systems in a 500 MHz system at NUDP points as a consequence of smaller DME values. Among the two TOA based algorithms CN-TOAG shows a better performance compared to the LS-TOA algorithm in a 25 MHz system, because the CN-TOAG restricts the estimated location to land on a reference point in the radio map. However in a 500 MHz system CN-TOAG and LS-TOA algorithms show comparable

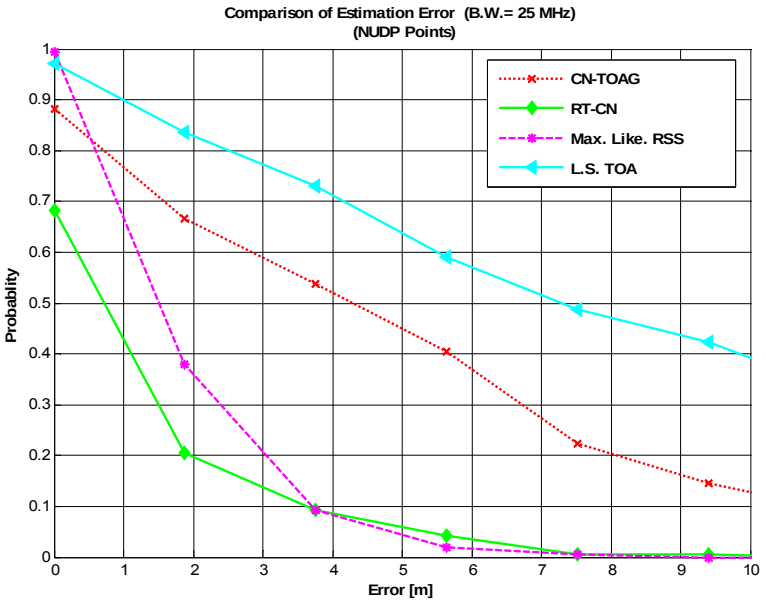

(a) BW: 25 MHz

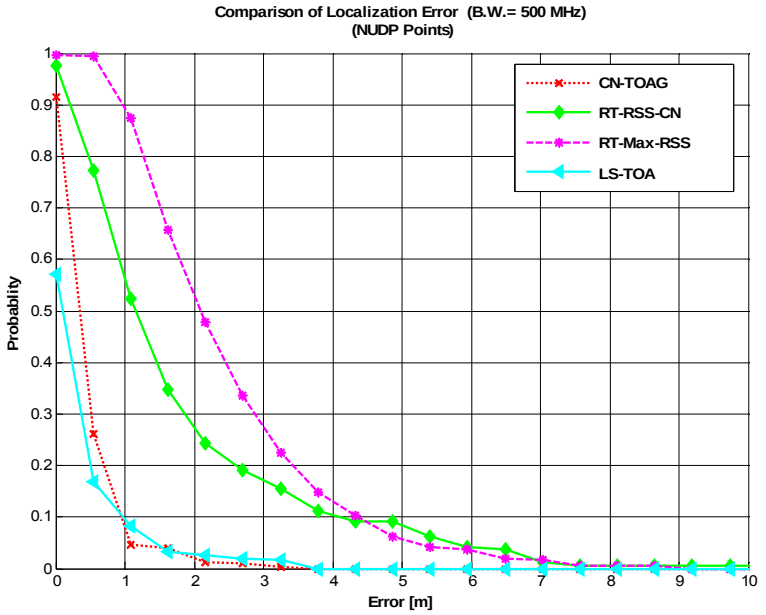

(b) BW: 500 MHz

Figure 4-14: Complementary CDF of localization error at NUDP points

results at NUDP points. The fact that LS-TOA is a distance based algorithm which does not require a reference radio map for localization, makes it the preferable choice for wideband TOA based localization in scenarios with NUDP conditions. As we discussed in Chapter 3 distance based localization algorithms are more scalable compared to the pattern recognition algorithms because the algorithm only needs to know the location of at least three reference points to perform the triangulation.

The initial and final points on our experimental path correspond to UDP points consequently we observe large errors at these locations. Although increasing the bandwidth reduces DME in TOA based algorithms, but in this scenario TOA techniques can not outperform RSS based systems at UDP points. This is shown in Figure 4-15 which shows the RMS of localization error at UDP points for each algorithm with different system bandwidths.

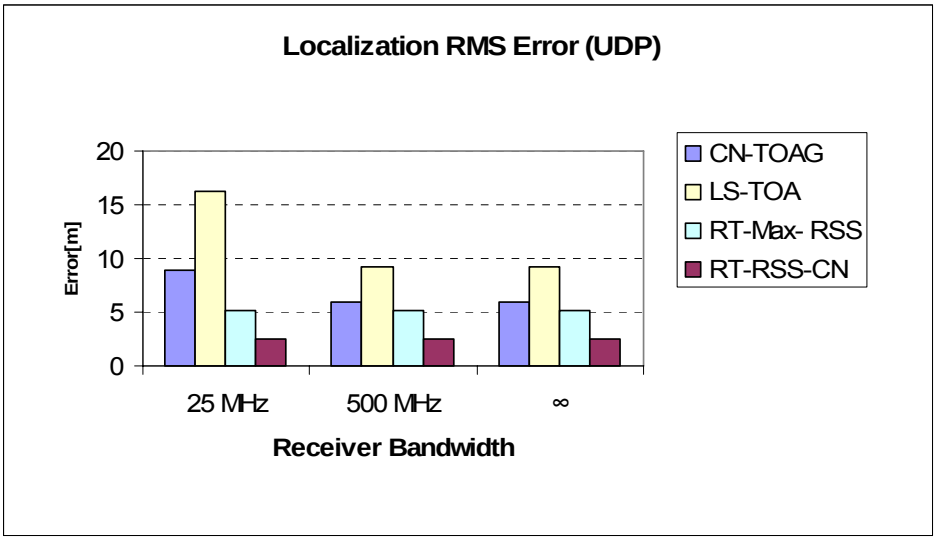

Figure 4-15: RMS of Localization error at UDP points

Statistical comparison of localization error among all four algorithms for 25 MHz and 500 MHz systems at UDP points are depicted in Figure 4-16 (a-b) respectively. Unlike the NUDP points, the localization performance of TOA based algorithms is inferior compared to the performance of RSS based algorithms even in 500 MHz system in this scenario. The poor performance of TOA based techniques is caused by large DME values as a result of UDP conditions. Among the two TOA based algorithms CN-TOAG shows a better performance compared to the LS-TOA algorithm especially at 500 MHz system, because the CN-TOAG restricts the estimated location to land on a reference point in the radio map. The overall CCDF of localization error at all points on the path is shown in Figure 4-17. The existing distribution of NUDP and UDP points in this scenario shows that, RSS based algorithms achieve a better localization performance compared to the TOA based techniques even in a 500 MHz system.

The existing data shows that, TOA based systems do not have much to offer in a system with bandwidths around 25 MHz, because TOA estimation suffers from large errors due to multipath, even in the absence of UDP conditions. However, for systems with bandwidths of at least 500 MHz TOA system can provide a better solution compared to RSS systems at NUDP points. In TOA based positioning systems using WPAN technologies, it is important to install the AP's at locations where they provide a comprehensive coverage as well as NUDP channel conditions within their coverage area. This may require increasing the number of AP's in certain areas in a building. In a practical system adding a new AP in a TOA based positioning system is more challenging compared to an RSS based system because TOA based localization requires

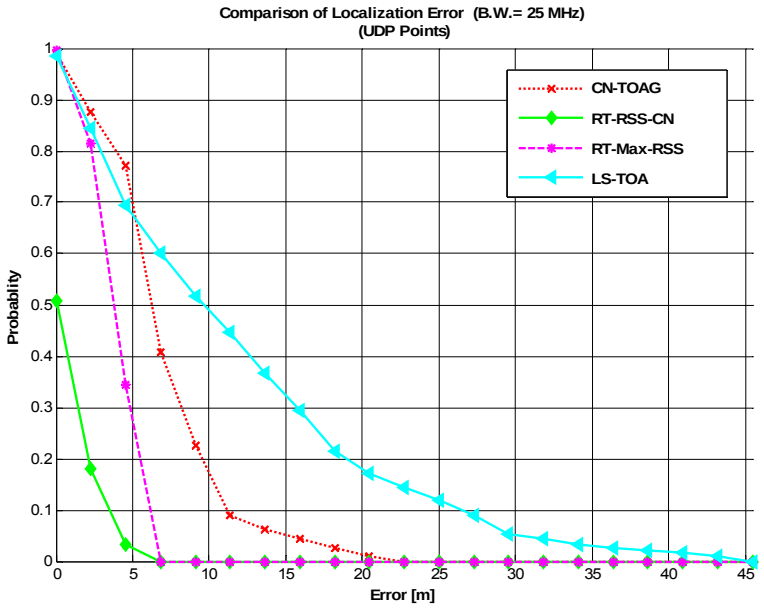

(a) BW: 25 MHz

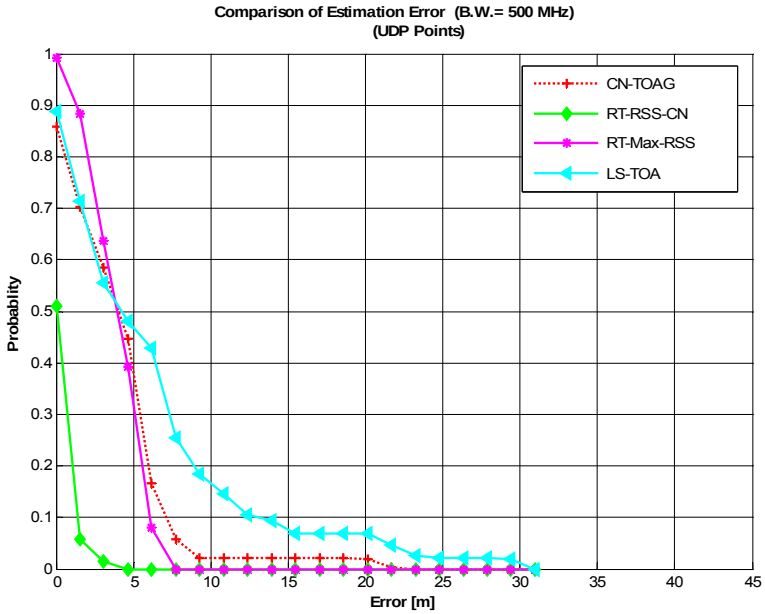

(b) BW: 500 MHz

Figure 4-16: Complementary CDF of localization error at UDP points

time synchronization mechanism between the MS and AP. On the other hand, in RSS based positioning systems the AP does not require to be connected to a network and there is no need for time synchronization between the MS and AP. Adding the number of AP's can improve the performance of RSS based positioning systems using WiFi technologies as well [69]. However, since the number of non-overlapping channels in IEEE 802.11b systems is limited adding new AP's may increase the interference in adjacent areas [44].

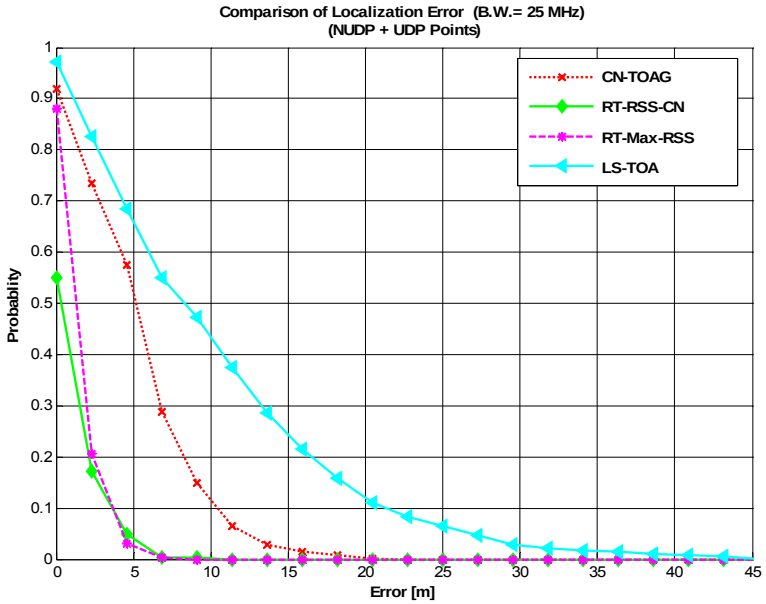

(a) BW: 25 MHz

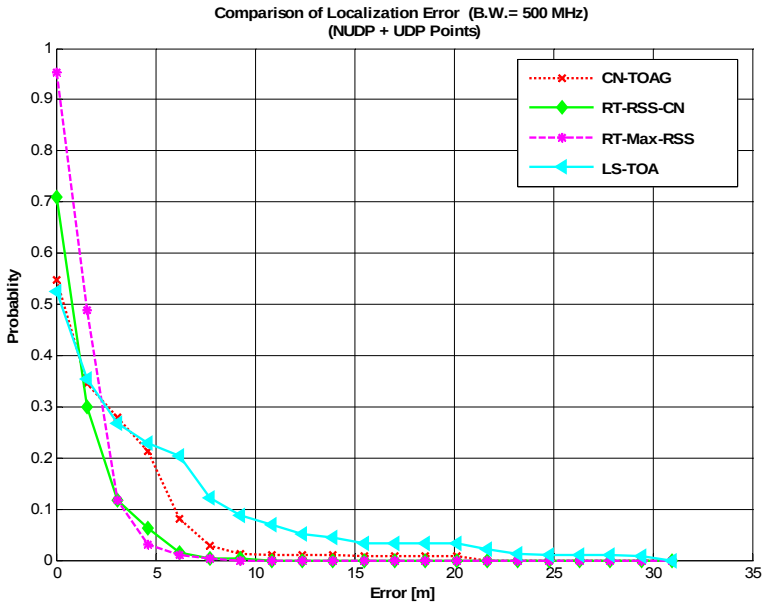

(b) BW: 500 MHz

Figure 4-17: Complementary CDF of error for all the points

4.4. TOA vs. RSS Based Localization Using Channel Measurements in Scenario II

This section presents a comparison between RSS and TOA based localization algorithms using UWB channel measurements. The experimental testbed for is the same setup that we used for UWB channel measurements in section 2.4.2.2 using scenario II. We used RT to generate the required reference radio map for pattern recognition algorithms and UWB measurements to emulate MS's signal observations from AP1-AP3 at 76 points along the measurement path (Figure 4-18). The components of this testbed are depicted in Figure 4-19. The UWB measurements are the same data set that we used in section 2.4.2.2 for channel simulations. We use RT; with the modified floor plan as discussed in section 2.4.2.2; to simulate channel profiles in a grid of 1040 reference points in scenario II.

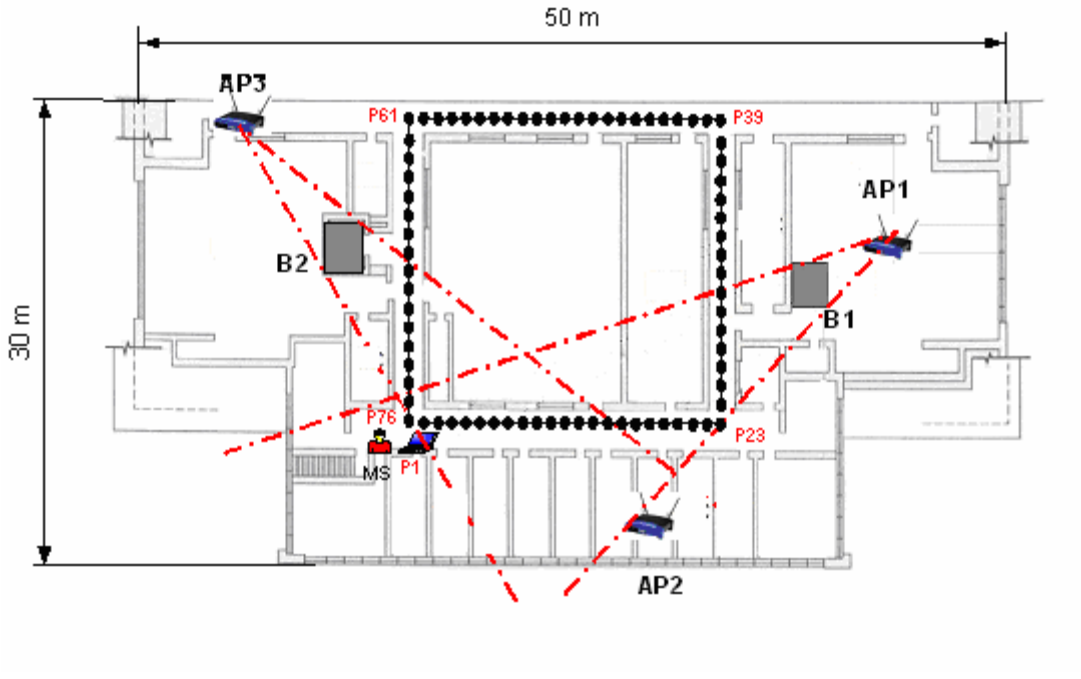

Figure 4-18: Third floor of Atwater Kent lab (scenario II)

The objectives of this experiment are as follows:

1. Using the updated floor plan create a new set of reference radio maps that can be used by RT-RSS-CN and RT-TOA-CN localization algorithms in a 25 MHz and 500 MHz system.

2. Provide a comparative performance evaluation among LS-TOA, CN-TOAG, and RT-TOA-CN from the TOA based class, and RT-RSS-CN from the RSS based class of localization algorithms with both 25 MHz and 500 MHz of system bandwidth.

Note that in this scenario the reference radio map is generated by RT, however the MS's observations are the actual channel measurements rather than RT simulations. We decided to use the RT-RSS-CN algorithm from the class of RSS based algorithms because for a high resolution radio map ($res. <= 1\ m$) the performance of RT-RSS-CN is superior to RT-MAX-RSS. We added the RT-TOA-CN algorithm instead because we believe that RT-TOA-CN can provide a better performance compared to the conventional TOA based algorithms especially under UDP conditions because RT-TOA-CN uses RT which provides additional environmental information; including possible UDP conditions; to the localization algorithm.

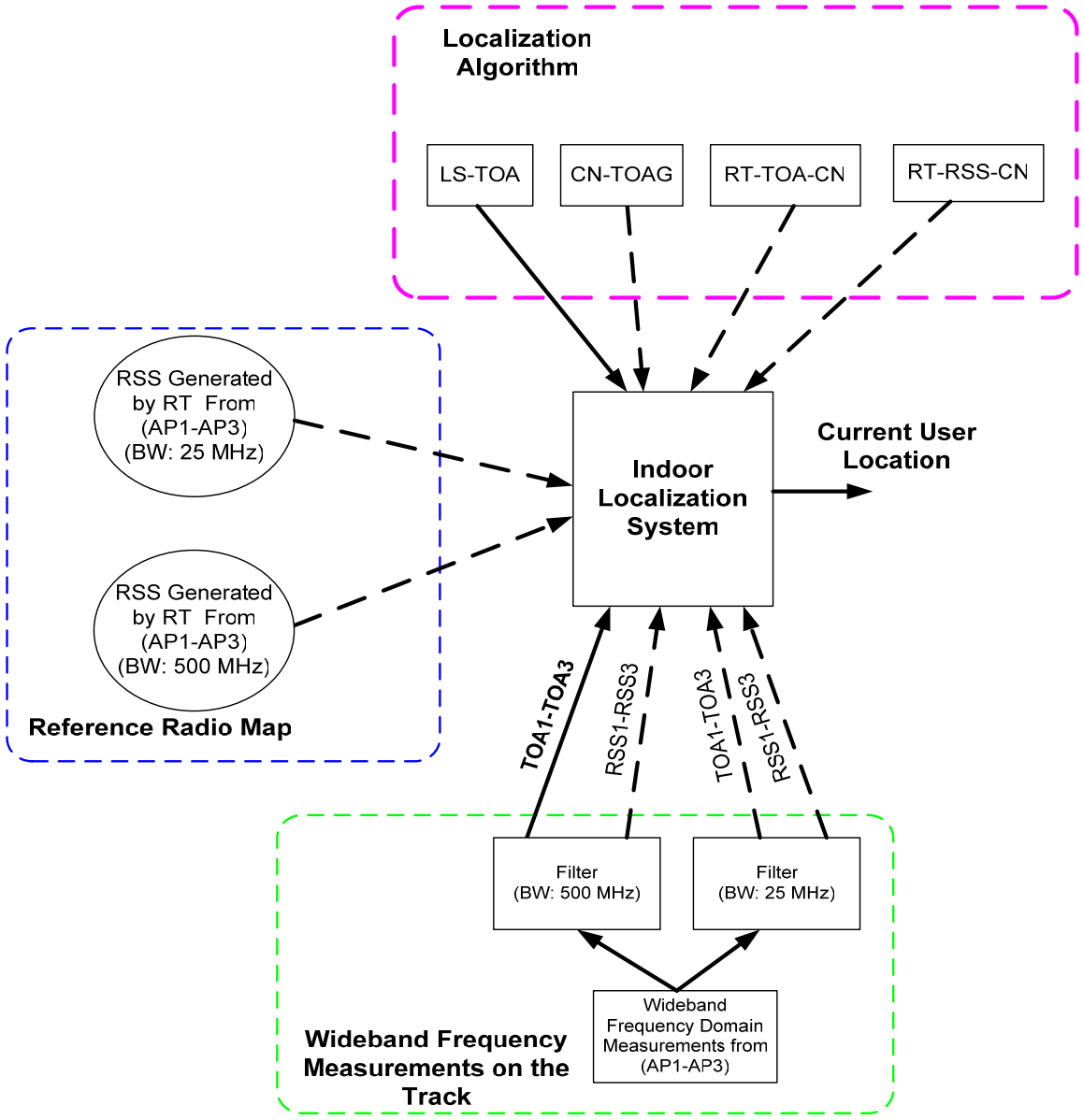

Figure 4-19: Major components of the testbed for scenario II

4.4.1. Results and Discussions

Statistical comparison of localization error among all four algorithms for 25 MHz and 500 MHz systems are depicted in Figure 4-20 (a-b) respectively. Unlike our original

results in section 4.3.1, the performance of wideband TOA based localization algorithms are superior to RT-RSS-CN. However, Figure 4-20 (b) illustrates that RT-RSS-CN provides the best performance compared to the other algorithms in a 25 MHz system which is in line with our previous results. Among the TOA based localization techniques pattern recognition based algorithms (CN-TOAG and RT-TOA-CN) result in a better estimation compared to distance based methods like LS-TOA in both 500 MHz and 25 MHz systems due to the existing UDP conditions.

These results show that, RT can be used as an alternative to the time and labor consuming wideband channel measurements in pattern recognition localization algorithms in both 25 MHz and 500 MHz systems. Moreover, by incorporating the RT generated channel information into the localization algorithms we can achieve better localization performance.

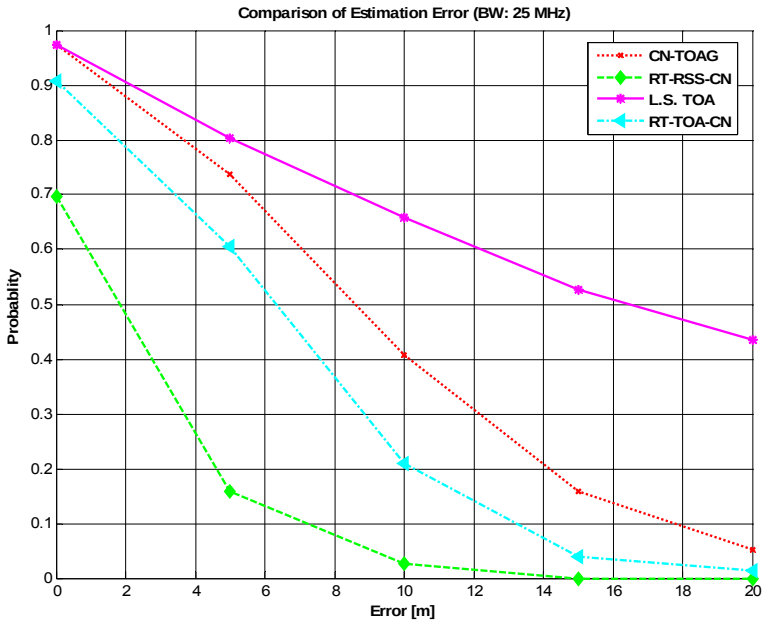

(a) BW: 25 MHz

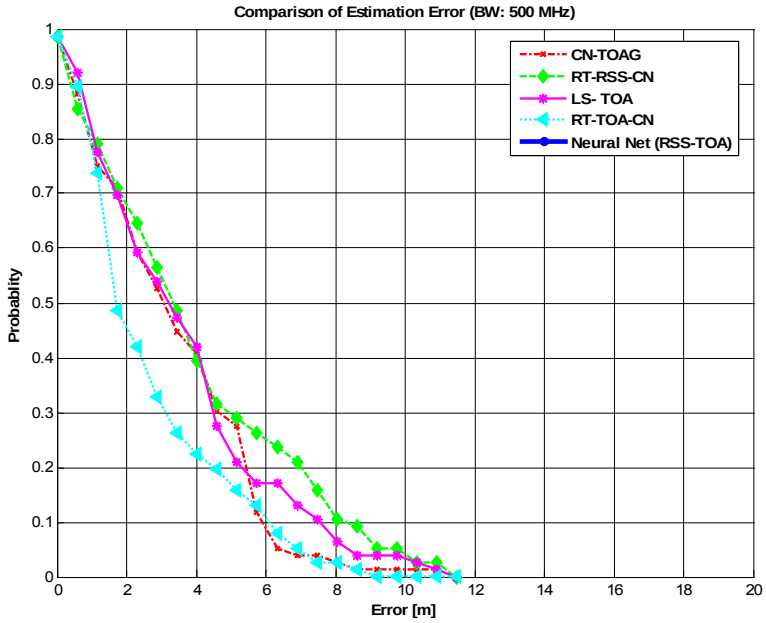

(b) BW: 500 MHz

Figure 4-20: CCDF of localization algorithms

4.5. Hybrid RSS-TOA Localization Using Channel Measurements in Scenario II

Motivated by the complementary behavior of TOA and RSS based localization algorithms in a wideband (BW=500 MHz) system as shown in Figure 4-12, in this section we use a hybrid RSS-TOA RT assisted algorithm using neural networks to achieve a better localization performance. The experimental testbed for this section is similar to the one explained in section 4.4. Thus, we can easily compare the performance of the new hybrid algorithm with our previous results in section 4.4.1.

We use a multilayer-perceptron (MLP) neural network (Figure 4-21) developed through supervised learning, as an underlying engine for a hybrid RSS-TOA based localization algorithm. Two sets of three input lines are assigned to RSS and TOA measurements from AP1-AP3 in this network. The output (x, y) is the current location of MS. It has been shown that a MLP with a single hidden layer is sufficient to approximate any continuous function to some desired accuracy provided that we use sufficient number of neurons [67]. We use a single hidden layer network with 20 neurons. The performance function has the form of a sum of squares:

$$\mathrm{E}(w) = \frac{1}{2}\sum_{i=1}^{N}(T_i - \mathrm{O_i}(w))^2 \qquad (4\text{-}1)$$

Where T_i and $\mathrm{O_i}(w)$ are the target and current output values for pattern i as a function of the network weights w and N is the number of training points. We use *tan-sigmoid*

defined by (4-2) and the identity function as transfer functions for the hidden layer and the output layer respectively.

$$\text{tansig}(x) = \frac{2}{1+e^{-2x}} - 1 \qquad (4\text{-}2)$$

This neural network is trained with RT generated radio map using *Levenberg-Marquardt* algorithm [68].

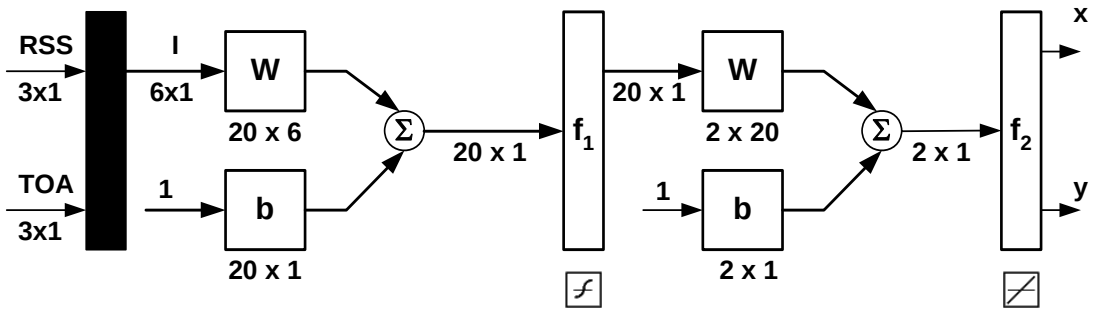

Figure 4-21: Neural network architecture for hybrid RSS-TOA based localization

4.5.1. Results and Discussions

The CCDF of LS-TOA, LS-TOA, RT-TOA-CN, RT-RSS-CN, and the new hybrid localization algorithms in a 25 MHz and 500 MHz system are compared in Figure 4-22 (a-b) respectively. The superior performance of the new algorithm compared to the other algorithms in a 500 MHz system is obvious. The underlying neural network relies on the

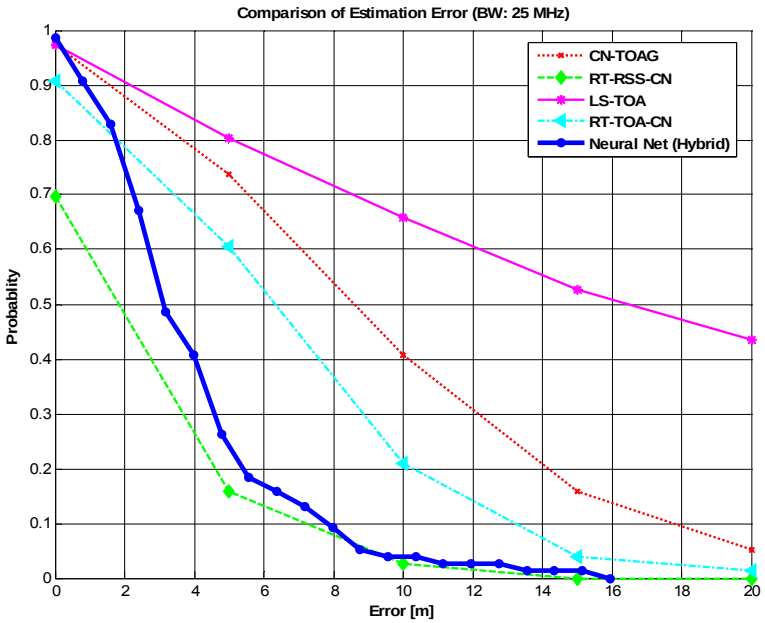

(b) BW: 25 MHz

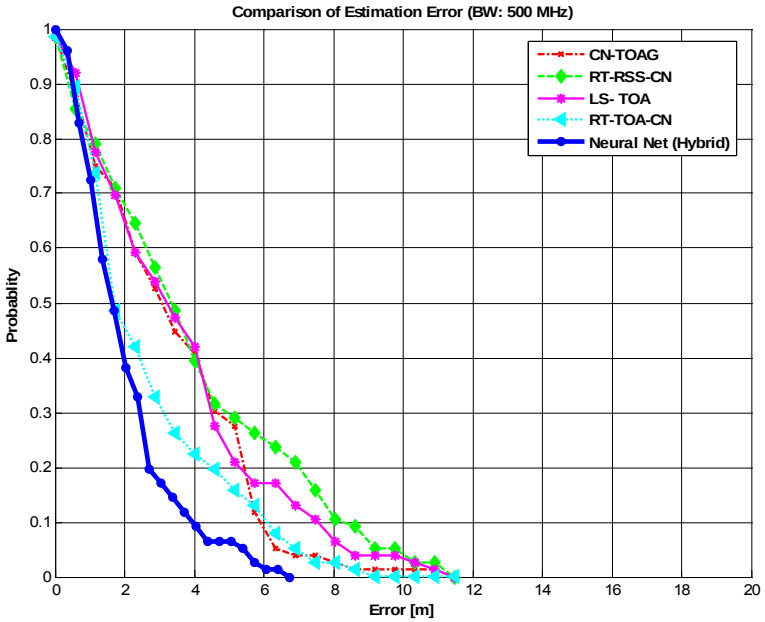

(b) BW: 500 MHz
Figure 4-22: CCDF of localization error

more accurate TOA, and RSS information at NUDP and UDP points respectively. The neural network implicitly identifies NUDP and UDP points using RT generated training data. However, in a 25 MHz system the performance of the hybrid algorithm is better than TOA based techniques and worse than RT-RSS-CN. In other words it seems that the TOA data does not provide any additional information for the hybrid algorithm. In order to further investigate this phenomenon, we used the existing RT generated radio map to create a new scenario. We use half of the reference points in the RT generated radio map as training points and use the other half as performance evaluation points and compare the performance of three separate neural networks with similar architectures. The first neural network uses RSS information, the second network uses TOA information and finally the third network uses both TOA and RSS information. We train all three networks with the corresponding RSS, TOA, and RSS-TOA information at all the training points and compare the localization performance of each network. Figure 4-23 (a-b) compare the performance of these three networks in 25MHz and 500MHz systems respectively. Figure 4-23(b) confirms that the performance of the hybrid network is better than both sole TOA and sole RSS based network in a 500MHz systems. This result is in line with our previous results in Figure 4-22(b). On the other hand in a 25 MHz system, the performance of the hybrid network is better than the TOA based network and worse than the RSS based network. In other words combining TOA and RSS information enhances the localization performance in a 500MHz system because the algorithm relies more heavily on TOA information at NUDP points and weighs more on RSS information at UDP points. However, in a 25MHz system TOA information is less accurate than RSS

information at both UDP and NUDP points. Thus, the hybrid algorithm is mislead with the additional TOA information in a 25 MHz system.

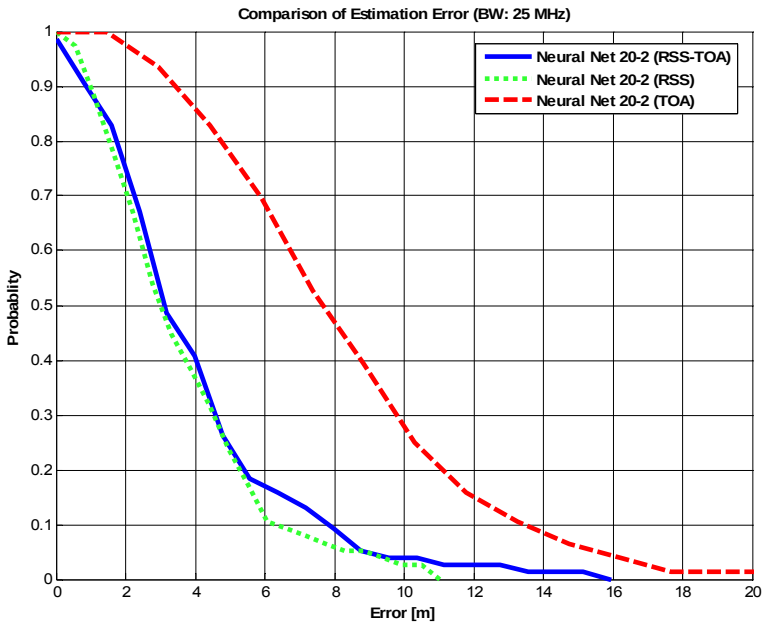

(a) BW: 25 MHz

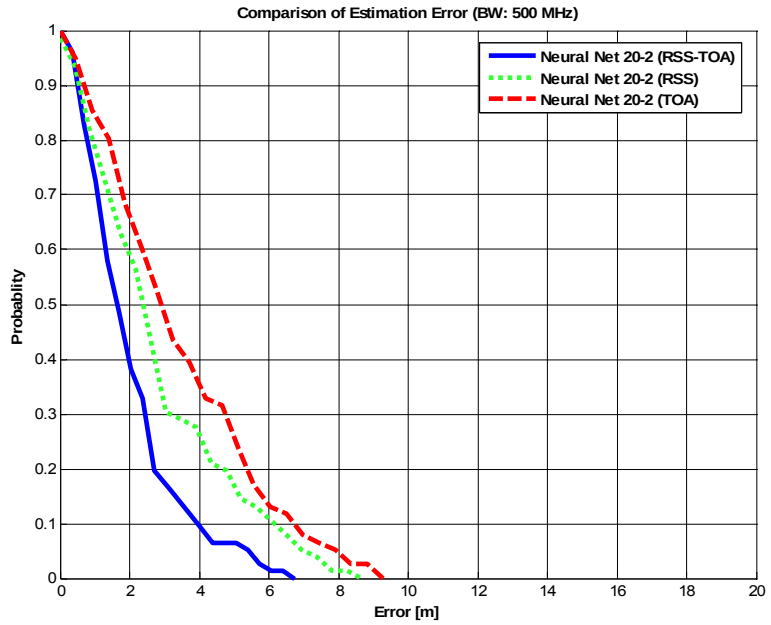

(b) BW: 500 MHz

Figure 4-23: CCDF of localization error for neural network based algorithm

Chapter 5

Conclusions and Future Research

This dissertation introduced applications of channel modeling techniques for indoor localization algorithms. Generating a reference radio map via on site measurements for pattern recognition based algorithms, and comparative performance evaluation of localization algorithms are two major challenges in any practical deployment of indoor positioning systems. Methodologies for using channel modeling techniques to cope with both of these problems are proposed. Channel modeling techniques are considered as an integrated part of a set of channel model assisted localization algorithms to eliminate the time consuming training process in pattern recognition based methods. Moreover, indoor channel modeling methods are used to create a repeatable framework for comparative performance evaluation of indoor localization algorithms.

RT-RSS-CN, RT-MAX-RSS, and RT-TOA-CN are introduced as a set of new RT assisted localization algorithms which use RSS and TOA attribute of a signal for localization. These algorithms use RT to reduce deployment cost and improve the performance of a localization system.

Two sets of empirical data obtained by radio channel measurements are used to create a baseline for comparative performance evaluation of localization algorithms. The first database is obtained by WiFi RSS measurements in the first floor of the Atwater Kent laboratory (Scenario I); an academic building on the campus of WPI; and the other by UWB channel measurements in the third floor of the same building (Scenario II).

The performance of measurement trained and channel model assisted localization algorithms are compared in scenario I. The performance of measurement trained and channel model assisted algorithms are very close except for the times, when the number of training points is increased substantially. In particular, on the average the performance of the RT assisted algorithm is less than 2 meters worse than the average localization error of a system which is trained by on site measurements in scenario I. This difference can be easily compensated by increasing the number of reference points in the reference radio map using channel modeling techniques.

Channel modeling techniques are used for comparative performance evaluation of TOA and RSS based localization in WLAN and WPAN systems in scenario II. RSS based localization using WLAN technologies are less sensitive to multipath and system bandwidth. TOA based localization algorithms are better than RSS based systems in NUDP conditions, but they may perform even worse than RSS based algorithms in UDP areas. The conventional TOA based algorithms do not have much to offer in a WLAN system with bandwidths around 25 MHz, because TOA estimation suffers from large errors due to multipath, even in the absence of UDP conditions. However, for WPAN

systems with bandwidths of at least 500 MHz TOA based algorithms can provide a better solution compared to RSS based techniques. For example the average localization error in scenario II with 25 MHz of bandwidth for LS-TOA and RT-RSS-CN algorithms were 16 and 2 meters respectively. On the other hand, in the same scenario with 500 MHz of bandwidths at NUDP points the average localization error achieved by LS-TOA and RT-RSS-CN were 50 cm and 1.5 meter respectively.

A novel hybrid TOA-RSS based algorithm using neural networks is introduced that utilizes the complementary behavior of RSS and TOA based localization and achieves a better performance in a WPAN system in scenario II. The hybrid algorithm shows a 5 meters improvement in localization error compared to the other algorithms in scenario II. The average localization error is reduced by using the hybrid algorithm to less than 2 meters in the same scenario.

For the future there are several aspects of indoor localization problem that can be studied. The coverage of an indoor localization system using existing network infrastructure and the coverage of the wireless access network are two interrelated problems. The performance of a localization system improves by adding more AP's with overlapping coverage areas. However, network operators are looking for methods to reduce the overlapping coverage areas to minimize the deployment cost and interference in their wireless access networks. Thus, analyzing the relationship between the number of AP's and the localization accuracy is a useful research study. Design of algorithms with tracking capabilities using spatial diversity embedded in measurements obtained in

neighboring locations can improve the performance of the algorithms and needs to be investigated. Designing neural network algorithms which are trained with other parameters such as arrival time and strength of other paths can improve the performance of localization and is another area of interest. Developing new algorithms to detect occurrence of UDP conditions and adjust the location estimate with the associated bias caused by UDP is another important contribution for future work. More advanced algorithms that use other paths to detect the arrival time of the direct path also deserve to be considered for future research. Analyzing the effects of clustering on the performance of channel model assisted algorithms to reduce the complexity of the algorithm is another important research topic.

Appendix A

WiFi RSS Measurements in Scenario I

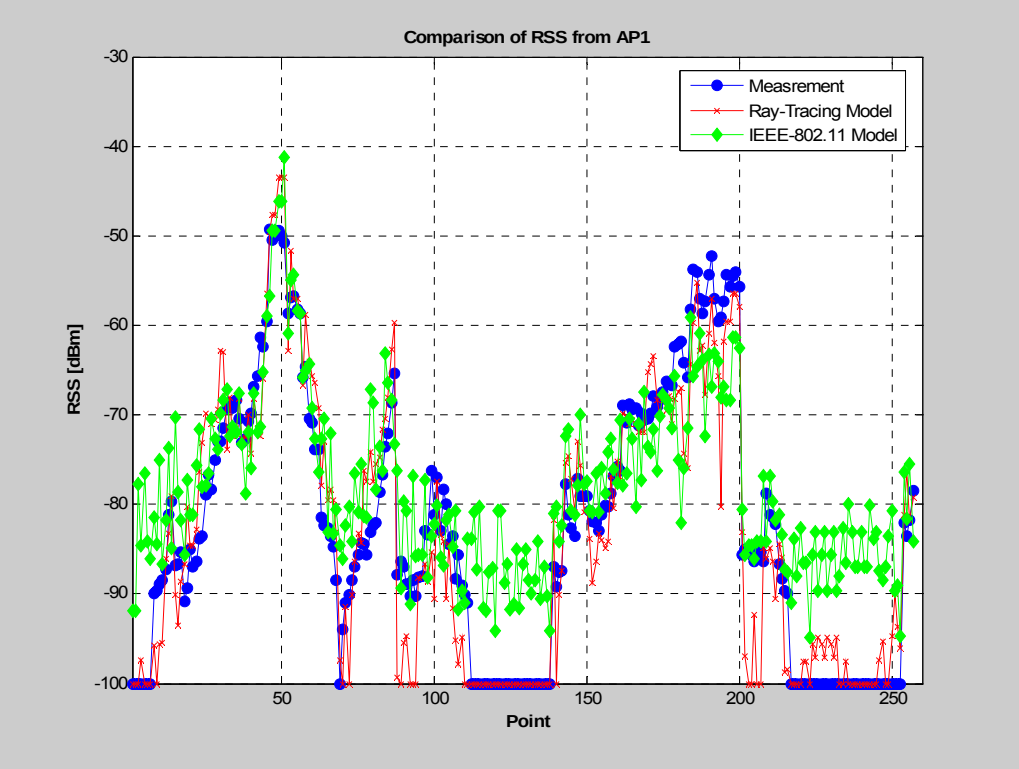

Figure A. 1: Channel models vs. measurements at AP1

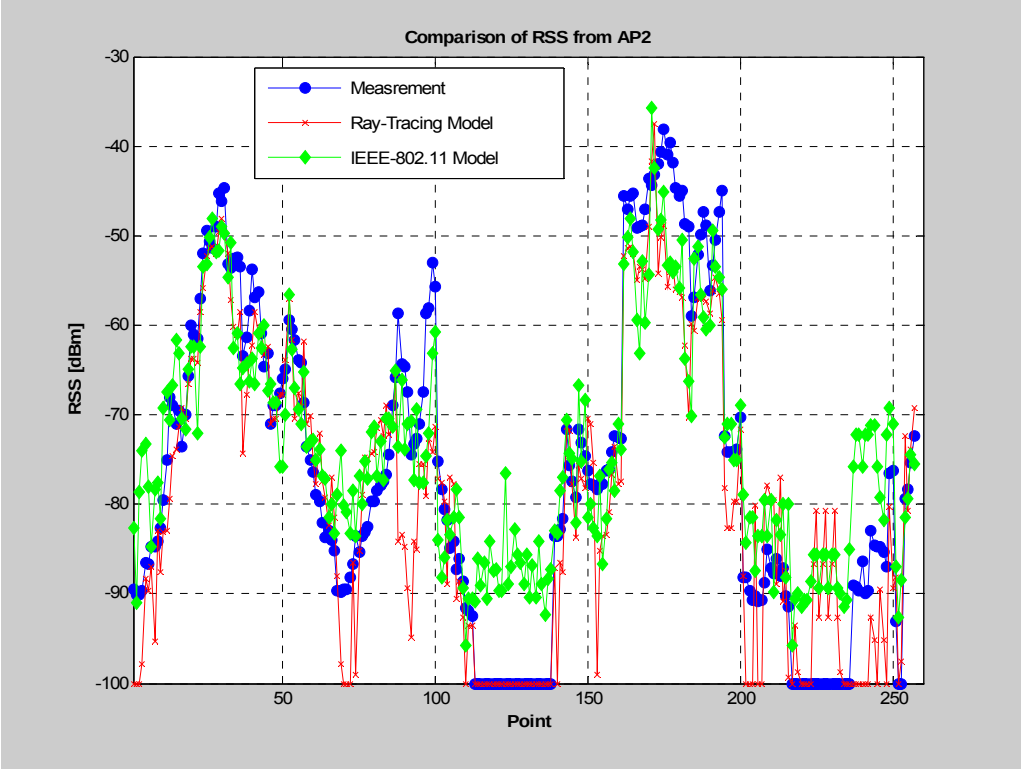

Figure A. 2: Channel models vs. measurements at AP2

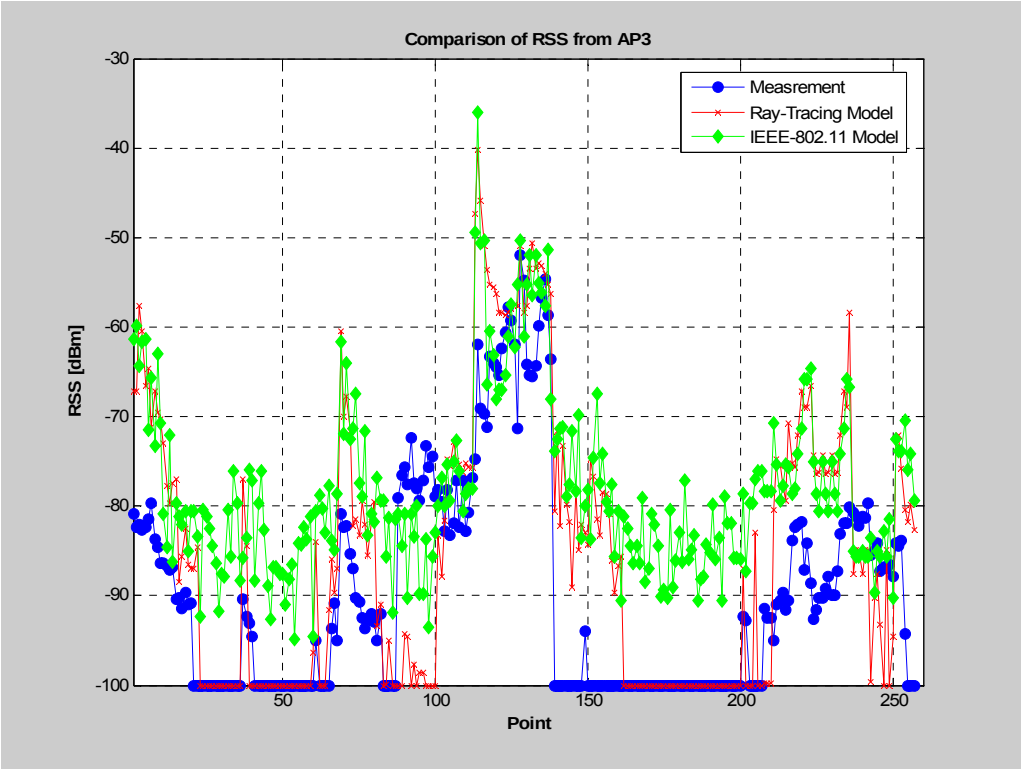

Figure A. 3: Channel models vs. measurements at AP3

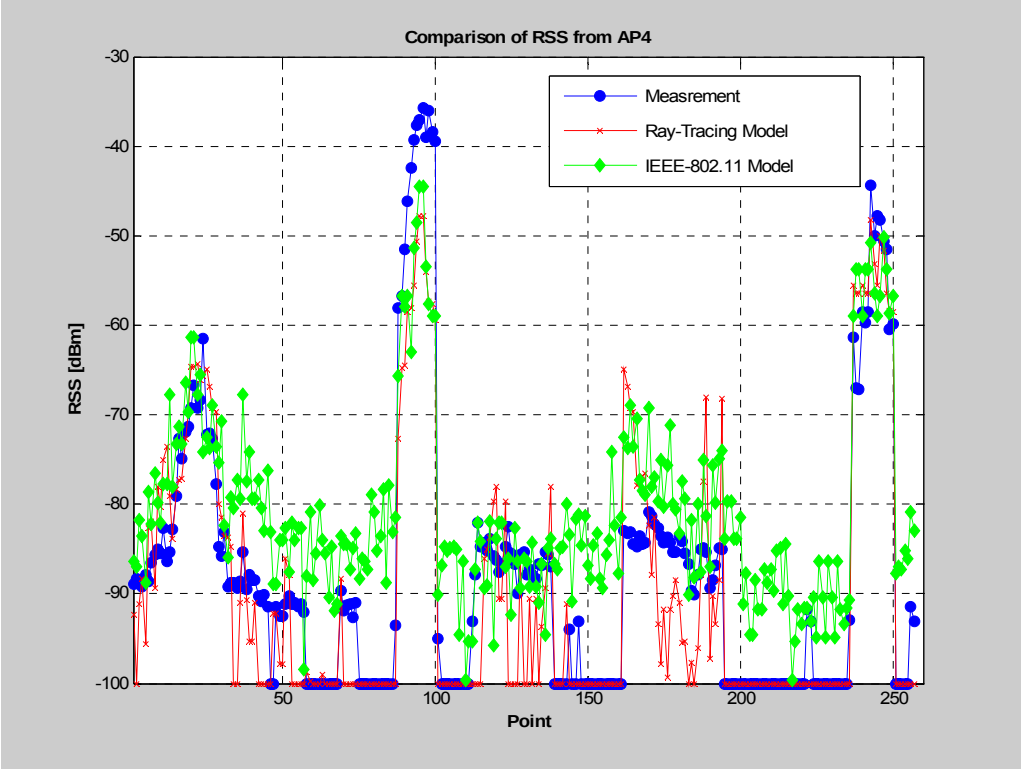

Figure A. 4: Channel models vs. measurements at AP4

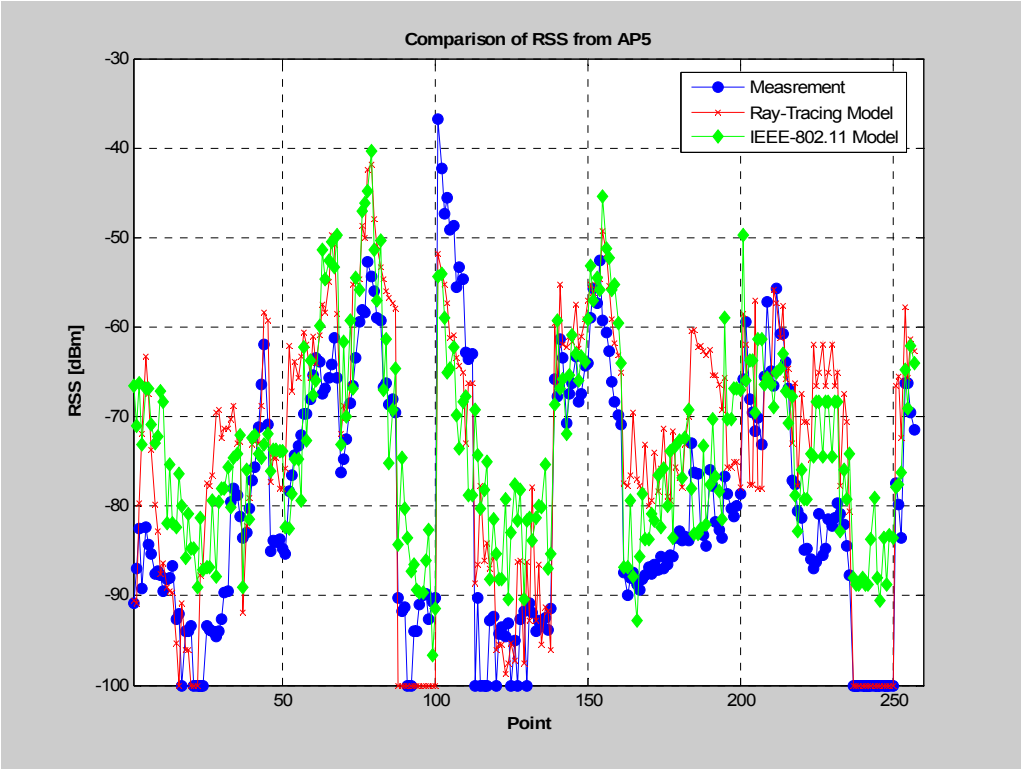

Figure A. 5: Channel models vs. measurements at AP5

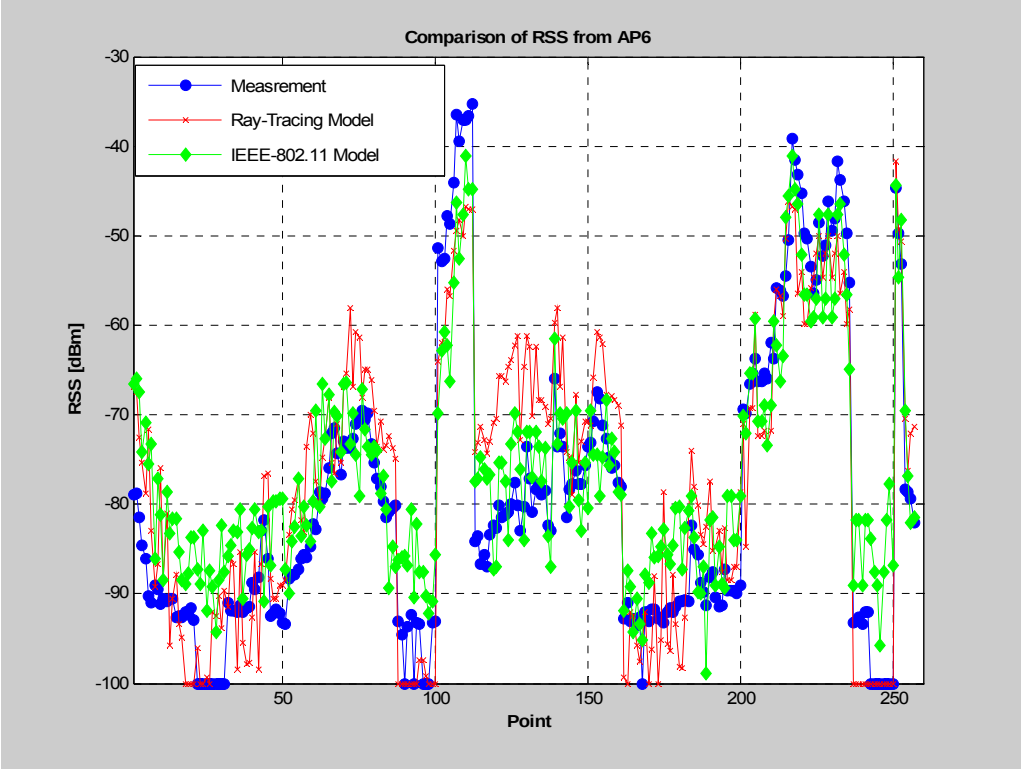

Figure A. 6: Channel models vs. measurements at AP6

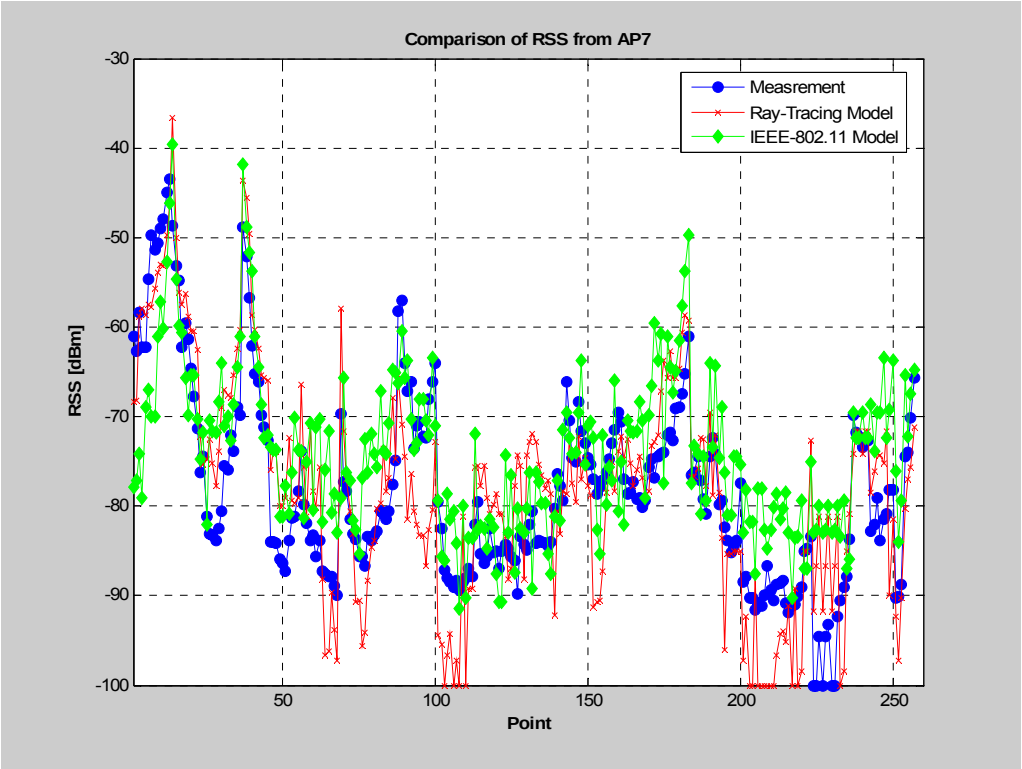

Figure A. 7: Channel models vs. measurements at AP7

Appendix B

Neural Networks

Neural networks are composed of simple interconnected elements (*Neurons*) operating in parallel. The overall function of the network is largely determined by the connection of neurons. A neural network can be trained to perform a complex pattern recognition function by adjusting the connection between neurons [62]. In most application a neural network is trained so that a particular input generates a predefined target output.

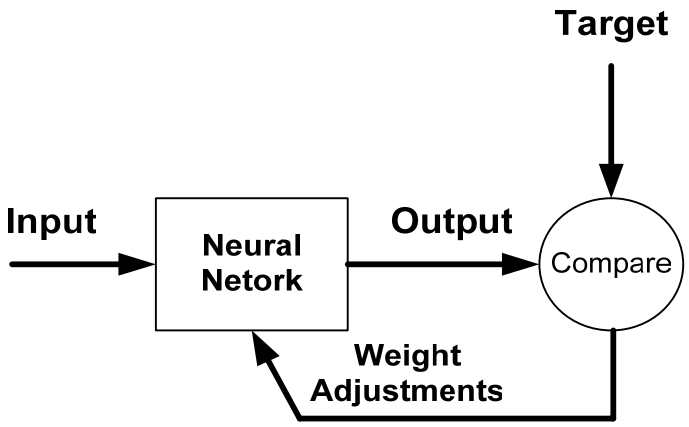

Figure B.1: Supervised learning in a neural network

The neural network in Figure B.1 is adjusted based on a comparison of the output and the target signal. In a practical system many pairs of input target values are used in this *supervised learning* process to train this network.

The basic component in a neural network is a neuron. An example of such a neuron is shown in Figure B.2 This neuron consists of a set of R input links which are weighted with weight matrix $\mathbf{W}$ and summed to a bias b. The summer output goes to a transfer function f which produces the scalar neuron output a calculated as:

$$a = \mathrm{f}(\mathbf{W}\mathbf{p} + b) \qquad \text{(B-1)}$$

Both $\mathbf{W}$ and b are adjustable parameters of the neuron. Typically the transfer function is chosen by the designer and then the parameters $\mathbf{W}$ and b will be adjusted by some learning rule so that the neuron input/output relationship meets some specific goal. The transfer function is chosen to satisfy the specification of the problem that the neuron is attempting to solve. Two functions that have been used in this document are *linear* and *tansig* transfer functions defined by (B-2) and (B-3) respectively.

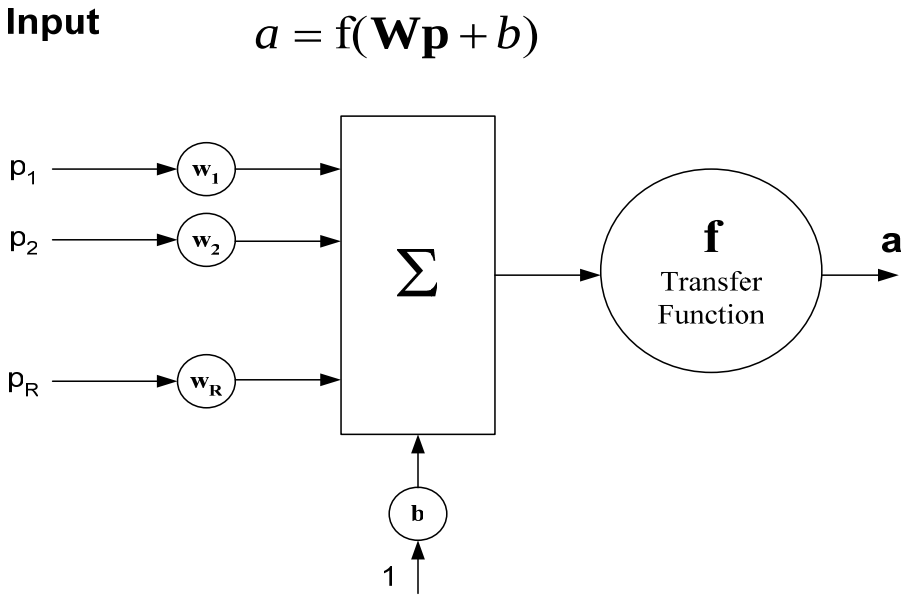

Figure B.2: An R-element input neuron

$$\text{purelin}(x) = x \tag{B-2}$$

$$\text{tansig}(x) = \frac{2}{1+e^{-2x}} - 1 \tag{B-3}$$

In order to model more complex functions multiple neurons are interconnected in parallel in a *layer* on neurons. A single layer of S neurons is shown in Figure B.3. Note that each of the R inputs is connected to each of the neurons and the corresponding weights are shown on the connecting lines. The weight matrix $\mathbf{W}$ now has S rows and defined as:

$$W = \begin{bmatrix} w_{1,1} & w_{1,2} & w_{1,3} & \cdots & w_{1,R} \\ w_{2,1} & w_{2,2} & w_{2,3} & \cdots & w_{2,R} \\ . & . & . & \cdots & . \\ w_{S,1} & w_{S,2} & w_{S,3} & \cdots & w_{S,R} \end{bmatrix} \tag{B-4}$$

It is common for the number of inputs to be different from the number of neurons. The output of this single layer is given by:

$$\mathbf{a} = \begin{bmatrix} a_1 \\ a_2 \\ \\ a_S \end{bmatrix} = \text{f}\left(\begin{bmatrix} w_{1,1} & w_{1,2} & w_{1,3} & \cdots & w_{1,R} \\ w_{2,1} & w_{2,2} & w_{2,3} & \cdots & w_{2,R} \\ . & . & . & \cdots & . \\ w_{S,1} & w_{S,2} & w_{S,3} & \cdots & w_{S,R} \end{bmatrix} \begin{bmatrix} p_1 \\ p_2 \\ . \\ p_R \end{bmatrix} + \begin{bmatrix} b_1 \\ b_2 \\ . \\ b_S \end{bmatrix} \right) \tag{B-5}$$

Multiple layers of neurons can be connected in series and the resulting network is called a *multi-layer-perceptron* (MLP). Each layer has its own weight matrix $\mathbf{W}$, its own bias vector $\mathbf{b}$, its own input net $\mathbf{n}$, and its own output vector $\mathbf{a}$. We use superscript numbers to distinguish between different vectors in different layers.

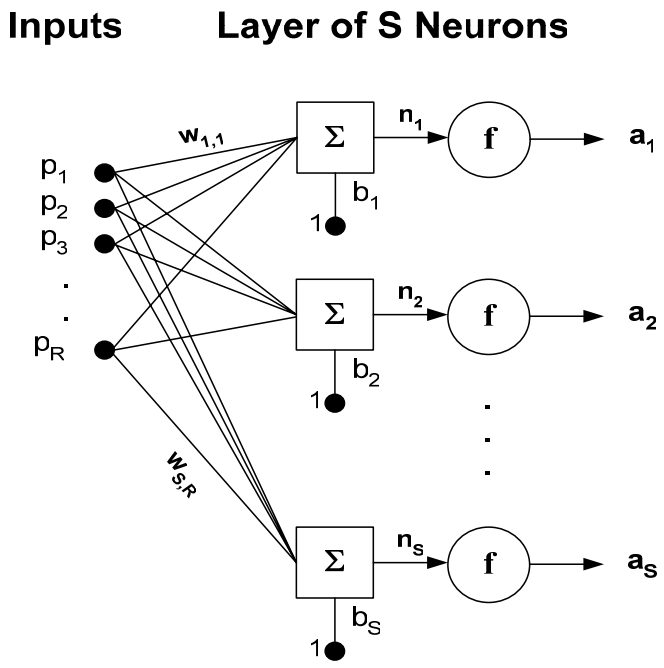

$$\mathbf{a} = \mathrm{f}(\mathbf{Wp} + \mathbf{b})$$

Figure B.3: Layer of S Neurons

Figure B.4 shows a three layer perceptron with R inputs and S^3 outputs. The first, second, and third layers contain S^1, S^2 and S^3 neurons respectively. A layer whose output layer is the output of the network is called the *output layer* and the other layers are called *hidden layers*. The output of the network shown in Figure B.4 as a function of input vector can be written as:

$$\mathbf{a}^3 = \mathrm{f}^3(\mathbf{W}^3\,\mathrm{f}^2(\mathbf{W}^2\,\mathrm{f}^1(\mathbf{W}^1\mathbf{p} + \mathbf{b}^1) + \mathbf{b}^2) + \mathbf{b}^3) \qquad \text{(B-6)}$$

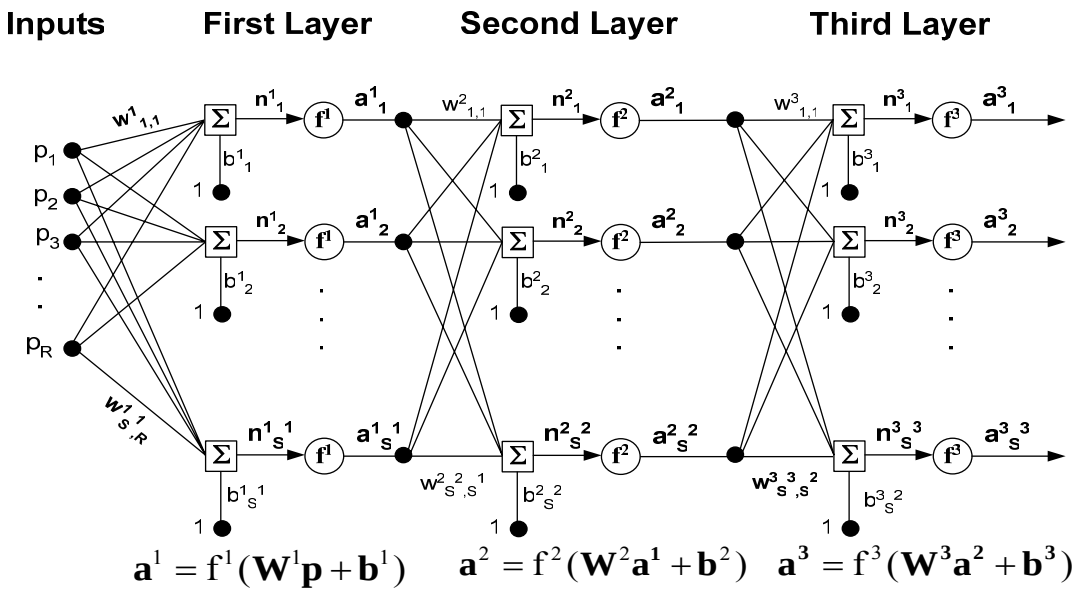

Figure B.4: Three layer neural network

The same network architecture is drawn in Figure B.5 in an abbreviated notation.

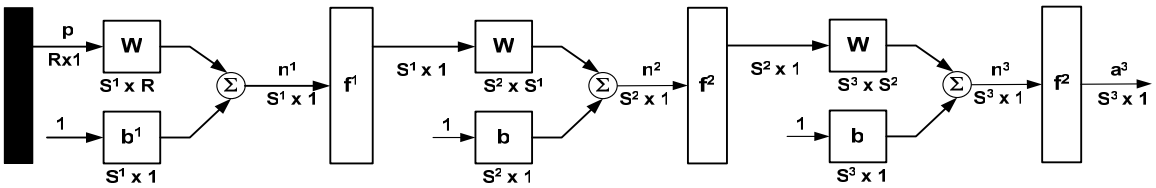

Figure B.5: Three layer neural network using abbreviated notation

Appendix C

Sample Results of UWB Measurements

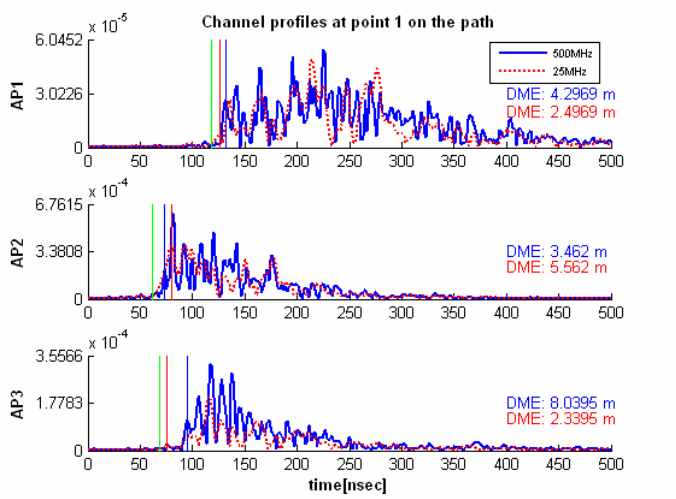

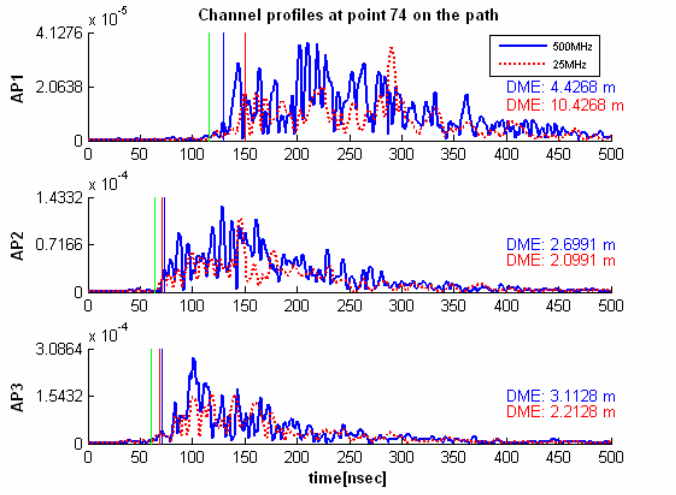

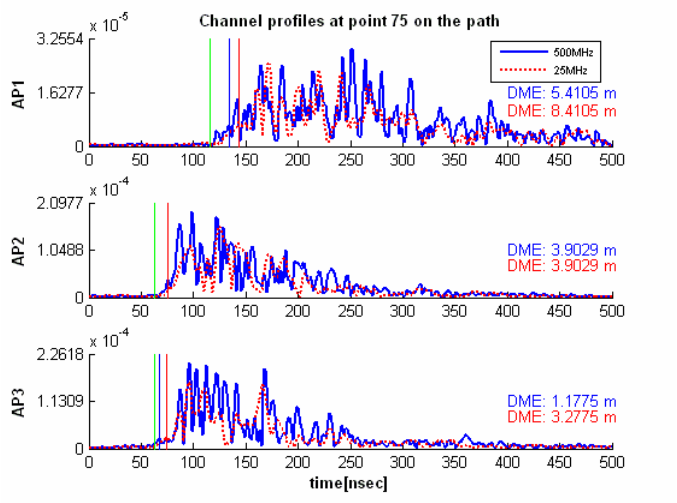
Channel profiles at point 75 on the path
x 10^-5
3.2554
1.6277
0
AP1
500MHz
25MHz
DME: 5.4105 m
DME: 8.4105 m
x 10^-4
2.0977
1.0488
0
AP2
DME: 3.9029 m
DME: 3.9029 m
x 10^-4
2.2618
1.1309
0
AP3
DME: 1.1775 m
DME: 3.2775 m
0 50 100 150 200 250 300 350 400 450 500
time[nsec]

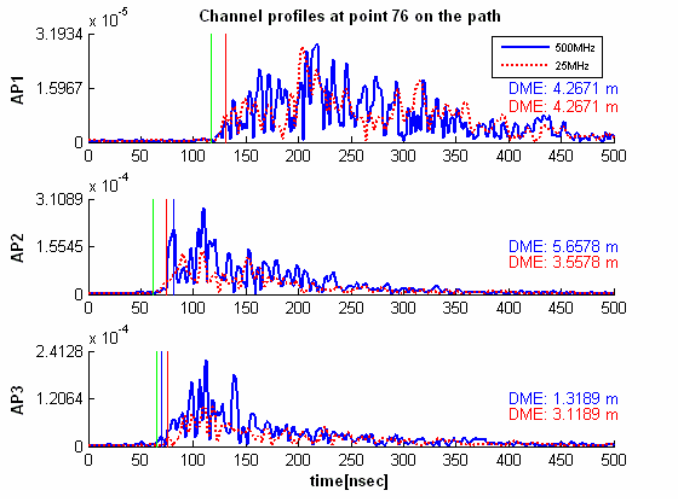
Channel profiles at point 76 on the path
x 10^-5
3.1934
1.5967
0
AP1
500MHz
25MHz
DME: 4.2671 m
DME: 4.2671 m
x 10^-4
3.1089
1.5545
0
AP2
DME: 5.6578 m
DME: 3.5578 m
x 10^-4
2.4128
1.2064
0
AP3
DME: 1.3189 m
DME: 3.1189 m
0 50 100 150 200 250 300 350 400 450 500
time[nsec]

Bibliography

[1] "Location-based services: Finding their place in the market, " In-Stat/MDR, San Jose, CA, Tech. Rep., Feb. 2003.

[2] Pahlavan, K.; Xinrong Li; Makela, J.P., "Indoor geolocation science and technology," IEEE Comm. Mag., vol. 40, no. 2, pp. 112-118, Feb. 2002.

[3] H. Koshima and J. Hoshen, "Personal locator services emerge," *IEEE Spectrum*, Feb. 2000, pp. 41-48

[4] G. J. Pottie and W. J. Kaiser, "Wireless integrated network sensors, " *Commun.. ACM*, May 2000, pp. 51-58

[5] Kaveh Pahlavan, P. Krishnamurthy, and Jaques Beneat, "Wideband radio propagation modeling for indoor geolocation application," *IEEE Communications Magazine*, vol. 36, no. 4, pp. 60-65, 1998.

[6] Schilit, B.; Adams, N.; Want, R, " Context-aware computing applications," *IEEE Workshop on Mobile Computing Systems and Applications*, pp. 85 – 90, Dec. 1994.

[7] Thomas C. AGOSTON, Tatsuro UEDA, and Yukari NISHIMURA, "Pervasive Computing in a Networked World," WebPage, *INET 2000 Proceedings*, [Online]. Available: http://www.isoc.org/inet2000/cdproceedings/

[8] Ali H. Sayed, Alireza Tarighat, and Nima Khajehnouri, "Network-Based Wireless Location, " *IEEE Signal Processing Mag*., 2005.

[9] P. Jensfelt, "Approaches to mobile robot localization in indoor environments", PhD Thesis, Royal Institute of Technology, Stockholm, Sweden, 2001.

[10] K. Pahlavan, P. Krishnamurthy, A. Hatami, M. Ylianttila, J. Mäkelä, R. Pichna, J. Vallström, "Handoff in Hybrid Mobile Data Networks," *IEEE Personal Communications Magazine*, Vol.7 No.2, April 2000, pp. 34-47.

[11] Y. Ko and N. H. Vaidya, "Location-aided routing (LAR) in mobile ad hoc networks, " *Proc. ACM/IEEE MOBICOM '98*, Dallas, TX, 1998.

[12] R. Jain, A. Puri, and R. Sengupta, "Geographical routing using partial information for wireless ad hoc networks, " *IEEE Pers. Commun.*, Feb. 2001, pp. 48-57

[13] "FCC Docket No. 94–102. Revision of the commissions rules to insure compatibility with enhanced 911 emergency calling systems, " Federal Communications Commission Tech. Rep. RM-8143, July 1996.

[14] B. Alavi and K. Pahlavan, K., "Analysis of undetected direct path in time of arrival based UWB indoor geolocation," IEEE 62nd Vehicular Technology Conference, VTC-2005-Fall, Vol. 4, 25-28 Sep., 2005. Page(s):2627 – 2631.

[15] P. Krishnamurthy and Kaveh Pahlavan, "Distribution of range error and radio channel modeling for indoor geolocation applications," *Proc. Of PIMRC*, Kyoto, Japan, Sept. 1999

[16] P. Bahl and V.N. Padmanabhan, and A. Balachandran, "Enhancements to the RADAR User Location and Tracking System,"*Tech. Rep. MSR-TR-00-12, Microsoft Research,* Feb. 2000.

[17] R. Fontana, "Advances in ultrawideband indoor geolocation systems," *presented at the 3rd IEEE Workshop on WLAN*, Boston, Sept. 2001.

[18] Ahmad Hatami, Bardia Alavi, Kaveh Pahlavan, and Muzaffer Kanaan, "A Comparative Performance Evaluation of Indoor Geolocation Technologies," submitted to *Interdisciplinary Information Sciences*, Japan.

[19] P. Krishnamurthy, "Position location in mobile environments," in *Proc. NSF Workshop on Context-Aware Mobile Database Management (CAMM)*, Providence, RI, Jan. 2002.

[20] J. Werb and C. Lanzl, "Designing a positioning system for finding things and people indoors," *IEEE Spectrum*, pp. 71-78, Sept. 1998.

[21] Teemu Roos, Petri Myllymaki, Henry Tirri, , "A statistical modeling approach to location estimation," *IEEE Trans. Mobile Comput. International Journal of Wireless Information Networks*, vol. 1, no. 1, pp. 59-69, March 2002.

[22] P. Bahl and V.N. Padmanabhan, "RADAR: An in-Building RF-based user location and tracking system," *Proc. Of IEEE INFOCOM 2000*., vol. 2, pp. 775 - 784 , March 2000.

[23] Teemu Roos, Petri Myllymaki, Henry Tirri, Pauli Miskangas, and Juha Sievanen, "A probabilistic approach to WLAN user location estimation," *International Journal of Wireless Information Networks*, vol. 9, no. 3, pp. 155-164, July 2002.

[24] J. A. Tauber, "Location systems for pervasive computing," Area Exam Report, Massachusetts Institute of Technology, Aug. 2002.

[25] R. Want, A. Hopper, V. Falcao, and J. Gibbons, "The active badge location system," *ACM Transactions on Information Systems*, vol. 40, no. 1, pp. 91-102, Jan. 1992.

[26] Ahmad Hatami, and Kaveh Pahlavan, "Comparative statistical analysis of indoor positioning using empirical data and indoor radio channel models," *Proc. Of the IEEE CCNC* 2006.

[27] J. Hightower and G. Borriello, "Location systems for ubiquitous computing," *IEEE Computer*, 34(8):57–66, August 2001.

[28] Kanaan. M.; Pahlavan K, "CN-TOAG: a new algorithm for indoor geolocation," *Proc. of IEEE PIMRC 2004*.

[29] Ahmad Hatami, and Kaveh Pahlavan, "In-building intruder detection for WLAN access," Position Location and Navigation Symposium, PLANS 2004.

[30] Ahmad Hatami, and Kaveh Pahlavan, "On RSS and TOA based Indoor Geolocation − A Comparative Performance Evaluation," *Proc. of the IEEE WCNC*, 2006.

[31] Ahmad Hatami, and K. Pahlavan, "Performance Comparison of RSS and TOA Indoor Geolocation Based on UWB Measurement of Channel Characteristics," submitted to *PIMRC'2006*, Helsinki, Finland, 2006.

[32] K. Pahlavan, F. Akgul, M. Heidari, H. Hatami, J. Elwell and R. Tingley, "Indoor Geolocation in the Absence of Direct Path, ", accepted for publication in IEEE Wireless Magazine, 2006.

[33] Ahmad Hatami, and K. Pahlavan, "Hybrid TOA-RSS Based Localization Using Neural Networks," submitted to *IEEE Globecom,* 2006.

[34] K. Pahlavan and A. Levesque, *Wireless Information Networks*, 2nd ed., John Wiley & Sons, 2005.

[35] John G. Proakis, *Digital Communications*, 4th ed., McGrawHill International Edition, 2001.

[36] B. Alavi and K. Pahlavan, "Bandwidth effect on distance error modeling for indoor geolocation," *Proc. IEEE PIMRC'03*, Beijing, China, Sept. 2003.

[37] Erceg V. et al., "TGn Channel Models," *IEEE 802.11 document 03/940r4*, May 2004.

[38] J. Medbo and P. Schramm, "Channel models for HIPERLAN/2," ETSI/BRAN document no. 3ERI085B.

[39] G. A. Deschamps, "Ray techniques in electromagnetics, " *Proc. IEEE,* vol. 60, no. 9, pp. 1022-1035, Sept. 1972.

[40] T. Holt, K. Pahlavan, and J. F. Lee, "A graphical indoor radio channel simulator using 2-D ray tracing, " presented at the *IEEE Inf.* Symp. *Personal, Indoor and Mobile Radio Communications,* Boston, MA, Oct.1992.

[41] Ganning Yang; Pahlavan, K.; Holt, T.J., "Sector antenna and DFE modems for high speed indoor radio communications," *IEEE Trans. on Vehicular Technology*, vol. 43, no. 4, pp. 925-933,1994.

[42] M. C. Lawton, R. L. Davies and J. P. McGeehan, "A ray launching method for the prediction of indoor radio channel characteristics, " in *Proc. IEEE Int. Symp. Personal. Indoor and Mobile Radio Communications,* King's College London (U.K.), pp. 104-108, Sept. 1991.

[43] Yan Xu, Report on Ray Tracing Software, Directed Research under Prof. K. Pahlavan, CWINS, Worcester Polytechnic Institute, Jan. 1998

[44] Kamol Kaemarungsi, Design of Indoor Positioning Systems Based on Location Fingerprinting, PhD thesis, University of Pittsburgh, Pittsburgh, PA, 2005.

[45] K. Pahlavan and S. J. Howard, " Frequency domain measurements of the indoor radio channel, " *Electron. Lett.,* vol. 25, pp. 1645-1647, Nov.1989.

[46] S. J. Howard and K. Pahlavan, "Measurement and analysis of the indoor radio channel in the frequency domain, " *IEEE Trans. Instrum. Meas.,* vol. 39, no. 5, pp. 751-755, Oct. 1990.

[47] V. Zeimpekis, G. M. Giaglis, and G. Lekakos, "A taxonomy of indoor and outdoor positioning techniques for mobile location services," *Journal of ACM Special Interest Group on Electronic Commerce*, vol. 3, pp. 19-27, 2002.

[48] T. S. Rappaport, J. H. Reed, and B. D. Woerner, "Position location using wireless communications on highways of the future," *IEEE Commun. Mag.*, vol. 34, no. 10, pp. 33-41, Oct. 1996.

[49] B. Alavi and K. Pahlavan, "Studying the Effect of Bandwidth on Performance of UWB Positioning Systems, " *IEEE WCNC 2006*, Las Vegas, USA, April 3-6, 2003.

[50] Neal Patwari, Joshua N. Ash, Spyros Kyperountas, Alfred O. Hero III, Randolph L. Moses, and Neiyer S. Correal, "Locating the Nodes Cooperative localization in wireless sensor networks," *IEEE Signal Proc. Mag.*, vol. 22, no. 4, pp. 54–69, July 2005.

[51] F. Gustafsson and F. Gunnarsson, "Mobile positioning using wireless networks," *IEEE Signal Proc. Mag*., vol. 22, no. 4, pp. 41–53, July 2005.

[52] T. S. Rappaport, *Wireless Communications: Principles and Practice*, 2nd ed. , Prentice Hall, Upper Saddle River, NJ, 2002.

[53] Papoulis, *Random Variables, and Stochastic Processes*, Third ed., McGrawHill, 1991.

[54] A. Harter, A. Hopper, P. Steggles, A.Ward, and P.Webster, "The anatomy of a context-aware application," in *Proc. ACM International Conference on Mobile Computing and Networking (MOBICOM'99)*, Seattle, WA, Aug. 1999.

[55] N. B. Priyantha, A. Chakraborty, and H. Balakrishnan, "The cricket location-support system," in *Proc. ACM International Conference on Mobile Computing and Networking (MOBICOM'00)*, Boston, MA, Aug. 2000, pp. 32-43.

[56] IEEE Std. 802.11-1999, Part 11: Wireless LAN medium access control (MAC) and physical layer (PHY) specifications, Reference number ISO/IEC 8802-11:1999(E), IEEE Std. 802.11, 1999 edition.

[57] P. Prasithsangaree, P. Krishnamurthy, P.K. Chrysanthis, "On indoor position location with wireless LANs," *IEEE PIMRC2002*, vol. 2, pp. 720 - 724 , Sept. 2002.

[58] A.H. Sayed, *Fundamentals of Adaptive Filtering*, John wiley, 2003.

[59] W.C. Davidon, "Variance algorithm for minimization," *Computer Journal*, Vol. 10, pp. 406-410, 1968**.**

[60] M. Kanaan, K. Pahlavan, "*Algorithm for TOA-based Indoor Geolocation,*" IEE Electronics Letters, October, 2004.

[61] P-C. Chen, "A non-line-of-sight error mitigation algorithm in location estimation," *Proceedings of the IEEE Wireless Communications and Networking Conference*, 1999

[62] M. Hagan, H. Demuth, and M. Beale, *Neural Network Design*, PWS Publishing Company, 1996.

[63] R. Battiti, A. Villani, and T. Le Nhat, "Neural network models for intelligent networks: deriving the location from signal patterns," in *Proceedings of AINS2002*, (UCLA), May 2002.

[64] C. Nerguizian, C. Despins, and S. Affes, "Geolocation in mines with an impulse response fingerprinting technique and neural networks," *IEEE Transactions on Wireless Comm.*, vol. 5, no. 2, pp. 603-611, March 2006.

[65] S. Saha, K. Chaudhuri, D. Sanghi, and P. Bhagwat, "Location determination of a mobile device using ieee 802.11b access point signals," in *Proc. IEEE WCNC'03*, New Orleans, LA, Mar. 2003, pp. 1987{1992.

[66] R. Battiti, "Location-aware computing: a neural network model for determining location in wireless lans," Universita degli Studi di Trento, Tech. Rep. DIT-0083, Feb. 2002. [Online]. Available: http://rtm.science.unitn.it/~battiti/archive/83.pdf

[67] Kurt Hornik. Approximation capabilities of multilayer feedforward networks. *Neural Networks*, 4:251–257, 1991.

[68] Bates, D. M. and Watts, D. G., *Nonlinear Regression and Its Applications*, New York: Wiley, 1988.

[69] *Ekahau Positioning Engine 2.1*, User Guide, Ekahau, Inc., 2003. [Online]. Available: http://www.ekahau.com

[70] R. Battiti, M. Brunato, and A. Villani, "Statistical learning theory for location fingerprinting in wireless lans," Technical Report, Oct. 2002. [Online]. Available: http://rtm.science.unitn.it/~battiti/archive/86.pdf